NUREG/CR-0649
SAND77-1371
R-3

Spent Fuel Heatup Following Loss of Water During Storage

Allan S. Benjamin, David J. McCloskey, Dana A. Powers, Stephen A. Dupree

Printed March 1979

Sandia Laboratories

SF 2900 Q(7-73)

Prepared for
U. S. NUCLEAR REGULATORY COMMISSION

NOTICE

Available from
National Technical Information Service
Springfield, VA 22161

NUREG/CR-0649
SAND77-1371
R-3

SPENT FUEL HEATUP FOLLOWING LOSS OF WATER DURING STORAGE

Allan S. Benjamin
David J. McCloskey
Dana A. Powers
Stephen A. Dupree

Date Published: March 1979

Sandia Laboratories
Albuquerque, New Mexico 87185
operated by
Sandia Corporation
for the
U.S. Department of Energy

Prepared for
U.S. Nuclear Regulatory Commission
Washington, DC 20555
Under Interagency Agreement DOE 40-550-75
NRC FIN No. A2050

ACKNOWLEDGEMENTS

The authors wish to thank Mr. R. E. L. Stanford, U.S. Nuclear Regulatory Commission, for his assistance and perceptive review of the manuscript, and Dr. D. E. Bennett, Sandia Laboratories, for his contribution in defining the decay heat characteristics of the spent fuel.

ABSTRACT

An analysis of spent fuel heatup following a hypothetical accident involving drainage of the storage pool is presented. Computations based upon a new computer code called SFUEL have been performed to assess the effect of decay time, fuel element design, storage rack design, packing density, room ventilation, drainage level, and other variables on the heatup characteristics of the spent fuel and to predict the conditions under which clad failure will occur. Possible storage pool design modifications and/or onsite emergency action have also been considered. It has been found that the likelihood of clad failure due to rupture or melting following a complete drainage is extremely dependent on the storage configuration and the spent fuel decay period, and that the minimum prerequisite decay time to preclude clad failure may vary from less than 10 days for some storage configurations to several years for others. The potential for reducing this critical decay time either by making reasonable design modifications or by providing effective emergency countermeasures has been found to be significant.

CONTENTS

ILLUSTRATIONS

ILLUSTRATIONS (Continued)

TABLES

TABLES (Continued)

1. INTRODUCTION

With the current U.S. moratorium on spent fuel reprocessing, high priority is being given to the expansion of facilities that store spent fuel under water in a retrievable configuration. To accomodate the growing quantities of used fuel bundles, existing storage pools are being enlarged and adapted to higher storage densities. In the process, storage racks have evolved from widely spaced, open frame structures to tightly packed, closed frame steel containers. This has necessitated reevaluation of the safety design basis of spent fuel storage facilities.

To assess the safety of such facilities, a range of postulated accidents may be considered, and predictions of the probability of occurrence of these accidents and the resulting consequences may be made. Such a process can provide perspective concerning the overall public risk caused by operation of the facility. The process is useful not only for delineating the safety bounds of the system but also for suggesting design or operational changes which may broaden these bounds.

This study addresses the most severe type of spent fuel storage accident that has been hypothesized, one that leads to a complete drainage of the water from the pool. The objective is to analyze the thermal-hydraulic phenomena involved when the storage racks and their contents become exposed to air, and to determine the conditions which could lead to clad failure due to overheating. Accident initiation mechanisms, the probability of occurrence, the magnitude of radioactive release, or the public consequences are not addressed.

The likelihood of a severe spent fuel pool drainage accident is judged to be extremely low.* Many spent fuel pools are constructed below grade, essentially precluding complete drainage of the pool due to structural failure. Numerous design features are incorporated in all facilities to minimize the likelihood of a loss of pool water, including (1) the conservative design philosophy of building the concrete structure, racks, cooling system, and support structures to withstand the forces that might result from a large earthquake or tornado, (2) design of the racks to assure that the geometry of stored spent fuel is maintained in a subcritical configuration, (3) location of pool penetrations to prevent draining or siphoning of water through associated piping systems, (4) inclusion of mechanical interlocks and operating procedures to prevent the crane from passing over the pool with heavy loads, and (5) provision of multiple water level, water temperature, and radioactivity monitors which actuate alarms in the control room. Stringent security measures are enforced to prevent sabotage. A complete drainage of a spent fuel pool, therefore, has to be considered as an extremely unlikely occurrence.

Postulating a complete pool drainage, however, the fuel elements will heat up, tending to reach a steady-state temperature distribution when the thermal power produced by radioactive decay is balanced by that removed by natural convection, thermal radiation, and other means. Undesirable releases of radioactive materials will occur only if the maximum attained temperature is high enough at some location in the pool to cause the Zircaloy clad to rupture as a result of internal pressure, or to undergo rapid exothermic oxidation leading to clad melting. (Coincidentally, the best available

---

*The Reactor Safety Study[1] evaluated the probability as being in the range of 10^{-5} to 10^{-7} per year. Handling or storage of spent fuel was not found to be a significant contributor to the overall public risk caused by nuclear power plant operations.

estimate for clad rupture temperature[2,3] is quite close to the temperature at which the air oxidation reaction becomes self-sustaining, both being in the neighborhood of 850 - 950° C.) The likelihood of reaching a deleterious temperature varies inversely with the amount of time that has elapsed since shut-down of fission power (i.e., the decay time), since longer times imply reduced decay heats.

A method of predicting the spent fuel heatup following drainage of the pool has been formulated[4,5] and implemented within a computer code called SFUEL (documented in Appendices A and D). Computations have been performed to assess the effect of decay time, fuel element design, storage rack design, packing density, room ventilation, and other variables on the heatup characteristics of the spent fuel, and to investigate such issues as complications caused by incomplete drainage, possible design modifications to promote heat removal, and emergency action that can be undertaken to maintain coolability after the accident has occurred. The problems considered, methods used, and results obtained are described in the following text, with mathematical details and a program listing being included in the appendices.

2. DESIGN CHARACTERISTICS

2.1 Pool Configurations

Excepting capacity and the design of the racks, the configuration of spent fuel storage pools is similar for most nuclear reactor and away-from-reactor (AFR) storage facilities. The pools are rectangular in cross section and approximately 40 feet deep. Fuel assemblies are placed vertically in storage racks which maintain an adequate spacing to prevent criticality and to promote natural convective cooling in a water medium. The pools themselves are constructed of reinforced concrete with sufficient thickness to meet radiation shielding and structural requirements, and are lined with stainless steel plates of approximately 1/4-inch thickness to insure a leak-tight system.

Boiling water reactors (BWRs) are designed with the spent fuel storage pool within the secondary containment. On Mark I and II plants, the bottom of the pool is usually elevated approximately 50 feet above ground level, which places the top of the pool at the level of the operating floor. More recent BWR designs, however, call for a ground-level storage pool to reduce seismic loads.

Pressurized water reactors (PWRs) use a ground-level spent fuel storage pool which is exterior to the reactor building, in the auxiliary building. Both BWR and PWR reactor pools typically range from 30 to 60 feet in length and 20 to 40 feet in width, with a spent fuel capacity of between 1 and 2 cores.

Away-from-reactor (AFR) storage pools generally have larger capacity than reactor pools. The General Electric facility at Morris, Illinois, for example, has the capability to store 750 metric tons, which is the equivalent of about five BWR cores or eight PWR cores, and has applied for authorization to double that capacity. A photograph of the G.E. Morris storage pool is shown in Fig. 1.

In the analysis to be described (Section 3), it was assumed that the walls and floor of the pool were comprised of thick reinforced concrete and lined with a 1/4-inch stainless steel liner.

2.2 Storage Rack Configurations

The design of storage racks and fuel element holder configurations varies considerably from facility to facility, both in general appearance and in details. Fig. 2 shows a sampling of the various types of racks currently in use.

An earlier storage rack design for PWR spent fuel (e.g., original Sequoyah and Savannah River designs) consists of an open frame arrangement with a 21-inch center-to-center spacing (Fig. 2a). The racks are made of stainless steel and are approximately 14 feet high. Criticality control is provided by the relatively large fuel element spacing together with borating of the water.

Subsequent PWR rack designs employ solid stainless steel holder walls to provide the neutron shielding required for a higher density storage configuration (Figs. 2b through 2d). The cylindrical "baskets" shown in Fig. 2b are used in the G.E. Morris facility, for example, and provide a 12.75-inch center-to-center fuel element spacing. The inlet for water circulation through these elements at G.E. Morris is provided by a 1.5-inch diameter hole, drilled through each basket near the baseplate.

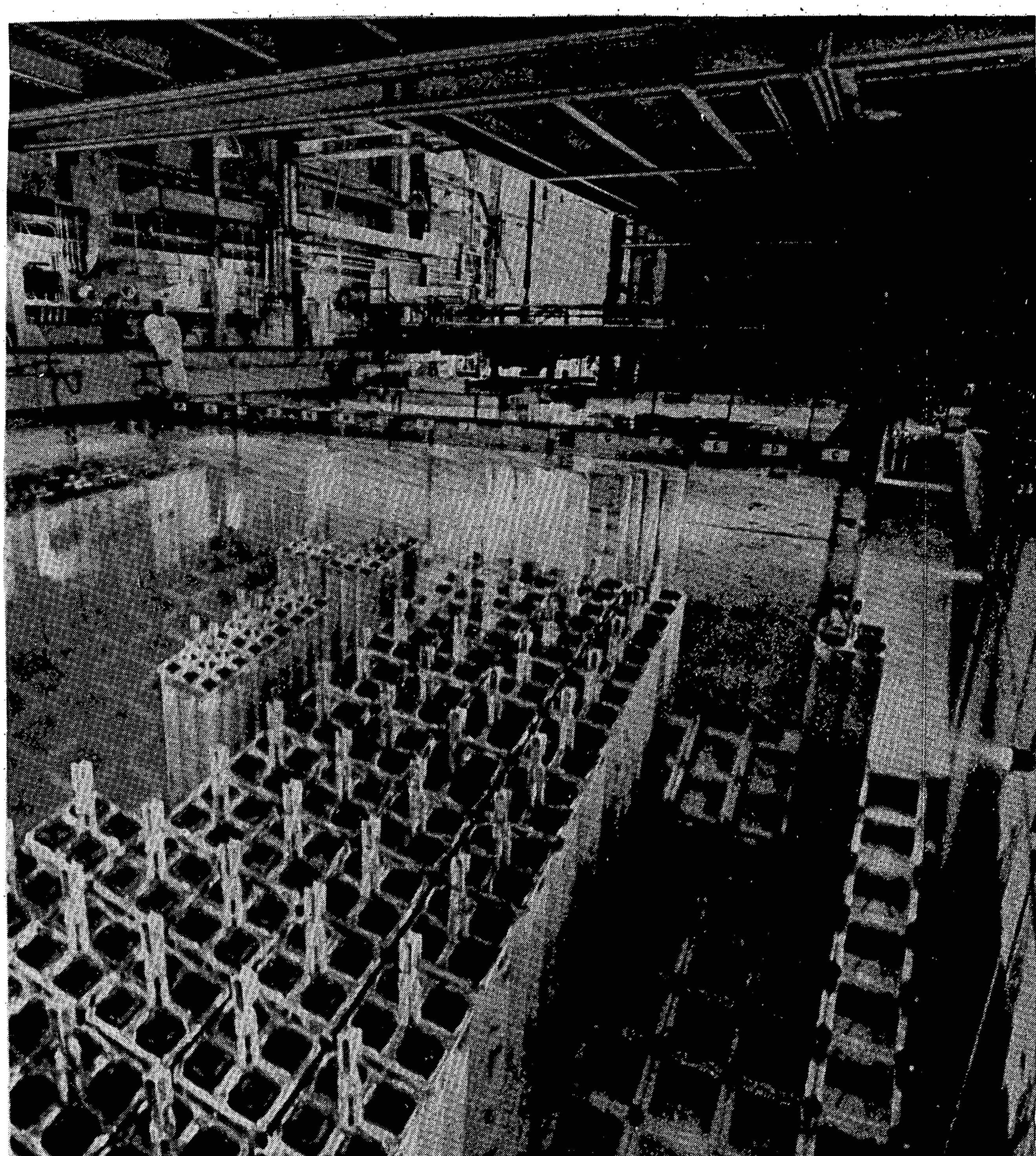

Figure 1. Spent Fuel Storage Pool at G.E. Morris Operation, Morris, Illinois

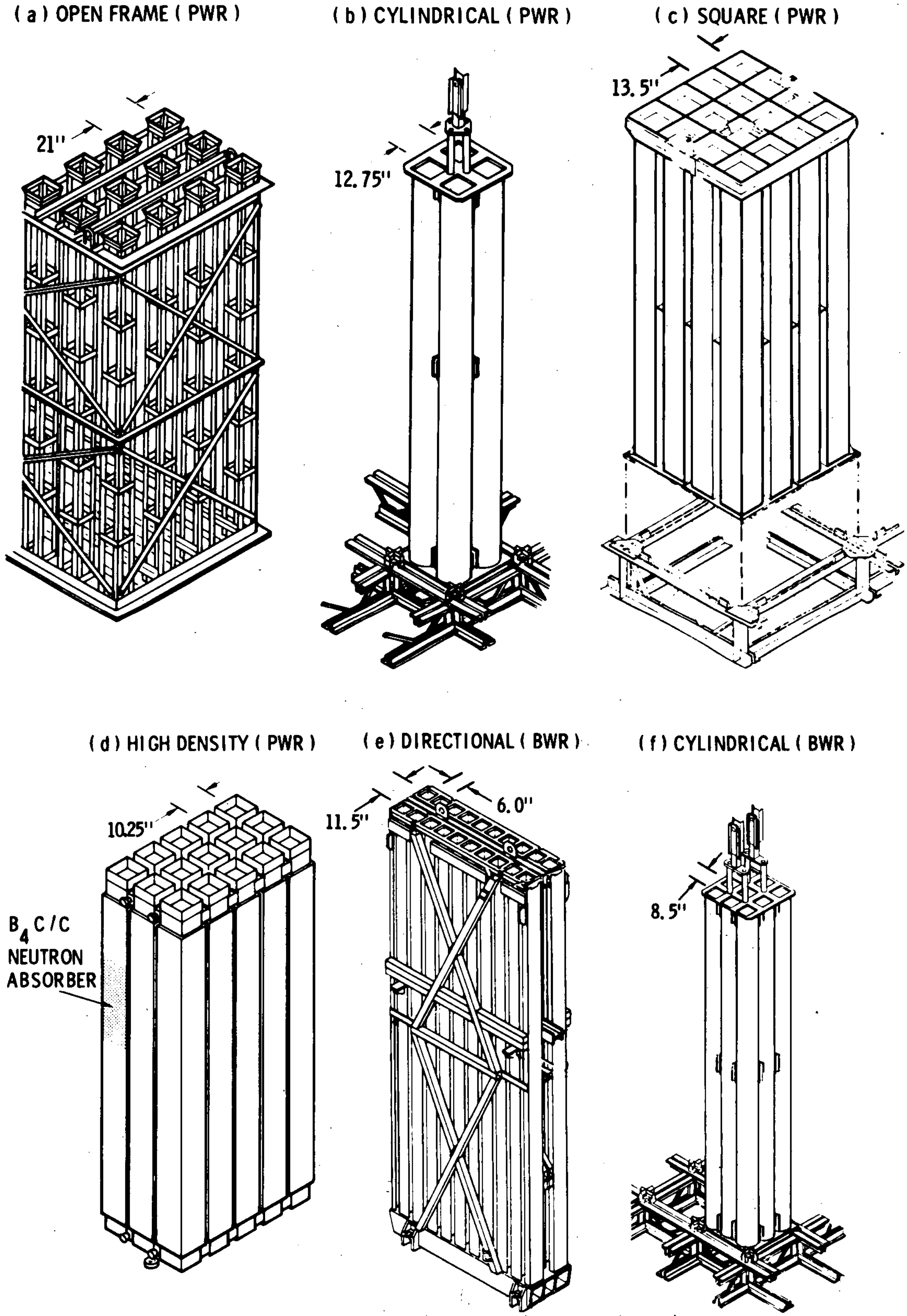

Figure 2. Spent Fuel Storage Racks Considered in Drained Pool Analysis

The square-shaped rack configuration in Fig. 2c is used or has been proposed (with some variations) for the Sequoyah, Oconee, and H. B. Robinson PWR power plants, among others. These racks include a 13- to 14-inch center-to-center fuel element spacing and provide for water flow through a baseplate hole of varying diameter (3.0 inches for H.B. Robinson).

The high density racks shown in Fig. 2d, being used at the Palisades Nuclear Generating Station as well as being considered for other installations, provide a 10.25-inch center-to-center spacing. Neutron absorption is accomplished by holder walls which consist of two 1/8-inch stainless steel plates sandwiched around a 1/4-inch absorber plate made of 50 percent boron carbide (by volume) in a carbon matrix. A 5.0-inch baseplate hole is included for water circulation.

Typical BWR spent fuel storage racks are shown in Figs. 2e and 2f. The earlier BWR rack design shown in Fig. 2e (e.g., original Peach Bottom reactor design) is made of aluminum and holds 20 fuel assemblies in two rows of 10. The fuel element center-to-center spacing is 6.0 inches in the long direction and 11.5 inches across the rows. The cylindrical "basket" arrangement shown in Fig. 2f is made of stainless steel, provides a 8.5-inch center-to-center spacing, and is used, for example, at G.E. Morris and at the Brunswick Steam Electric Plant. The water inlet at G.E. Morris consists of a 1.5-inch hole drilled into the bottom part of the basket, whereas Brunswick uses a 3.625-inch baseplate hole.

Since it was found during the study that rack configuration was an important variable in the heat transfer problem for a drained pool, each of the configurations shown in Fig. 2 was analyzed separately. Schematics of these configurations together with dimensions used are shown in Fig. 3. It was assumed in most cases that a 16-inch open space is maintained

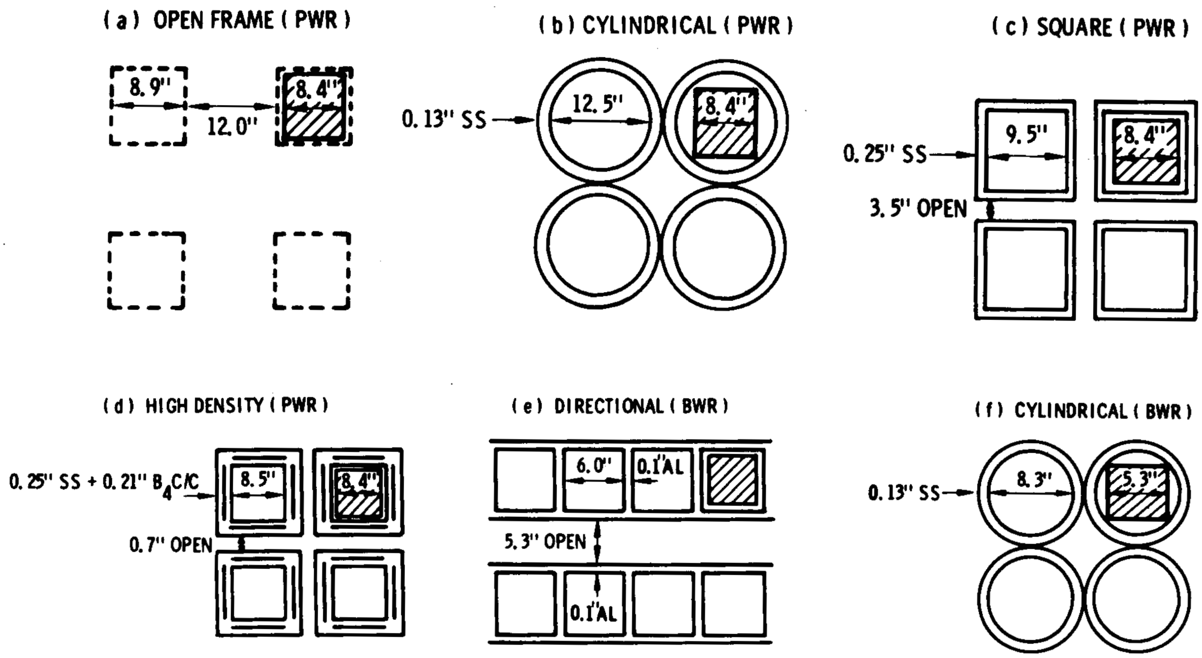

Figure 3. Cross Sectional Dimensions of Spent Fuel Holders Shown in Fig. 2.

between the baseplate and the bottom of the pool and between the sidewalls and the outermost basket or holder, allowing a low resistance path for air flow from above the pool to below the fuel elements. This assumption is generally valid, since most storage rack configurations do provide a 1 to 1-1/2 foot allowance around the sides of the pool and over the bottom. The high density storage configuration (Fig. 2d), however, is an exception in that the design allows racks to be placed within 1/2 inch of the walls of the pool. Special calculations were made for this case to investigate possible flow constrictions that might occur from full utilization of the racks.

2.3 Fuel Subassemblies

Schematics of PWR and BWR fuel assemblies are shown in Fig. 4 and quantitative details are given in Table I. The PWR subassemblies considered in this analysis consisted of 15 x 15 and 17 x 17 fuel pin arrays, characteristic of older

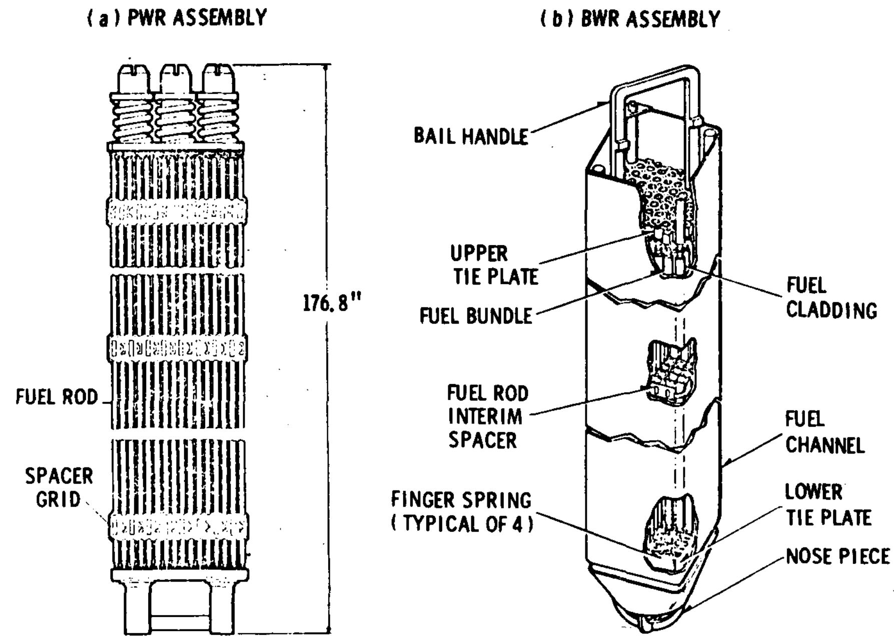

Figure 4. Typical PWR and BWR Fuel Assemblies

Table I

Design Properties of Fuel Assemblies Used in the Analysis

	Older PWR	Newer PWR	Older BWR	Newer BWR
Rod array	15 x 15	17 x 17	7 x 7	8 x 8
Number of fuel rods per assembly	208	264	49	63
Number of non-fuel rods per assembly	17	25	0	1
Active fuel height (In.)	144	144	144	148
Rod center-to-center pitch (In.)	0.558	0.496	0.738	0.640
Fuel rod outside diameter (In.)	0.420	0.374	0.563	0.493
Clad thickness (In.)	0.026	0.023	0.032	0.034
Channel thickness (In.)	-	-	0.08	0.12
Metric tons uranium per assembly (MTU)	0.456	0.461	0.195	0.189
Number of assemblies per core, typical reactors	177	193	764	732

and newer fuel element designs, respectively. Heatup characteristics were computed both with and without the control rods. The BWR subassemblies were comprised of 7 x 7 and 8 x 8 fuel pin arrays, and the computations were performed both with and without the Zircaloy channel walls. Standard practice at many facilities (e.g., G.E. Morris) is to remove control rods and channel walls before storage, but these practices are not universal.[6]

3. HEAT TRANSFER MODELS

3.1 Decay Heat Generation

Decay heat produced by spent fuel elements varies strongly with time since removal from the core as well as the operating conditions and burnup experienced in the core.[7] For the decay times of interest here, namely 10 days to several years, the effect of reactor experience and, in particular, the burnup are of great importance. Consequently, a review of operating practice was made and new decay power computations were undertaken to account for realistic operating conditions. These computations were accomplished with a Sandia version of the ORIGEN code,[8,9] the Sandia version having been updated with respect to the cross section data and in particular the neutron absorption characteristics of ^{133}Cs, which is an important contributor for the longer decay times. During personal communications with Tal England at LASL (January 1978), it was determined that results from the Sandia and Los Alamos versions of ORIGEN are substantially in agreement.

Burnups achieved in operating practice for PWR fuel in Zion units 1 and 2 and for BWR fuel in Dresden units 2 and 3 and Quad Cities units 1 and 2 are shown in Table II, these data having been obtained from personal communications with Bruce Momsen at Commonwealth Edison of Illinois (February 1978). It may be noted that for the PWR fuel in Zion unit 1, the projected equilibrium burnup is in the range of 31,000 - 33,000 MWD/MTU*, depending on location in the core, and that the projected burnup after Cycle 3 is considerably higher than

*Megawatt-days per metric ton of uranium the equilibrium value. For this reason, two operating histories were considered for the PWR, the first (standard case) corresponding to a 33,000 MWD/MTU burnup and the second (perturbed case) corresponding to a 36,900 MWD/MTU burnup, both involving three cycles of operation.

Table II.

Reported Fuel Burnups Achieved in Operating Practice

Reactor	Type/ Pin Array	Cycle	Actual/ Projected	Average Burnup (MWD/MTU)	Peak Burnup (MWD/MTU)
Zion Unit 1	PWR (15 x 15)	1	Actual	18,343	19,290
		2	Actual	30,310	32,185
		3	Projected	35,550	38,700
		Equil.	Projected	31,000	33,000
Zion Unit 2		1	Actual	19,470	20,540
		2	Projected	29,020	30,200
Dresden Unit 2	BWR (7 x 7)	5	Actual	21,429	22,813
Dresden Unit 3		4	Actual	18,255	19,369
Quad Cities Unit 1		3	Actual	19,310	20,689
Quad Cities Unit 2		2	Actual	17,662	19,139

The results for total decay heat obtained from ORIGEN for the PWR cases are shown in Table III. These results

TABLE III

Thermal Decay Power of PWR Spent Fuel as a Function of Decay Time and Discharge Cycle

Cycle of Discharge \ Decay Time	10d	30d	90d	180d	1 yr	2 yr	3 yr	5 yr	10 yr
(1) Standard Case: 3 cycles @ 3.3% wt. enrichment. Operating power = 37.3 MW/MTU. Total burnup = 33,000 MWD/MTU. 30-day down time between cycles, 35-day down time within cycles, 295 oper. days per cycle.									
1	75.4*	43.4	21.3	11.4	5.05	2.22	1.25	0.607	0.368
2	81.1	48.6	26.0	15.6	8.20	4.07	2.46	1.30	0.779
3	86.6	53.2	30.0	19.2	11.0	5.90	3.76	2.12	1.28
(2) Perturbed Case: Same as above except total burnup = 36,900 MWD/MTU. 30-day down time between cycles, no down time within cycles, 330 oper. days per cycle.									
1	79.5	46.7	23.4	12.6	5.68	2.52	1.42	0.689	0.414
2	86.3	52.8	28.9	17.5	9.35	4.69	2.84	1.50	0.888
3	92.9	58.3	33.7	21.8	12.7	6.88	4.41	2.50	1.49
(3) Reference Case (Non-practicable): Continuous operation for 1100 days @ 3.3% wt. enrichment. Operating power = 30 MW/MTU. Total burnup = 33,000 MWD/MTU.									
-	75.5	47.9	27.9	18.2	10.7	5.83	3.68	2.10	1.27

*Units of decay power in this table are KW/MTU include heating contributions from fission products, actinides, and structural components, the first of these being the most important for the decay times being considered. For purposes of determining decay heats in the event of a whole core discharge, the values presented include decay heats for early discharges (i.e., discharges occurring after the completion of an intermediate cycle) as well as the normal discharge after three cycles. A reference case involving continuous operation at an 80 percent power level with a 33,000 MWD/MTU burnup is included for comparison. A comparison of decay heating characteristics for PWR spent fuel assemblies after various cycles of discharge is shown in Fig. 5.

The specification refueling cycle for BWR's is somewhat more complicated than for PWR's, some of the fuel assemblies being utilized for four cycles and others for three. The fuel in a typical BWR core of 748 assemblies is divided into 5 categories, each having different amounts of burnup ranging from 24,600 to 30,600 MWD/MTU, owing to differences in operating power, number of cycles, or percent enrichment.[10] Table IV shows the decay heating power as a function of decay time and cycle of discharge for each of these five categories of BWR fuel assemblies.

For the drained pool heatup calculations, both whole core discharges and normal discharges were considered. For reactor storage, it was assumed that the pool had a capacity of 1.75 cores, with full loading as shown in Table V. In a typical calculation, the hottest fuel elements would comprise about 20 percent of the total fuel load, with elements of progressively lower radioactivity comprising the remainder. The same proportions of fuel element loading as were used for reactor storage were typically assumed to apply for away-from-reactor storage as well, although parametric variations of the fuel loading proportions were also considered in that case.

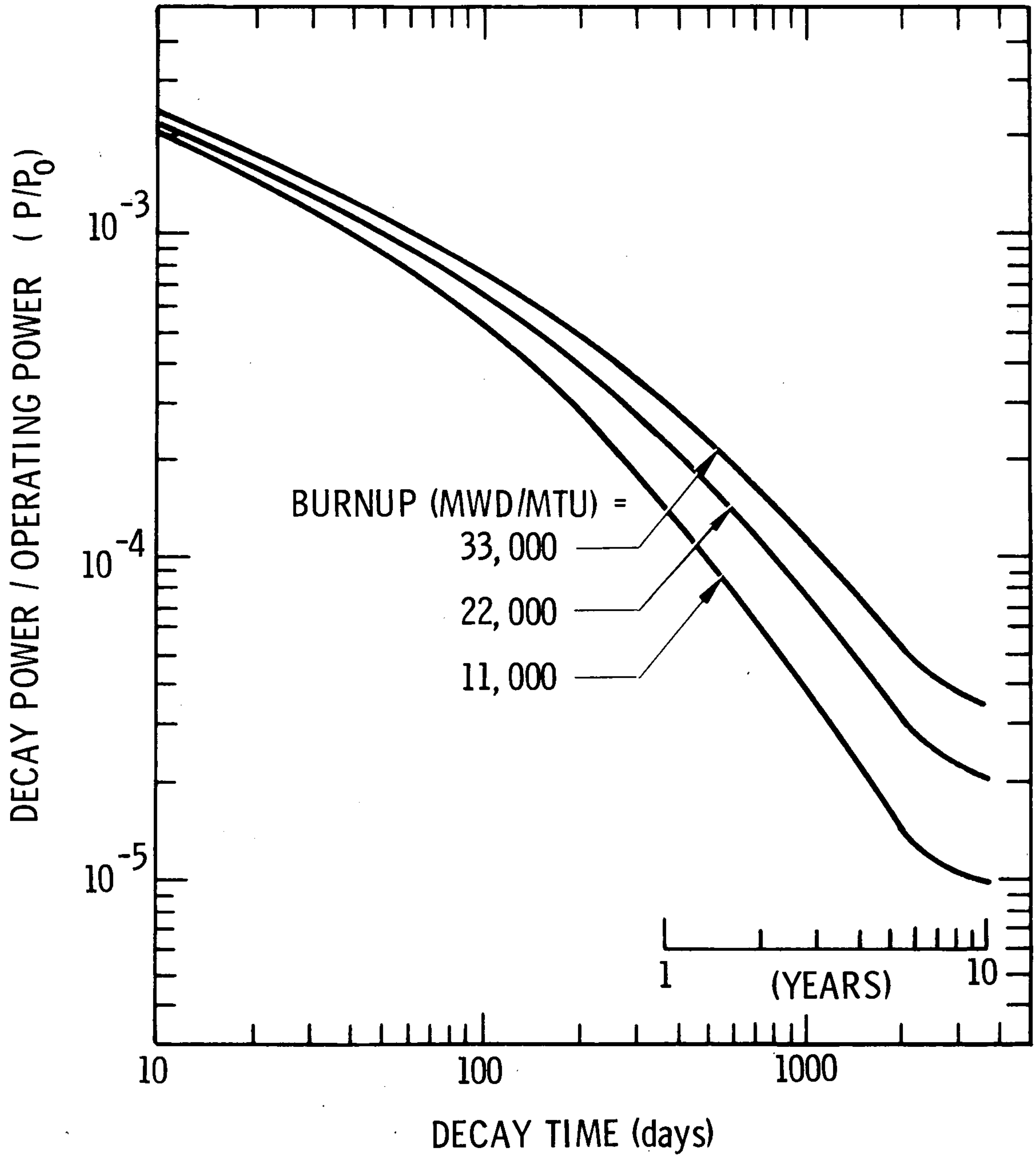

Figure 5. Normalized Decay Power Versus Decay Time for PWR Spent Fuel

TABLE IV

Thermal Decay Power of BWR Spent Fuel as a Function of Decay Time and Discharge Cycle

Cycle of Discharge \ Decay Time	10d	30d	90d	180d	1 yr	2 yr	3 yr	5 yr	10 yr
Standard Case*									
(1) 272 assemblies out of core: 4 cycles @ 2.83% wt. enrichment. Total burnup = 30,600 MWD/MTU. Operating power, first cycle = 30.1 MW/MTU, second cycle = 29.0, third cycle = 27.2, fourth cycle = 25.1. 30-day down time between cycles, 50-day down time within cycles, 275 operating days per cycle.									
1	59.7**	33.8	16.3	8.71	3.82	1.67	0.940	0.459	0.284
2	61.4	36.2	19.1	11.4	5.92	2.92	1.76	0.942	0.586
3	60.9	36.9	20.6	13.1	7.43	3.94	2.51	1.44	0.907
4	59.5	36.9	21.5	14.3	8.58	4.80	3.19	1.94	1.24
(2) 272 assemblies out of core: Same as (1) except operating power fourth cycle = 12.6 MW/MTU. Burnup = 27,200 MWD/MTU.									
1	Decay power for early discharges same as for (1) above								
2									
3									
4	33.3	22.0	13.9	9.77	6.24	3.63	2.48	1.57	1.05

TABLE IV (continued)

(3) 96 assemblies out of core: 4 cycles @ 2.66% wt. enrichment. Total burnup = 29,600 MWD/MTU. Operating power, first cycle = 29.1 MW/MTU, second cycle = 27.9, third cycle = 25.7, fourth cycle = 25.1. 30-day down time between cycles, 50-day down time within cycles, 275 operating days per cycle.

1	57.6	32.6	15.8	8.41	3.70	1.62	0.911	0.444	0.274
2	59.1	34.8	18.4	11.0	5.72	2.83	1.70	0.907	0.564
3	57.5	34.9	19.5	12.4	7.07	3.75	2.39	1.37	0.863
4	59.1	36.6	21.2	14.0	8.39	4.67	3.09	1.87	1.20

(4) 96 assemblies out of core: Same as (3) except operating power fourth cycle = 12.6. Burnup = 26,200 MWD/MTU.

1	Decay power for early discharges same as for (3) above								
2									
3									
4	33.0	21.6	13.6	9.51	6.04	3.50	2.39	1.50	1.01

(5) ∿12 assemblies out of core: 3 cycles @ 2.66% wt. enrichment. Total burnup = 24,600 MWD/MTU. Operating power, first cycle = 30.1 MW/MTU, second cycle = 29.8, third cycle = 29.5. 30-day down time between cycles, 50-day down time within cycles, 275 operating days per cycle.

1	59.7	33.7	16.3	8.72	3.84	1.69	0.949	0.462	0.284
2	63.0	37.1	19.6	11.7	6.10	3.02	1.82	0.967	0.598
3	65.9	39.8	22.2	14.1	7.99	4.23	2.69	1.53	0.954

*Each of the 5 categories listed corresponds to a portion of a BWR-6 core. A full core discharge will therefore include elements from each category.

**Units of decay power in this table are KW/MTU.

TABLE V

Typical Fuel Loadings Assumed for Spent Fuel Storage at Reactor

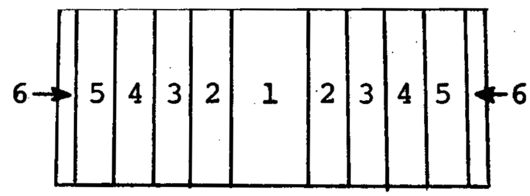

Section of Pool	Fraction of Core	Number of cycles in reactor	Burnup (MWD/MTU)	Decay Time
(A) Full-Core PWR Discharge				
1	1/3	3	33,000	T
2	1/3	2	22,000	T
3	1/3	1	11,000	T
4	1/3	3	33,000	T + 1 yr
5	1/3	3	33,000	T + 2 yrs
6	1/12	3	33,000	T + 3 yrs
(B) Normal PWR Discharge				
1	1/3	3	33,000	T
2	1/3	3	33,000	T + 1 yr
3	1/3	3	33,000	T + 2 yrs
4	1/3	3	33,000	T + 3 yrs
5	1/3	3	33,000	T + 4 yrs
6	1/12	3	33,000	T + 5 yrs
(C) Worst Case PWR Loading Pattern				
1	1/3	3	33,000	T
2	1/3	3	33,000	T
3	1/3	2	22,000	T
4	1/3	2	22,000	T
5	1/3	1	11,000	T
6	1/12	1	11,000	T
(D) Full-Core BWR Discharge				
1	1/8	4	30,600	T
2	1/4	3	23,700	T
3	1/4	2	16,300	T
4	1/4	1	8,300	T
5	1/8	4	27,200	T
6	3/4	4	30,600	T+1,2,3 yrs

To characterize the variation of decay power along the axis of a fuel rod, a chopped sine distribution having a peak-to-average variation of 1.5 was assumed. Thus the decay heat generation per unit length, L, of rod was taken to be

$$Q(z,t) = \frac{1.5\, W_U\, P_o(t)}{L} \sin \left[\frac{\pi(z + .025L)}{1.050L} \right] \qquad (1)$$

where P_o is the decay power per unit weight of uranium determined from ORIGEN and W_U is the uranium weight per assembly. All rods in a fuel assembly were assumed to have the same decay power variation. It may be seen from Equation (1) that the production of decay heat is symmetric about the midpoint ($z = 0.5L$).

3.2 Clad Oxidation

Oxidation of Zircaloy clad at elevated temperatures by air occurs primarily by the following reaction

$$Zr + O_2 \rightarrow ZrO_2$$

which liberates approximately 262 Kcal per mole of Zr. The rate of reaction depends upon whether the reaction is rate-limited or diffusion-limited, the latter case occurring when oxygen is unable to diffuse through nitrogen to the Zircaloy surface at a fast enough rate to sustain the kinetics of the reaction.

For a rate-limited reaction, the rate of oxidation is assumed to obey the parabolic rate law:

$$2\, w \frac{dw}{dt} = K_o \exp(-E_a/RT) \qquad (2)$$

where

w = weight gain (mg O_2 per cm^2)
t = time (seconds)
E_a = activation energy (cal)
R = gas constant = 1.987 cal/°K
T = temperature (°K)

As discussed elsewhere,[11] the assumption of parabolic kinetics for air oxidation of zirconium is an approximation, since it is known that the oxidation process is more complex than would be indicated by parabolic kinetics. For the times and temperatures encountered in this calculation, however, the assumption of parabolic kinetics has no visible effect on the accuracy of the results.

The amount of data available for oxidation of Zircaloy in air is not as substantial as that available for oxidation in steam. Hayes and Roberson[12] measured corrosion depths for pure zirconium in moist air for a wide range of temperatures, but their data contain considerable uncertainties in regard to the reported temperatures, since the techniques for measuring temperatures and maintaining isothermal conditions were not well refined at that time (1945). More recently (1967), White[13] obtained some fairly accurate data for the oxidation of pure zirconium in dry air, but the measurements were limited to high temperatures (above 1200°C). Probably the most reliable data for temperatures in the range of 900 to 1200 °C were reported by Leistikow[14] (1975), who exposed some Zircaloy-4 cladding tubes to an air environment for 5 to 10 minutes. The differences between Zircaloy-4 and pure zirconium are small enough, from a chemical point of view, to assume that their oxidation characteristics will be very similar.

The data of Hayes and Roberson, White, and Leistikow are shown in Fig. 6, together with the following suggested correlations:

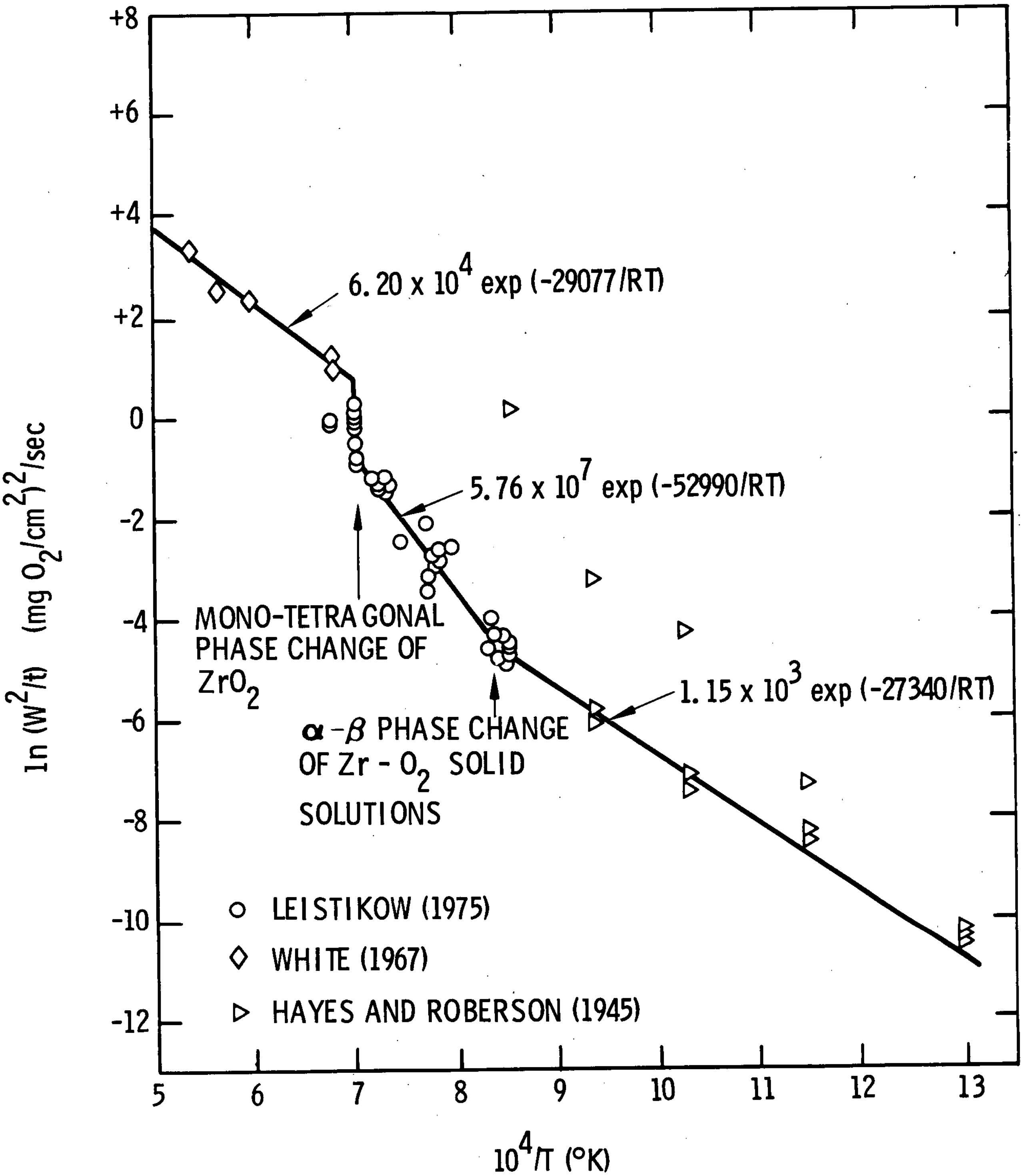

Figure 6. Reaction Rate Correlation For Air Oxidation of Zircaloy

$$K_o = 1.15 \times 10^3,\ E_a = 27340\ (T \leq 920°C)$$
$$K_o = 5.76 \times 10^7,\ E_a = 52990\ (920°C < T \leq 1155°C)$$
$$K_o = 6.20 \times 10^4,\ E_a = 29077\ (T > 1155°C)$$

The low-temperature correlation is identical to that proposed recently by Biederman et. al.[15] for Zircaloy oxidation in steam, and the fact that it agrees well with Leistikow's data at 900°C and is a lower bound to Hayes and Roberson's data below 900°C indicates a possible equivalence between steam oxidation and air oxidation at the lower temperatures. Above 900°C, air oxidation is clearly more efficient than steam oxidation, judging from the available data, and special correlations are required. At 1155°C, a change in the reaction rate is assumed to occur. While this discontinuity is primarily introduced to effect a matching of the data, there is some physical justification for such a discontinuity to occur based on the fact that the product of the reaction, namely ZrO_2, changes phase from monoclinic to tetragonal at about this temperature. Similarly, the slope discontinuity at 920°C may be rationalized in terms of the $\alpha \rightarrow \beta$ phase change of zirconium-oxygen solid solutions.

When the reaction is limited by the diffusion of oxygen to the reacting surface, a different model is required. It is assumed in this case that the heat and mass transfer analogy is appropriate, whereby the local Nusselt number for mass transfer is obtained from the local Nusselt number for heat transfer by substituting Schmidt number for Prandtl number. Thus

$$Nu_m = Nu_h\ (Re,\ Gr,\ Sc) \tag{3}$$

where Re is Reynolds number, Gr is Grashoff number, and Sc is Schmidt number, and

$$\frac{dw}{dt} = \frac{\rho_a\ \mathcal{D}_{on}\ Nu_m\ m_o}{x} \tag{4}$$

where ρ_a is the air density in the stream, $\mathcal{D}_{on}$ is the diffusion coefficient for oxygen in nitrogen, m_o is the mass fraction of oxygen in the steam, and x is the distance from the origin of the boundary layer (which is assumed to be the characteristic length in Nu_m). The reaction is diffusion-limited if dw/dt from Eqn. (2) is less than dw/dt from Eqn. (4). The correlation for Nusselt number is described in Appendix A.

When the reaction is rate-limited, the total amount of oxidation occurring as a result of heatup after the pool drainage will depend somewhat upon the initial oxide thickness. According to A. B. Johnson, Jr., of Battelle Pacific Northwest Laboratories (private communication, June 1977), the average uniform thickness of monoclinic ZrO_2 existing on spent fuel after reactor discharge is about 15-20 microns for PWR fuel and about 10 microns for BWR fuel, but the latter is much more variable than the former, having maximum local thicknesses as much as 100 microns. The initial oxide thickness was found to be a parameter of secondary importance in the heatup calculations, and a conservative value of 1.5 microns was used for most cases.

3.3 Heat Transfer Within Spent Fuel Pool

The heat removal problem for the drained spent fuel pool is considered in two parts: (1) the heat transfer problem within the confines of the pool, and (2) the removal of heat from the containment building. Section 3.3 discusses the first of these two heat transfer problems and Section 3.4 considers the second. Mathematical details of both problems are presented in Appendix A.

Schematics of the heat transfer problem for the spent fuel pool are shown in Figs. 7 through 9. Heat produced by decay within the spent fuel elements and by chemical oxidation of the clad is removed, in part, by buoyancy-driven air flows

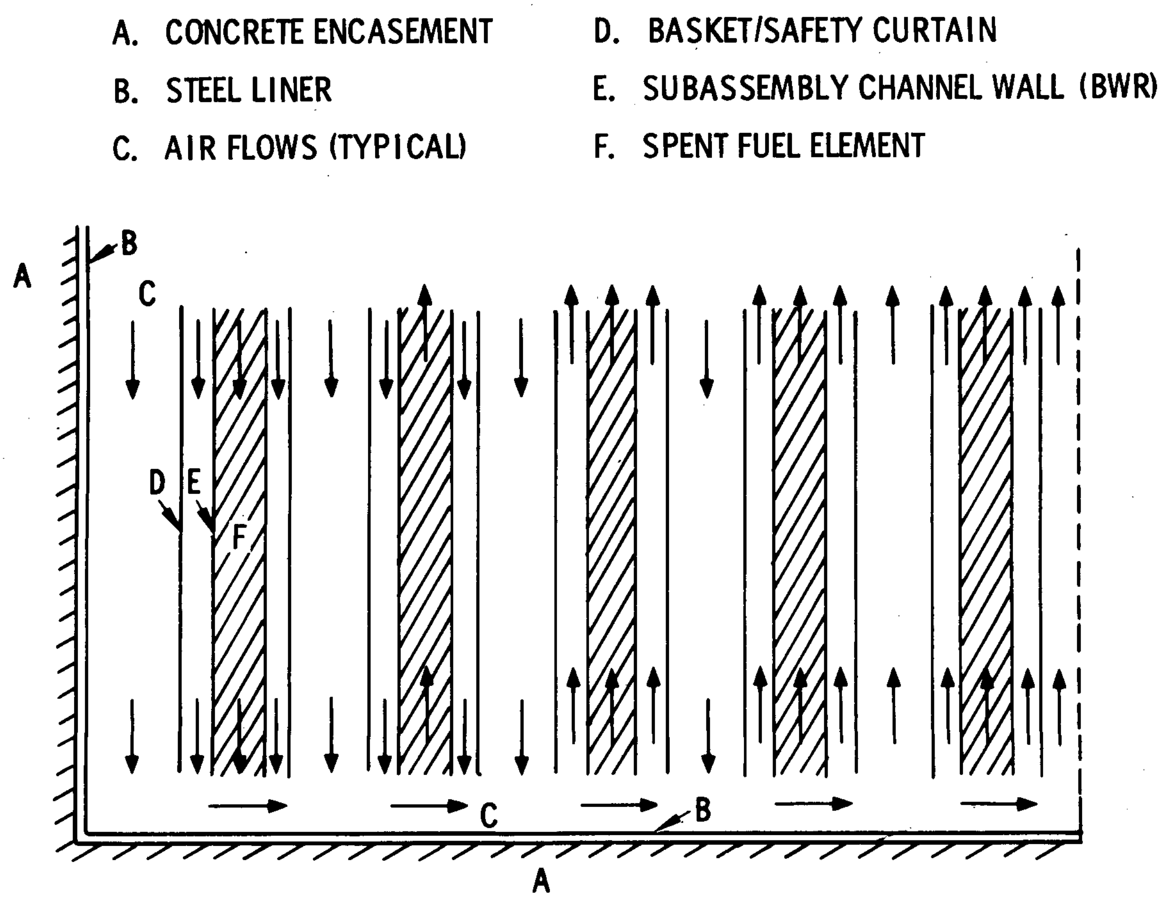

Figure 7. Schematic of Spent Fuel Storage Configuration and Natural Convection Flows Following a Complete Drainage

circulating in well-defined channels (Fig. 7). Transport of mass, momentum, and energy for the air flows is calculated within the code SFUEL through an iterative, finite-difference solution of the appropriate conservation equations, averaged over the cross-sections. Transient conduction equations are solved in the axial direction to determine the heatup of the fuel rods as a function of time and vertical location. Radiation between structural elements (i.e., fuel rods, subassembly channel walls if present, tie plates, holders or baskets, and pool liners) is accounted for, as is transient conduction into the concrete encasement (Figs. 8, 9).

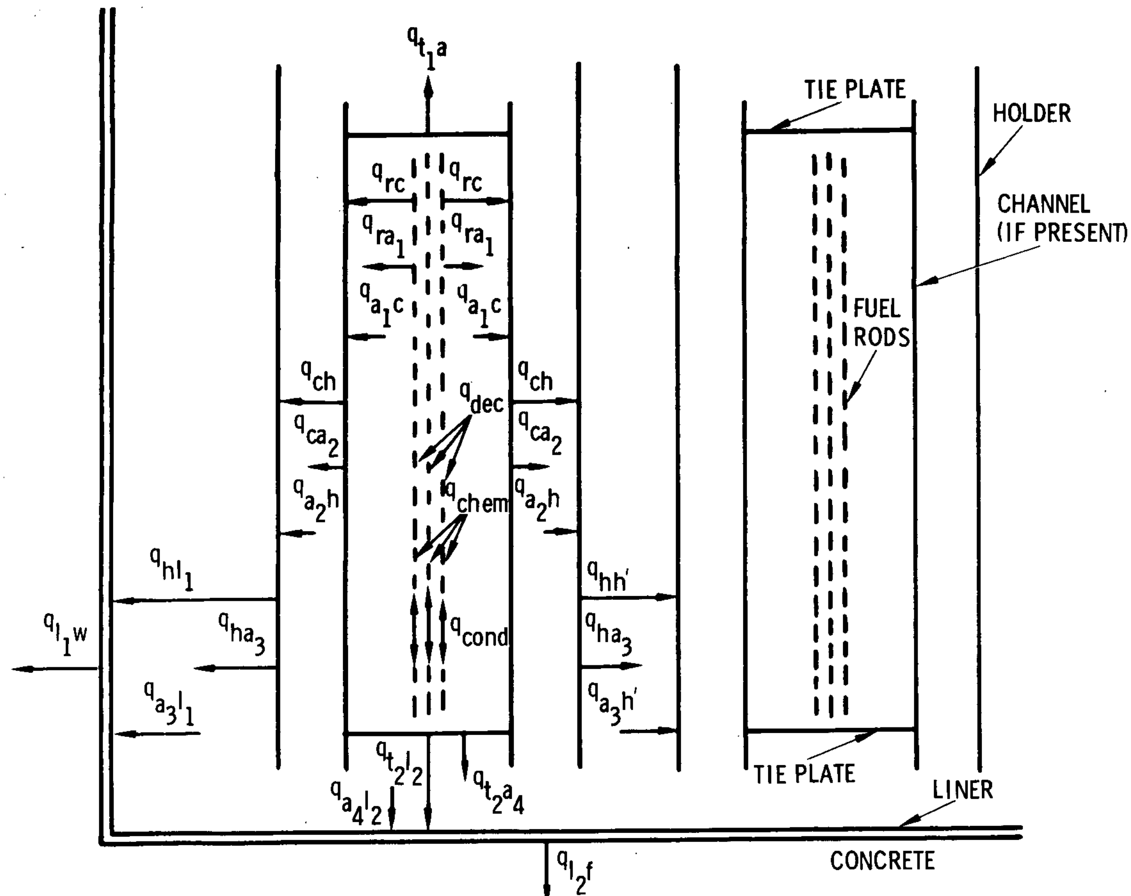

q_{dec} = DECAY HEAT INPUT TO FUEL RODS

q_{chem} = CHEMICAL OXIDATION HEAT INPUT TO FUEL RODS

q_{cond} = AXIAL CONDUCTION IN FUEL RODS

q_{rc} = RADIATION FROM RODS TO CHANNEL WALL

q_{ra_1} = CONVECTION FROM RODS TO AIR STREAM 1

q_{a_1c} = CONVECTION FROM AIR STREAM 1 TO CHANNEL WALL

q_{ch} = RADIATION FROM CHANNEL WALL TO HOLDER

q_{ca_2} = CONVECTION FROM CHANNEL WALL TO AIR STREAM 2

q_{a_2h} = CONVECTION FROM AIR STREAM 2 TO HOLDER

$q_{hh'}$ = RADIATION FROM HOLDER TO ADJACENT HOLDER

q_{ha_3} = CONVECTION FROM HOLDER TO AIR STREAM 3

$q_{a_3h'}$ = CONVECTION FROM AIR STREAM 3 TO ADJACENT HOLDER

q_{hl_1} = RADIATION FROM OUTERMOST HOLDER TO SIDEWALL LINER

$q_{a_3l_1}$ = CONVECTION FROM AIR STREAM 3 TO SIDEWALL LINER

q_{l_1w} = CONDUCTION INTO CONCRETE SIDEWALL

q_{t_1a} = RADIATION FROM UPPER TIE PLATE

$q_{t_2l_2}$ = RADIATION FROM LOWER TIE PLATE TO FLOOR LINER

$q_{t_2a_4}$ = CONVECTION FROM LOWER TIE PLATE TO AIR STREAM 4

$q_{a_4l_2}$ = CONVECTION FROM AIR STREAM 4 TO FLOOR LINER

q_{l_2f} = CONDUCTION INTO CONCRETE FLOOR

Figure 8. Identification of Heat Transfer Modes Considered in the Pool Region

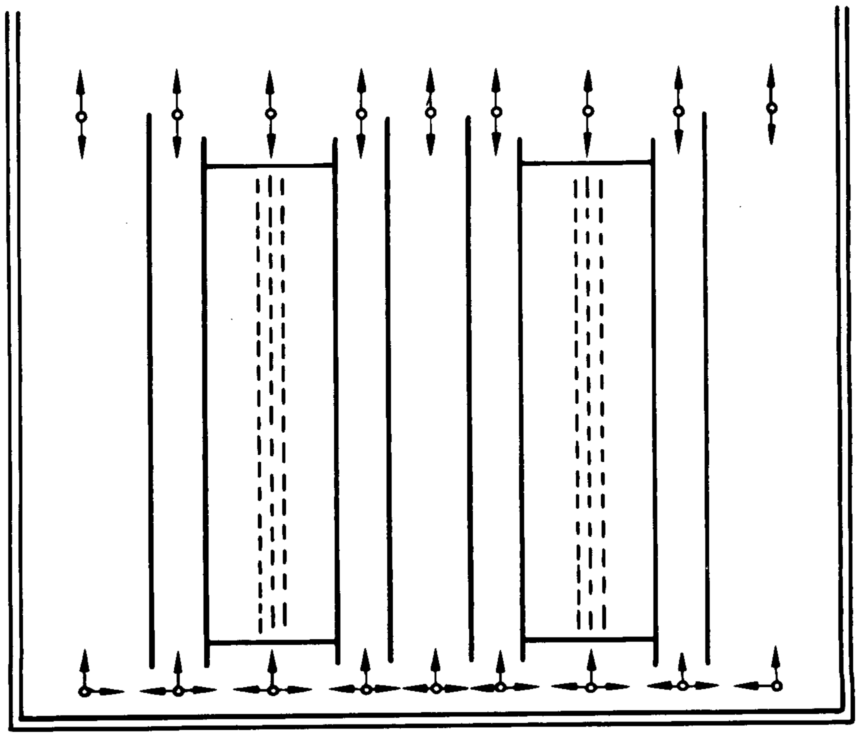

ITEMS	SYMBOLS	SOLUTION PROCEDURE, EACH TIME STEP
FLOW PATHS		SOLVE EQUATIONS OF MOMENTUM AND ENERGY CONSERVATION, ONE DIMENSION, TO DETERMINE AIR TEMPERATURE AND VELOCITY AS A FUNCTION OF POSITION.
JUNCTIONS		ITERATE UNTIL (1) MASS OUTFLOW EQUALS MASS INFLOW, (2) PRESSURES ON ALL SIDES OF JUNCTION ARE EQUAL, (3) ENTHALPY OUTFLOW EQUALS ENTHALPY INFLOW.
FUEL RODS		SOLVE TRANSIENT 1-D CONDUCTION EQUATION, INCLUDING INTERNAL HEAT GENERATION, TO DETERMINE FUEL ROD TEMPERATURE AS A FUNCTION OF POSITION.
STRUCTURAL ELEMENTS		APPLY TRANSIENT HEAT BALANCE EQUATION TO DETERMINE STRUCTURE TEMPERATURE AS A FUNCTION OF POSITION.
CONTAINMENT ATMOSPHERE	(NOT SHOWN)	APPLY HEAT AND MASS BALANCES TO DETERMINE BULK TEMPERATURE OF ROOM AIR.

Figure 9. Identification of Solution Procedures Used in Spent Fuel Heatup Problem

The primary assumptions embodied in the pool analysis are as follows:

(1) The water drains instantaneously, leaving the pool completely devoid of water.

(2) The geometry of the fuel assemblies and racks remains undistorted.

(3) Decay heat emanates from the fuel rods only, and not from the surrounding structure.

(4) Temperature variations across the fuel rods are neglected, and all rods in a particular assembly have the same vertical temperature distribution.

(5) The air flow patterns are locally one-dimensional and always occur in a vertical or horizontal direction, as shown in Fig. 7.

(6) Radiation view factors are based on projected areas. All radiating surfaces are gray bodies.

(7) The spent fuel placement is two dimensional and such as to have the hottest elements in the middle of the pool and the cooler elements progressively toward the ends of the pool (see Table V).

(8) Heat conduction is negligible for channel walls, holder walls, and liners. Conduction in the vertical direction is considered for fuel rods only.

(9) The spaces between adjacent basket walls are assumed to be closed to air flow (a special case of Figs. 7-9), except where specifically noted otherwise. The downcomer next to the edge of the pool and the base region beneath the racks are assumed to be open to air flow.

The implications of these assumptions are as follows: First, the assumption that the pool drains completely is not necessarily the most conservative assumption that can be made regarding the course of the accident. If the water ceased to drain when it reached the level of the baseplates or slightly below, and if all the flow inlets to the fuel elements were at or near the baseplate, as they are in many of the more recent storage rack designs, then the residual water could constrict the flow of air beneath the baseplate and essentially block the inflow to the elements. At the same time, possible heat transfer advantages to be gained by converting decay heat to boiling energy would be minimal, since the residual water level would be far removed from the location of maximum heatup. The question of incomplete drainage is discussed in Section 5.1.

The assumption that the pool drains instantaneously is somewhat conservative in that it disregards the fact that steam produced by boiling will enhance the natural convection owing to its high heat capacity.

The assumption that temperature variations are negligible in the horizontal direction across any fuel assembly has been found to be quite adequate, in view of the equalizing effect of thermal radiation from one fuel rod to another and the fact that the heatup time is on the order of hours. Variations in temperature from rod to rod in an assembly might occur as a result of variations in decay heat or differences in the thickness of the oxide coating, but these factors are difficult to predict and have not been accounted for.

The assumed air flow patterns, shown in Fig. 7, and the assumed spent fuel placement, shown in Table V, represent somewhat approximate attempts to account for a complex situation. It is felt, however, that the omission of the third dimension and the placement of the hottest fuel elements in the middle of the pool are fair approximations to what might be a worst case. It has been found, moreover, that the spent fuel heatup is more affected by the total decay heat production in the pool and by the availability of open spaces for air flows than by the precise placement of the spent fuel.

One of the larger uncertainties in the overall analysis relates to the storage rack or holder design, which has been found to be difficult to characterize for lack of detailed information and the variability from one facility to another. The assumption that certain flow paths are closed (Assumption (9) above) is postulated as a somewhat conservative approximation to the fact that the airflow is often retarded in the inter-holder spaces by structural obstructions such as those shown in Fig. 2. However, the amount of improvement to be gained by opening all the available flow paths has also been studied (Section 4.1). The philosophy has been to consider a fairly wide variation of design parameters so that the results will span at least a majority of the configurations currently in use.

The open frame configuration, Fig. 2a, has been treated specially because of the lack of defined channels for air flow. Appendix A, which provides mathematical details for the cases involving well-defined channels, also discusses the more approximate modeling techniques used for the open frame rack design.

3.4 Heat Removal From Containment Building

Removal of heat from the containment building under normal operation is accomplished by a forced ventilation system. For at-reactor spent fuel pools, ANS Standard 57.2 (dated 1976) requires a minimum of two complete air changes per hour. Under the accident conditions produced by a pool drainage, however, this amount of ventilation will generally not be sufficient to remove all the decay heat imparted to the room atmosphere by the exposed spent fuel rods (see Section 4.2). If the building is closed, therefore, it is possible for the room air to heat up significantly and to affect the natural convection process in the drained pool through a decay heat feedback process. On the other hand, it would be possible for the building designer to counteract this effect by utilizing the pressure buildup inside the building to open doors at ground level and in the ceiling, so as to provide a so-called "chimney effect".

Two situations have been considered. In the first case, it is assumed that ventilation provided through a powerful forced air system or through a chimney effect is sufficient to keep the room air at ambient conditions (i.e., equal to the outside air conditions). In the second case, it is assumed that no chimney effect exists and that aside from a prescribed forced ventilation rate, the direction of leakage is always from the inside of the building to the outside. The following discussion will pertain to the latter case, where the removal of heat from the containment building becomes an important issue.

To account for the containment building, the SFUEL code computes the amount of heat that is removed by a combination of forced ventilation, leakage of air through the building structure, heat storage by the structural heat sinks, and radiation/natural convection from the building exterior to the outside (see Fig. 10). Because of the large uncertainties in characterizing the nature of the building and the quantity of heat sinks, this portion of the model is necessarily approximate in nature. The following assumptions are utilized:

(1) The building is considered to be constructed of sheet metal having the properties of steel with an emissivity of 0.7. The heat capacity of all the heat sinks in the building are approximated by providing a 1/8-inch sheet metal wall and ceiling thickness.

(2) The building is assumed to be capable of withstanding an internal gage pressure of 2.0 psi before any leaking occurs, and then is assumed to leak at the rate required in order to keep the pressure from

exceeding 2.0 psi. All leakage is assumed to occur from the inside to the outside.

(3) The ventilation system is assumed to operate with a fixed volume rate of flow whose value is unaffected by internal temperature and pressure.

(4) The room air is considered to be well mixed (i.e., isothermal, isobaric, and homogeneous).

Mathematical details of the containment building portion of the model are included in Appendix A.

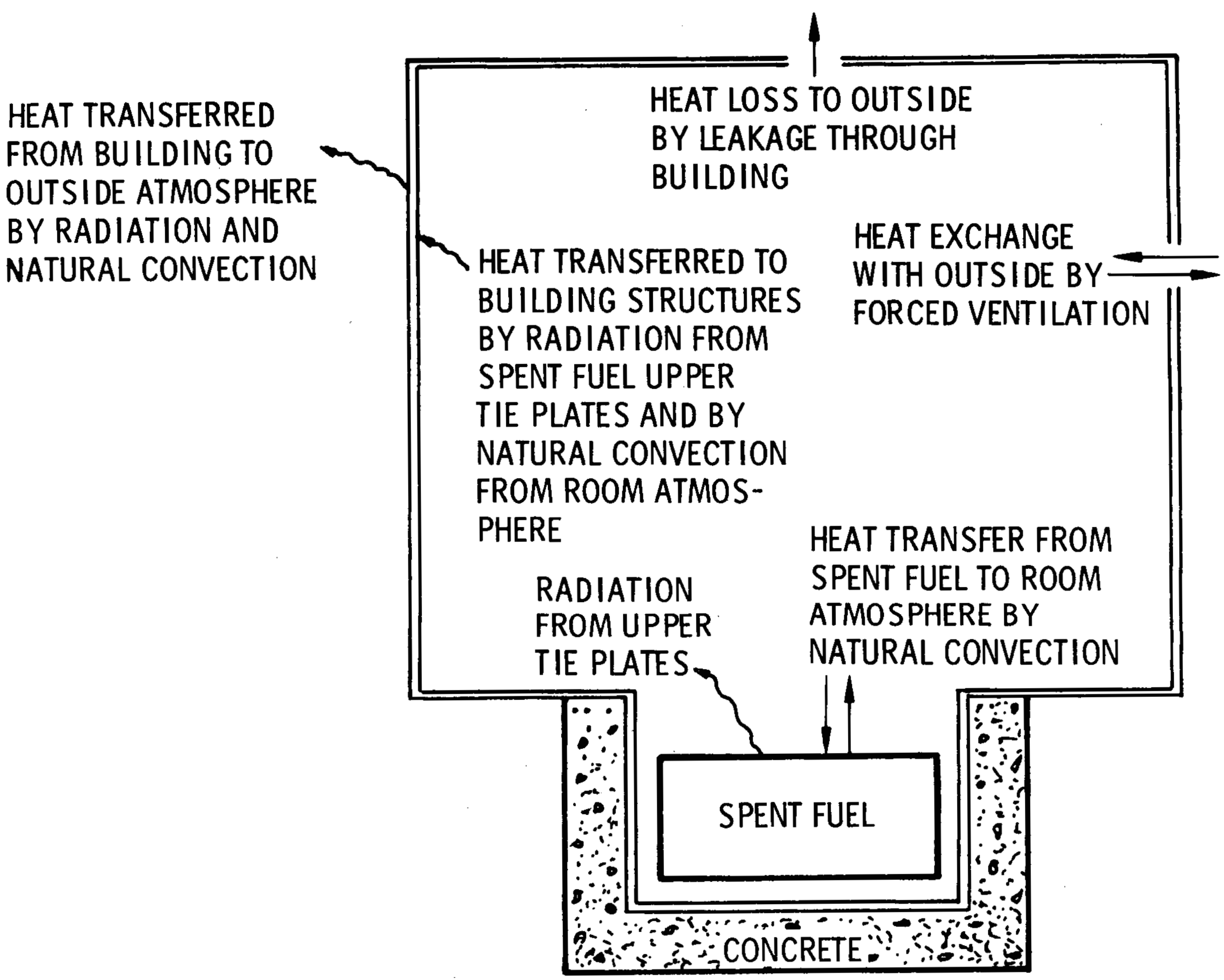

Figure 10. Heat Transfer Modes for the Containment Building and Outside Atmosphere

4. RESULTS

4.1 Perfect Ventilation

The results presented in this section correspond to the case where the air in the containment building is kept at ambient conditions, through the use of a high-powered ventilation system or a containment building design feature that produces a chimney effect. Section 4.2 treats the case of imperfect ventilation where some of the decay heat released to the air is recycled back into the spent fuel pool.

Because of the fact that the loading of spent fuel into the storage pool is not uniform, with fuel of varying ages and, hence, varying decay powers being present at the same time, the distribution of temperatures throughout the pool is also non-uniform. Figure 11 shows the clad temperature variation with distance along the fuel rod at six different locations in the pool for a typical case, 5 hours after the drainage. The figure also lists the velocities of the upward air flows through the fuel elements for each location in the pool, and shows the air flow temperature as a function of distance up the fuel rods for the hottest location. The particular case considered corresponds to a full core discharge (Table V Part A), 10 days after reactor shutdown.

As shown in Figure 11, the location of highest temperature does not generally correspond to the location of highest heat production. Whereas the maximum assumed decay heat is produced at the midpoint of the fuel rods (z/L = 0.5), the location of highest temperature moves with time from the midpoint toward the upper end of the fuel rods. The reason for this phenomenon

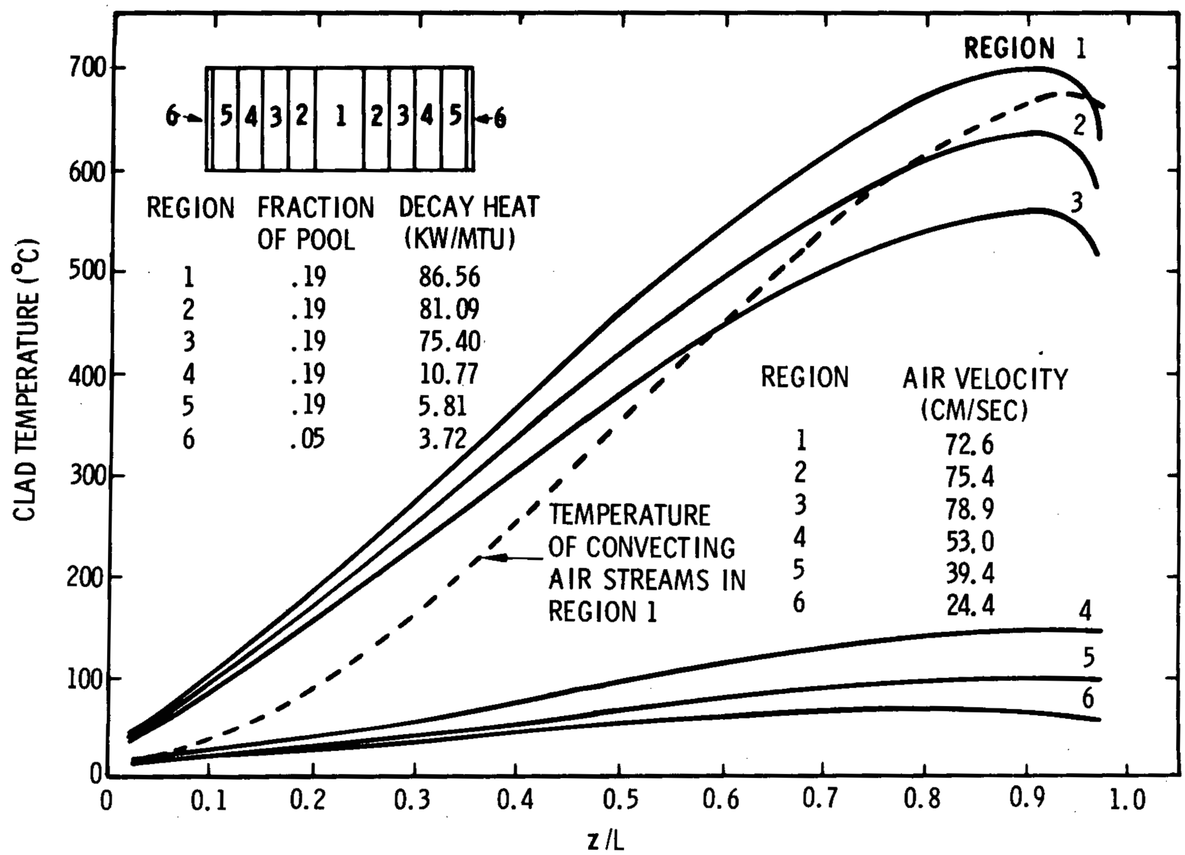

Figure 11. Typical Variation of Clad Temperature With Normalized Distance, Measured from Lowest End of Fuel Rod

is explainable by the dashed curve in Figure 11, which shows that the temperature of the air increases as it streams from the bottom to the top of the fuel element, owing to absorption of heat from the fuel rods. Since the air stream becomes hotter at the upper end of the fuel rods, the fuel rods must also become hotter. (Parenthetically, this heatup of air in the flow channels is responsible for the fact that the temperature achieved by the fuel rods in a drained spent fuel pool is much higher than the temperature that would be achieved by an isolated fuel rod in an open air environment.)

A sampling of heatup results of PWR spent fuel in cylindrical holders (Figure 2b) is presented in Figure 12. Here the peak clad temperature (i.e., the maximum clad temperature in the pool at a given time) is plotted as a function of the time after pool drainage for various baseplate hole sizes that are typical of operational practice (see Section 2.2). The calculations in this figure correspond to a loading pattern applicable to a full core discharge, 1 year after shutdown of the reactor, with a maximum burnup of 33,000 MWD/MTU (see Table V Part A). It may be noted that the results presented here and throughout the rest of Section 4.1 are more-or-less independent of pool size if the same fuel loading proportions are maintained, and that this independence results from the fact that the room is considered to be perfectly ventilated.

It may be seen from Figure 12 that the baseplate hole size can exert a marked effect on the heatup of the spent fuel, since a small baseplate hole tends to constrict the flow at the inlet to the fuel assembly. It may also be observed from Figure 12 that if the temperature of self-sustaining clad oxidation is not attained, the peak clad temperature tends to reach a steady-state maximum value that remains essentially invariant with time. If a sufficiently high temperature is achieved, however, the clad oxidation reaction can become self-sustaining, leading to a temperature divergence that results in local clad melting. The temperature at which clad oxidation becomes self-sustaining is a function of the storage configuration, but tends to occur around 900°C.

Before continuing on to other types of storage racks, it is interesting to observe the partitioning of heat that occurs in cases where a steady-state temperature distribution is obtained. As shown in Figure 13, most of the heat produced by radioactive decay is eventually removed by natural convection, with a much smaller portion being removed by radiation from

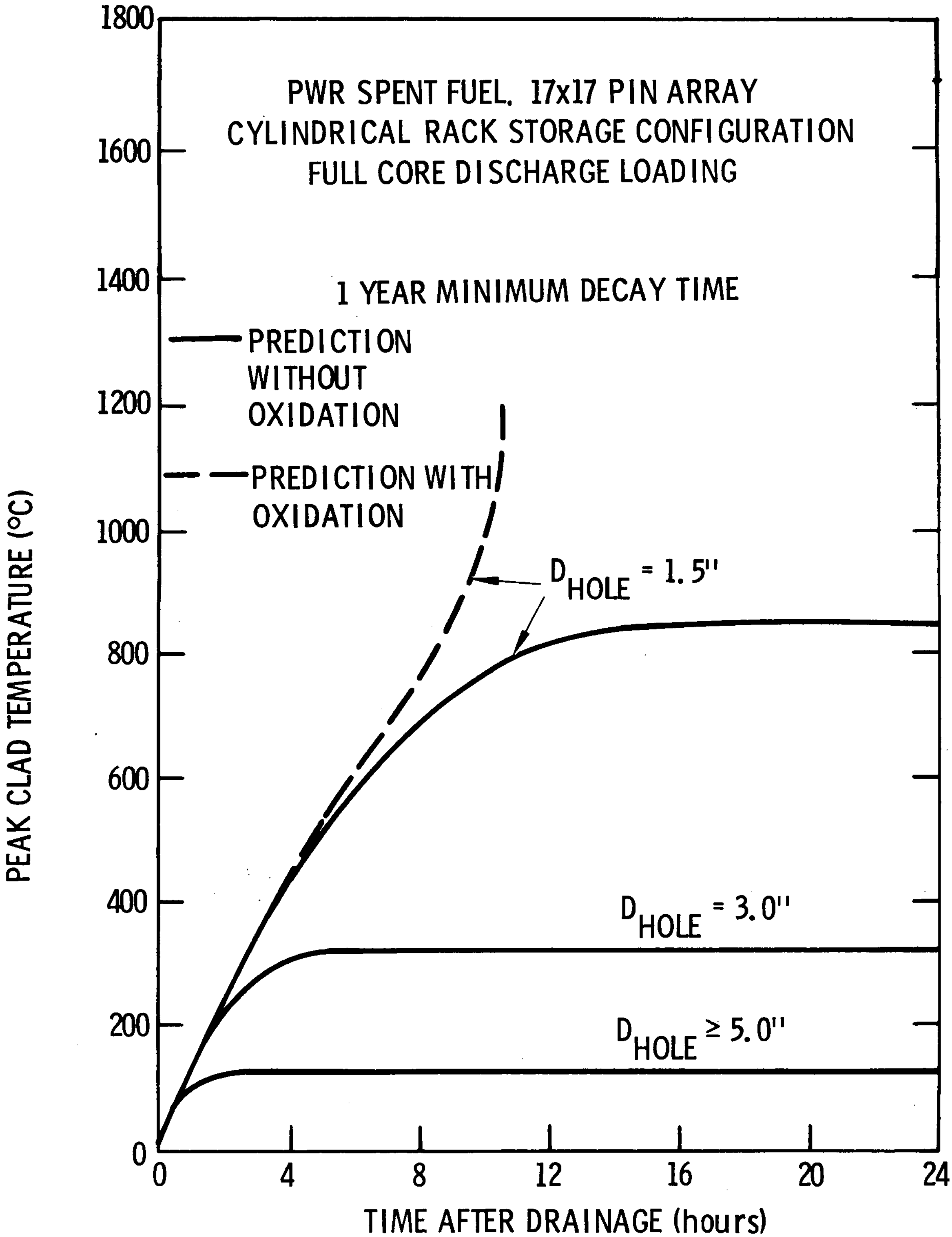

Figure 12. Effect of Baseplate Hole Size on Heatup of PWR Spent Fuel, Well-Ventilated Room

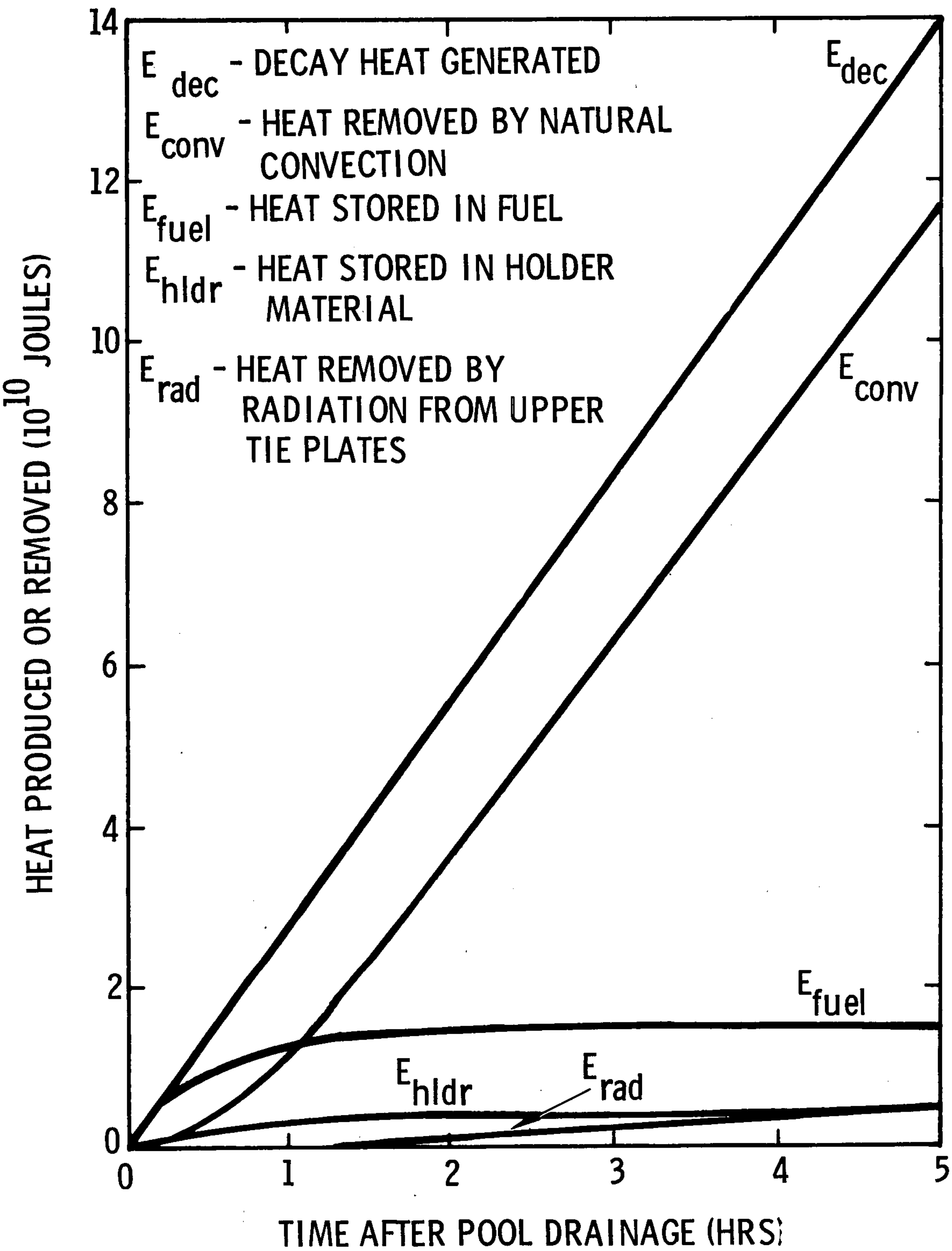

Figure 13. Typical Partitioning of Heat for a Drained Spent Fuel Pool in a Perfectly Ventilated Room

the upper tie-plates. The remainder of the energy is primarily accounted for by the temperature rise of the materials in the pool, with approximately 80 percent of that energy going to the fuel rods (including the fuel itself and the clad) and the other 20 percent going to the steel holders. The energy absorbed by the concrete encasement and the steel liners is negligible. Although Figure 13 applies to a particular case (viz., the case considered in Figure 11), the observations made above are applicable to a majority of the cases considered.

Although the clad heatup is not excessive for the cylindrical baskets as long as the baseplate holes are sufficiently large, a somewhat different situation may exist for other types of PWR storage rack configurations. As shown in Figure 14, the cylindrical holders rank second in heat removal effectiveness to the open frame construction, it being recognized that the computations for the open frame configuration are quite approximate due to the nature of the modeling assumptions. The "square" baskets of Figure 2c are somewhat less efficient than the cylindrical baskets, despite the larger center-to-center spacing, because of the smaller flow area within the baskets. The high density holders of Figure 2d are the least well-suited to heat removal, as expected, particularly if the spent fuel is packed wall-to-wall so as to preclude a downcomer space at the edge of the pool. The high density configuration is believed to be the only one where wall-to-wall storage is currently possible.

The effect of decay time on the clad heatup is illustrated in Figure 15, for the cylindrical holders with large baseplate holes, where it may be seen that the temperature rise is reduced by a factor of six in going from a minimum decay time of 10 days to 1 year. The term "minimum decay time" refers to the time since power shutdown for the most recently discharged fuel elements (i.e., the hottest elements in the pool). Also

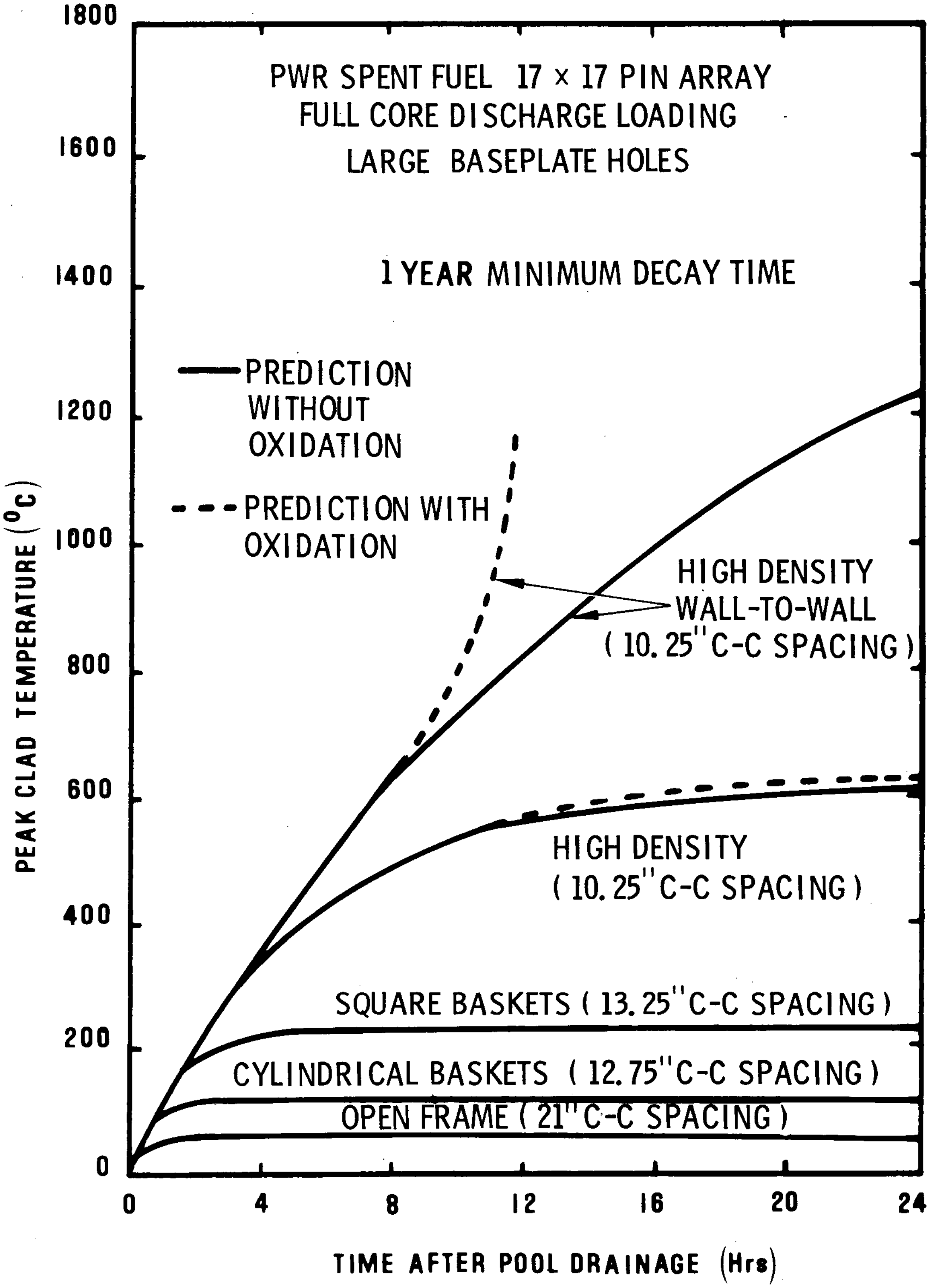

Figure 14. Effect of Storage Rack Configuration on Heatup of PWR Spent Fuel, Well-Ventilated Room

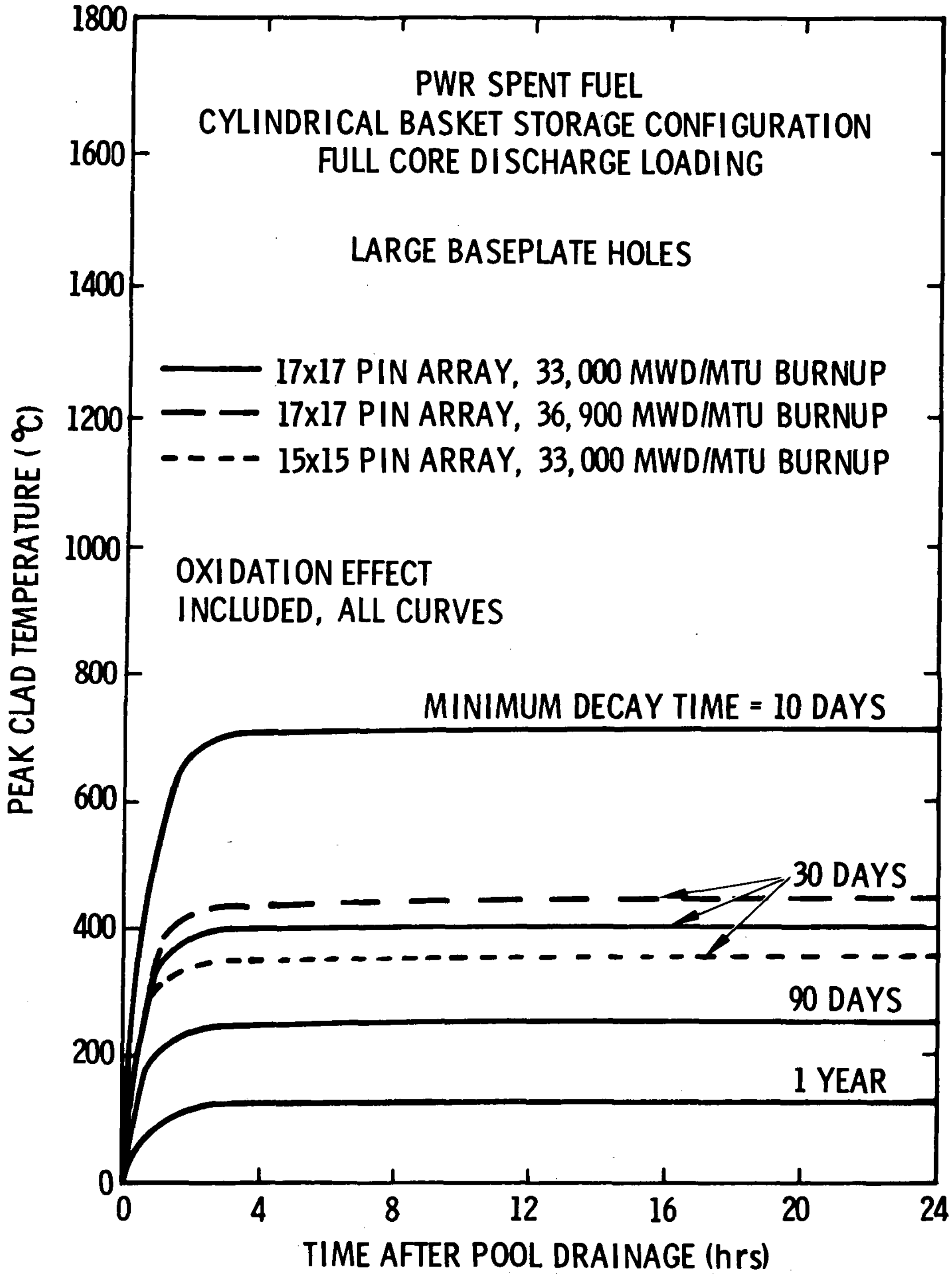

Figure 15. Effect of Minimum Decay Time, Burnup, and Sub-Assembly Type on Heatup of PWR Spent Fuel, Well-Ventilated Room

shown in Figure 15 is the effect of a higher burnup (36,900 MWD/MTU) on the clad heatup and the difference between the newer PWR fuel assemblies (17 x 17 pin array) and the older assemblies (15 x 15 array).

It has been assumed in the preceding discussions that the pool is loaded according to a full core discharge scenario and that the control rods have not been removed. While the calculations for the open frame, cylindrical, and square configurations are not very sensitive to these assumptions, it is possible to observe rather significant differences in the response with the high density configuration if these assumptions are changed. As shown in Figure 16, a 33 percent drop in the temperature rise can be achieved by simply removing the control rods (high density configuration only). It may also be observed that while there is little difference between the full core discharge loading pattern (Table V, Part A) where the decay times vary from 1 to 4 years, and the normal discharge loading pattern (Table V, Part B) where the decay times vary from 1 to 6 years, a significantly worse heatup problem would occur if the fuel were loaded according to the "worst case" loading pattern (Table V, Part C), where all the fuel elements are assumed to have the same decay time of 1 year.

A summary of results for PWR spent fuel in a drained storage pool is presented in Figure 17, which depicts the minimum allowable decay times for a variety of cases. The variables plotted here are the <u>maximum</u> peak clad temperature (i.e., the highest clad temperature attained at any point in the pool for all time) and the decay time of the most recently discharged elements. The critical, or minimum, allowable decay time for each case corresponds to the point at which the curve becomes vertical. All cases correspond to a full core discharge loading pattern with a 33,000 MWD/MTU maximum burnup

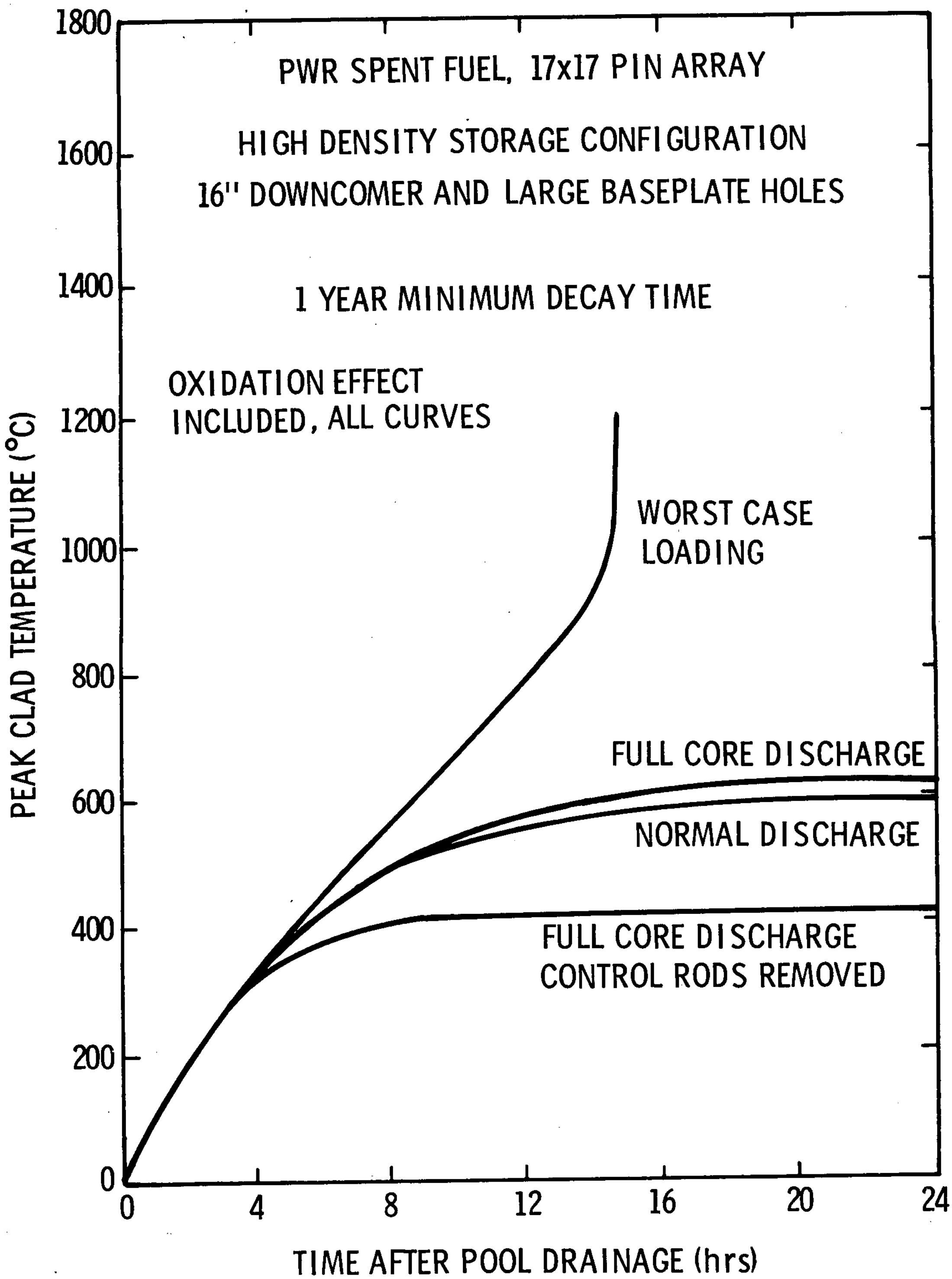

Figure 16. Effect of Fuel Loading and Control Rod Removal on Heatup of PWR Spent Fuel in High Density Configuration, Well-Ventilated Room

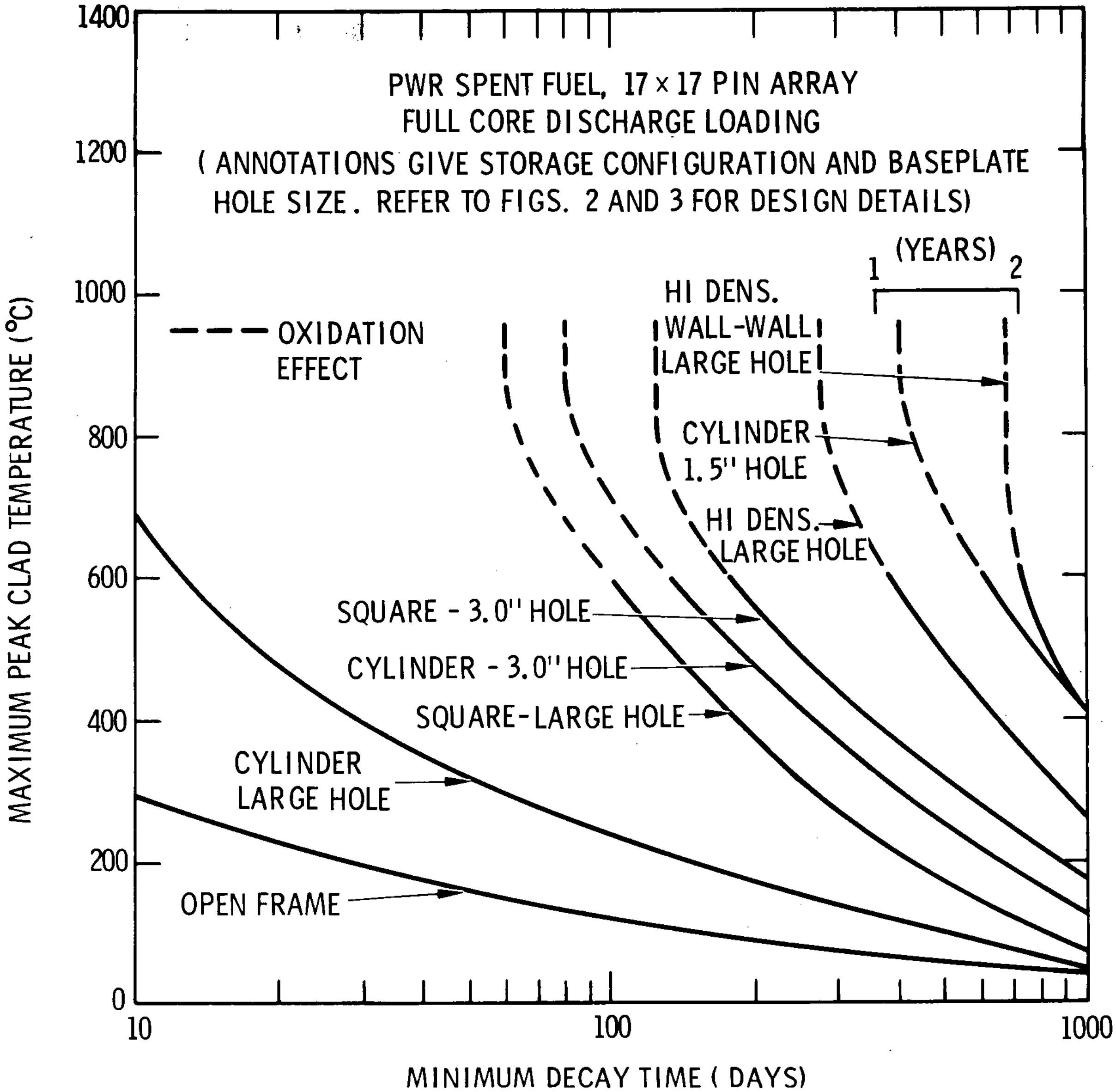

Figure 17. Summary of Heatup Results for PWR Spent Fuel, Well-Ventilated Room

and with control rods intact. As shown in Figure 17, the variation is critical decay times over the cases considered is extremely large, ranging from well under 10 days for the open frame configuration to nearly 2 years for the high density configuration with wall-to-wall placement. These results should be considered in context with the fact that according to current practice, decay times as short as 30 days in reactor-sited pools and 1 year in away-from-reactor pools are possible.

Similar results have been obtained for BWR spent fuel assemblies, and these are shown in Figures 18 through 20. By comparing Figures 12 and 18, it may be seen that the clad heat-up for BWR spent fuel tends to be significantly lower than for PWR spent fuel, primarily owing to the lower heat output per unit storage area. However, there can be considerable variations in the heatup response depending upon whether or not the BWR channels are removed, and depending upon the specific storage configuration used (Figure 19). The critical, or minimum allowable decay times computed for BWR spent fuel vary from under 10 days to about 150 days for the various cases considered (Figure 20). There is little difference in results between the older 7 x 7 pin array and the newer 8 x 8 pin array.

Before leaving the subject of spent fuel heatup under well-ventilated conditions, it is worth considering the amount of improvement that could be gained by making reasonable design changes in the existing storage rack configurations, while maintaining the original packing density. It has been noted that enlarging the baseplate holes and providing a downcomer space at the edge of the pool are both important considerations. In addition, a considerable improvement in the heat removal capability can often be effected by removing obstructions to flow <u>between</u> the baskets (i.e., those regions that were depicted in Figure 7 as being open to vertical air flows but that were treated as closed for purposes of the analysis). These paths are currently blocked by the presence of the baseplates, top plates, and other members that are used for structural support or spacing.

The amount of improvement that can be obtained by the modifications suggested here has been computed, and the

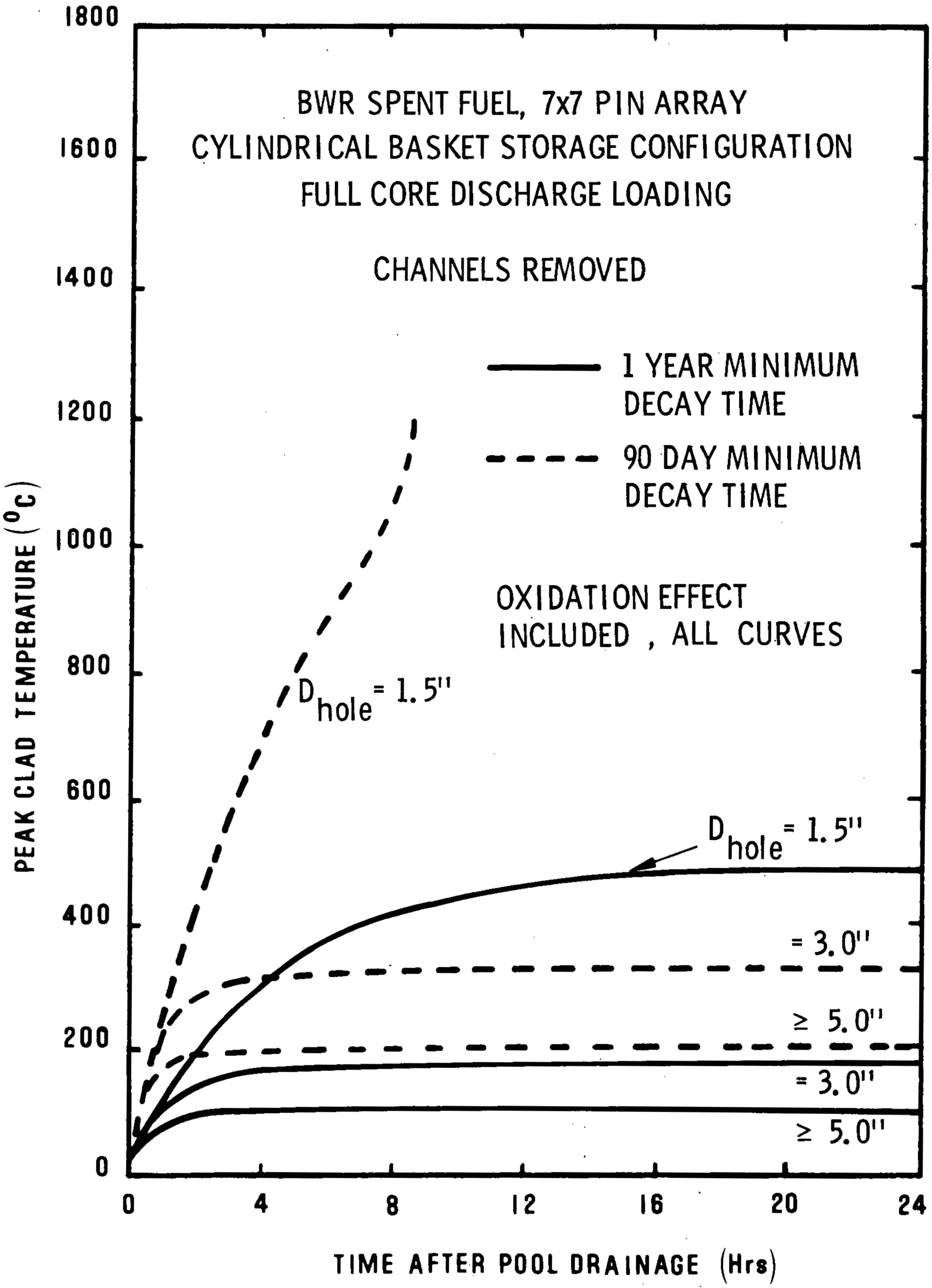

Figure 18. Effect of Baseplate Hole Size and Minimum Decay Time on Heatup of BWR Spent Fuel, Well-Ventilated Room

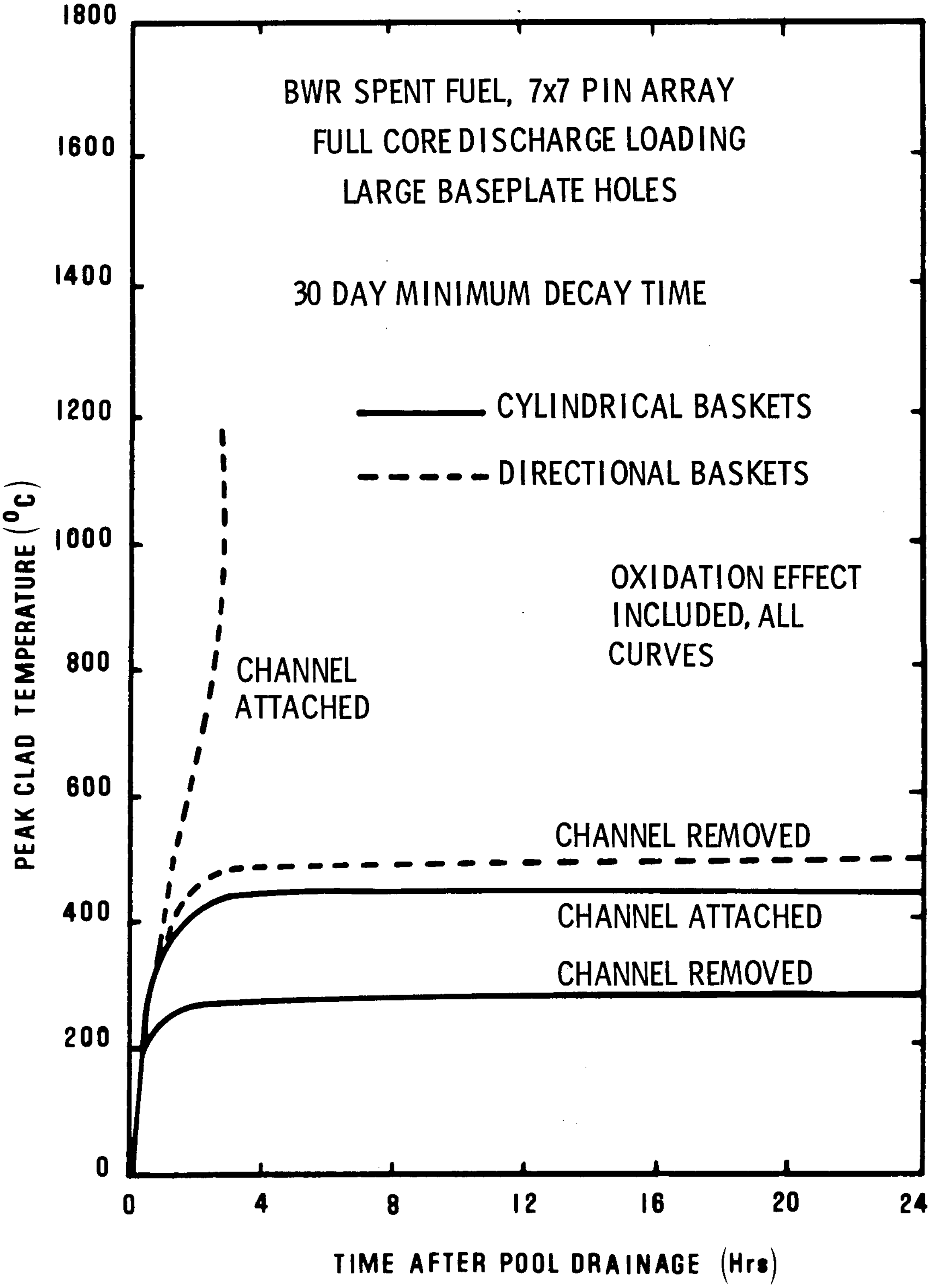

Figure 19. Effect of Storage Configuration on Heatup of BWR Spent Fuel, Well-Ventilated Room

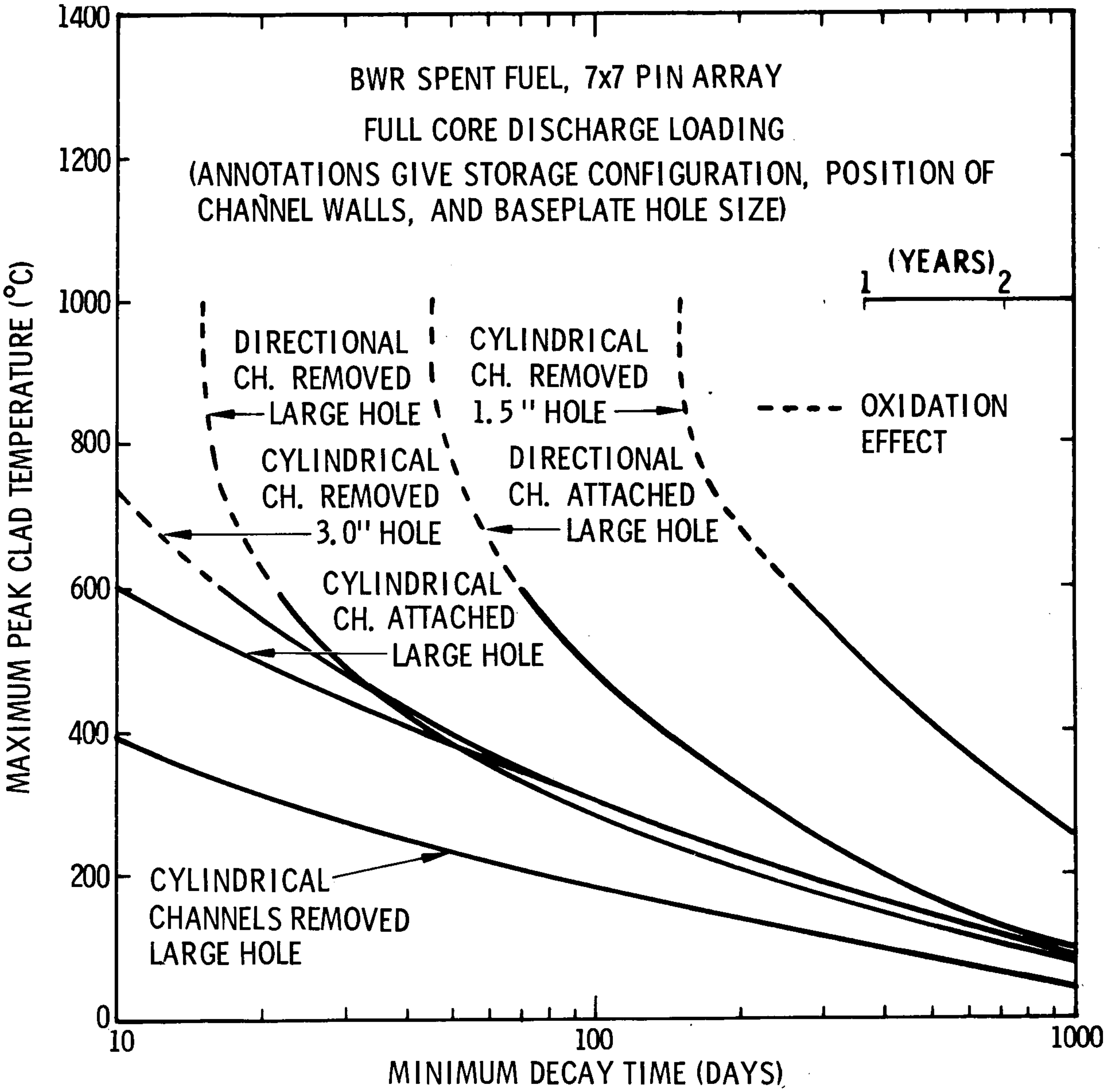

Figure 20. Summary of Heatup Results for BWR Spent Fuel, Well-Ventilated Room

results are summarized in Table VI. Observe that the reduction in the critical decay time is quite substantial in those cases that might be termed problem areas. According to the calculations, it should be possible, by making these modifications, to achieve allowable decay times as low as 80 days for the high density configuration and at least as low as 20 days for the other configurations.

TABLE VI

Reductions in Critical Decay Time Achievable by Modification of Storage Rack Design, Well-Ventilated Room

CASE	TYPE OF FUEL	STORAGE RACK DESCRIPTION	CRITICAL DECAY TIME (DAYS)	POSTULATED DESIGN MODIFICATIONS	NEW CRITICAL DECAY TIME (DAYS)
1	PWR	Open Lattice 21" C-C Spacing	<5	None	<5
2	PWR	Cylindrical Baskets 12.75" C-C Spacing 1.5" Baseplate Hole	400	Enlarge baseplate hole	8
3	PWR	Square Baskets 13.25" C-C Spacing 3.0" Baseplate Hole	130	Enlarge baseplate hole Promote flow outside baskets	20
4	PWR	High Density Baskets 10.25" C-C Spacing 5.0" Baseplate Hole	280* 700*	Leave 1.0 ft. to edge of pool Promote flow outside baskets	80
5	BWR	Cylindrical Baskets 8.5" C-C Spacing 3.63" Baseplate Hole	<5	None	<5
6	BWR	Cylindrical Baskets 8.5" C-C Spacing 1.5" Baseplate Hole	150	Enlarge baseplate hole	<5
7	BWR	Directional Baskets 11.5" C-C Across Rows 6.0" C-C Along Rows Channels Attached	45	Remove channels	15

*Higher figure represents full utilization (wall-to-wall storage arrangement). Lower figure corresponds to 1.0-foot downcomer space at edge of pool.

4.2 Imperfect Ventilation

Maintaining adequate ventilation in the event of a complete pool drainage requires either a powerful forced air ventilation system or a building design that promotes natural ventilation from the outside, such as from a chimney effect. Through an approximate analysis presented in Appendix B, estimates for the requirements of a forced ventilation system and/or a chimney design have been made, and the results are presented below.

Consider first the requirements of a forced air ventilation system. The analysis in the appendix shows that in order for the air temperature in the room to be kept below a specified value, T_r, the venting rate must satisfy the following inequality:

$$\dot{V}_{vent} \geq \frac{T_o}{T_r - T_o} \frac{RQ_{decay}}{p_o c_p} \tag{5}$$

where

$\dot{V}_{vent}$ = volume rate of exchange of air
R = gas constant
Q_{decay} = total decay heat produced in pool
p_o = outside (atmospheric) pressure
T_o = outside (atmospheric) temperature
c_p = specific heat of air

Table VII indicates the venting rates and air change rates (room air changes per hour) which would be required to keep the room temperature rise below 150°C, a reasonable value, for each of the following three cases:

(1) a PWR reactor-sited storage pool
(2) a BWR reactor-sited storage pool
(3) an away-from-reactor storage pool.

Table VII.

Estimates of Forced Air Ventilation Rates or Door/Chimney Hole Sizes Required to Keep Room Temperature Rise Below 150°C.

Case	1	2	3
Situation	PWR reactor-sited pool in auxiliary building, 2 core capacity filled after a full core discharge	BWR reactor-sited pool in reactor containment building, 2 core capacity filled after a full core discharge	Away-from-reactor storage pool, 750 MTU capacity filled with PWR spent fuel according to full core discharge loading pattern.
Postulated Room Dimensions: Length x Width x Height (Feet)	40 x 30 x 30	150 x 150 x 80	100 x 50 x 30
Minimum Decay Time (Days)	30	30	365
Decay Heat (Watts)	4.8×10^6	5.3×10^6	4.6×10^6
Desirable Venting Rate (Ft^3/hr)	3.0×10^6	3.3×10^6	2.8×10^6
Corresponding Room Air Changes Per Hour	83	2	19
Desirable Door/Chimney Hole Size (Ft^2)	77	51	74
Corresponding Side of Square (Ft.)	9	7	9

The room dimensions in Table VII were chosen to bracket the range of volumes that are likely to be encountered at existing storage pools, rather than to typify specific installations.

It is clear from Table VII that based on the ANS Specification of two air changes per hour, existing ventilation systems will generally be inadequate for Cases (1) and (3). For Case (2), however, the situation is more favorable owing to the large volume associated with the fact that BWR storage pools are located within the reactor containment building.

Now consider the question of providing for an adequate chimney effect. Assume that at the time of the pool drainage, a door of area A is opened at ground level to allow fresh air to enter the building, and that a chimney hole of similar area, A, is opened in the ceiling, above the pool, to allow hot air to escape. The analysis in the appendix shows that in order to keep the room temperature at or below a specified value, T_r, the opening A must satisfy the following inequality:

$$A \geq \frac{Q_{decay}}{C_D c_p \rho_o \sqrt{2gH}} \bullet \sqrt{\frac{T_r(T_o+T_r)}{T_o(T_r-T_o)^3}} \qquad (6)$$

where

C_D = discharge coefficient ($\sim$0.6)
ρ_o = outside (atmospheric) density
g = acceleration of gravity
H = height of ceiling above ground level.

Table VII presents the door/chimney hole sizes corresponding to Equation (6) with a 150°C room temperature rise, and illustrates that a square opening of 9 feet on a side will be sufficient for the three cases enumerated above.

The preceding estimates indicate that in most cases, existing ventilation systems will not be adequate to remove the decay heat from the building. Although additional ventilation could be obtained by other means, it appears that many current facilities do not have this provision. Consequently, calculations have been made to assess the effect of inadequate ventilation on the spent fuel heatup, utilizing the detailed pool heat transfer models discussed in Section 3.3 together with the containment building models described in Section 3.4. The results are typical rather than specific, in that attention has been focused more upon the mechanisms than upon the specifics of the building design.

Figure 21 shows that for a drained spent fuel pool in the auxiliary building of a PWR reactor, with a 30-day minimum decay time and a full core discharge loading pattern, the effect of inadequate ventilation will be to cause rapid overheating of the spent fuel. This is to be expected on the basis of Table VII, which showed that because of the small room size (36,000 cu. ft.), more than 80 room air changes per hour would be required to keep the room temperature at a reasonable level. This amount of ventilation is not feasible with forced air systems.

In the case of a typical away-from-reactor storage pool loaded with PWR spent fuel having a minimum decay time of one year (Figure 21), existing ventilation systems based on the ANS half-hour change rate will still be rather ineffective, despite the larger room size (150,000 cu. ft.). Again, this effect is to be expected on the basis of the results in Table VII, which showed that nearly 20 room air changes per hour would be necessary to eliminate the decay heat to the outside. Certainly, a half-hour change rate would provide little relief, as the figure shows.

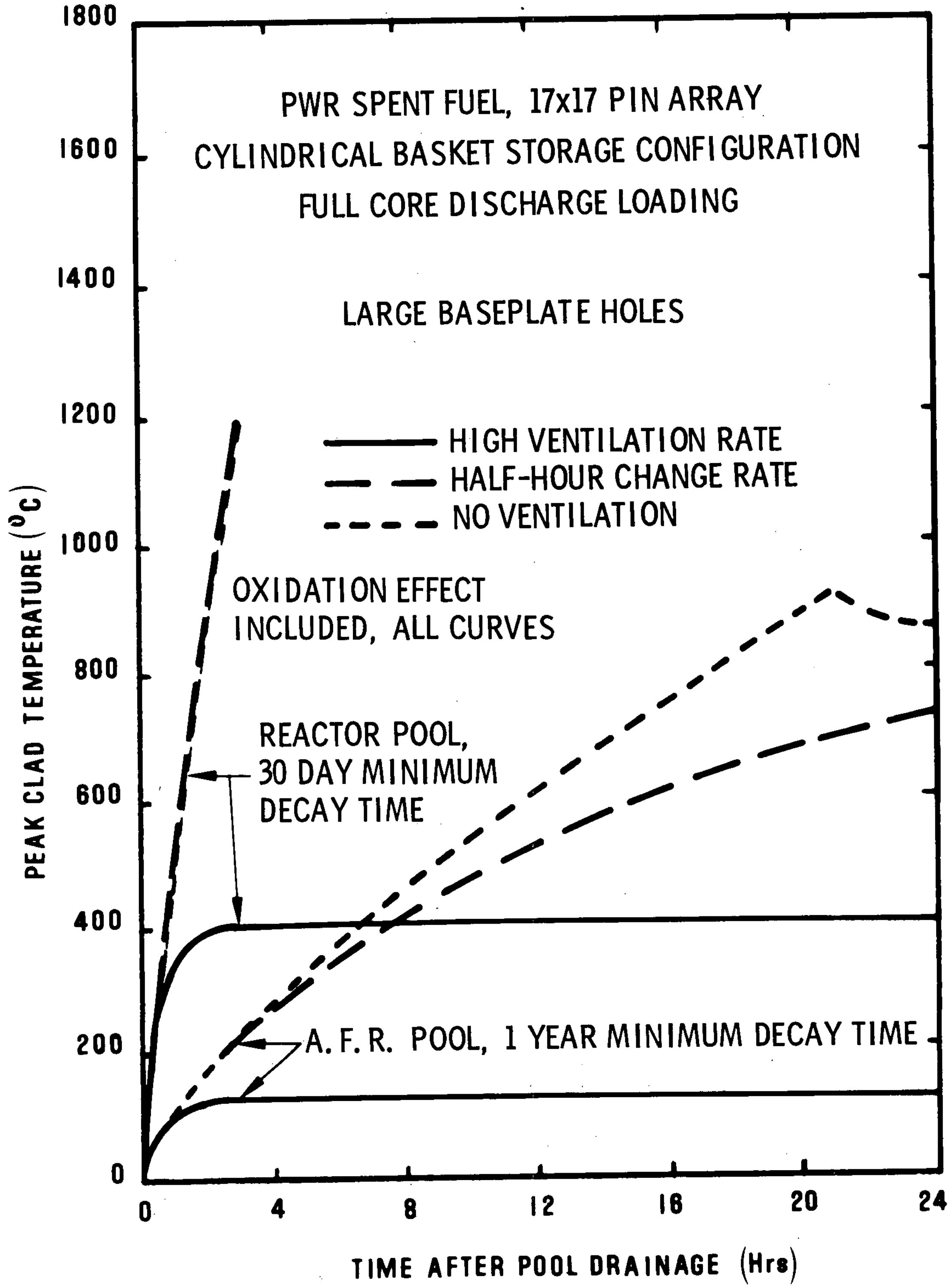

Figure 21. Effect of Ventilation Rate on Heatup of PWR Spent Fuel in Reactor Storage and Away-From-Reactor Storage

An interesting phenomenon occurs with the away-from-reactor storage arrangement and is worth pointing out. Because of the inadequate ventilation, the oxygen supply becomes depleted rather rapidly when clad oxidation starts to occur. When the oxygen disappears, the reaction terminates and the spent fuel temperatures correspondingly "peak out." As shown in Figure 21 and, more specifically in Figure 22, the clad temperature may not attain melting prior to the shutoff, or if melting is attained (as it is for the 1.5-inch baseplate hole, not shown), the period of melting may be too short for clad penetration to occur. On the other hand, clad failure may still develop via the rupture mechanism, which can occur at temperatures around 900°C. Another interesting result shown in Figure 22 is that the time to reach steady-state extends to the order of days when ventilation is inadequate.

Figure 23 shows the partitioning of heat that occurs for an unventilated, away-from-reactor storage building, corresponding to the less severe of the two heatup cases in Figure 22. When steady-state is attained, such that E_{fuel} and E_{hldr} remain constant, the majority of the heat produced by radioactive decay is thereafter removed by radiation and convection from the sheet metal exterior (69 percent), with a smaller portion being removed by air leakage to the outside (23 percent), and a still smaller portion by conduction into the concrete (8 percent). Storage of heat in the building structure is computed to amount to less than 1 percent of that stored in the spent fuel itself.

A composite of results for PWR spent fuel in away-from-reactor storage pools without ventilation is shown in Figure 24, these cases corresponding to a 3-year minimum decay time with a full core discharge loading pattern. Observe that for most of the cases considered, a 3-year decay period is sufficient to keep the clad temperatures within safe limits even when there is no ventilation at all. The

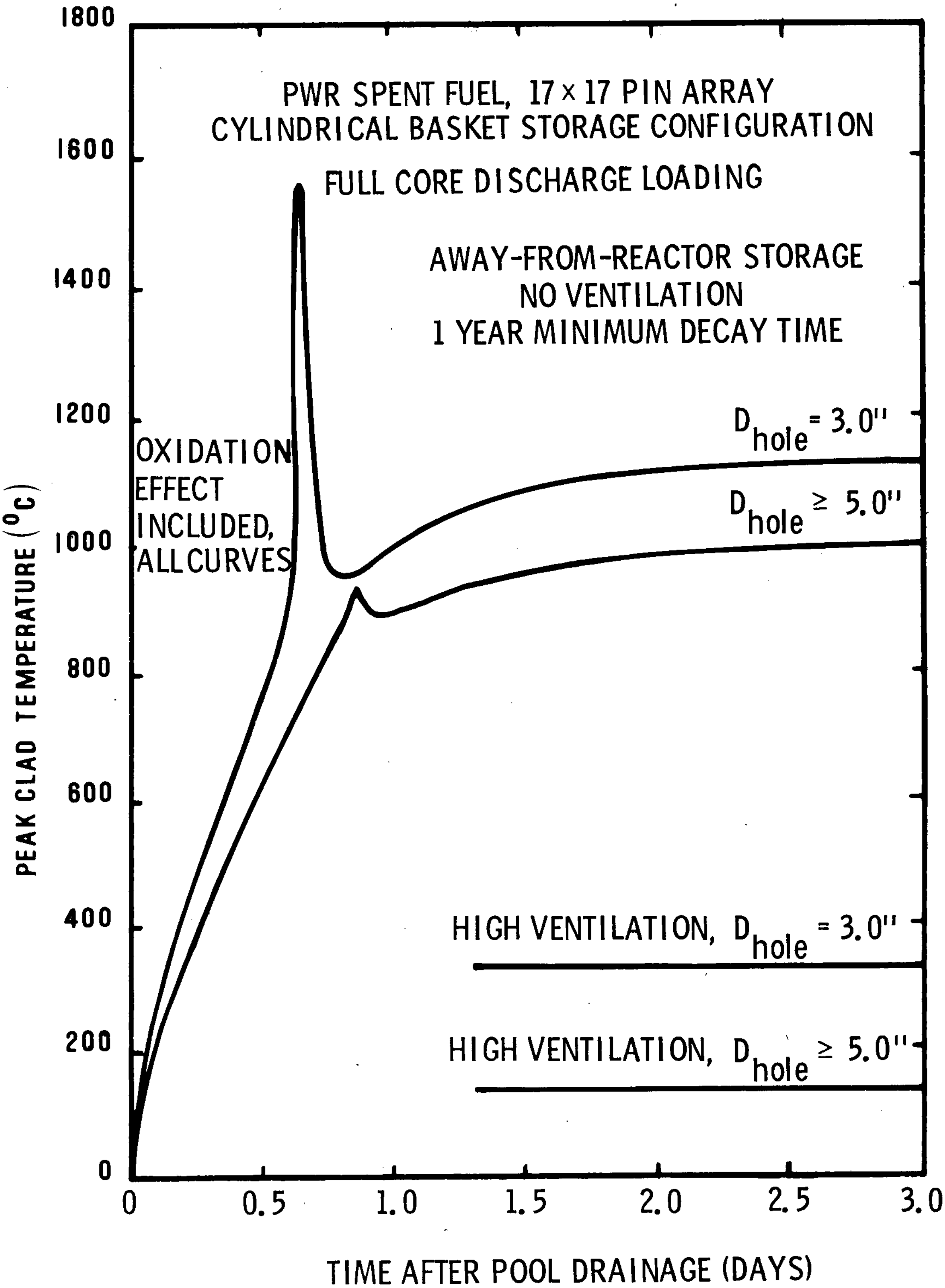

Figure 22. Heatup of PWR Spent Fuel With Complete Ventilation Failure in an Away-From-Reactor Storage Facility, One Year Minimum Decay Time

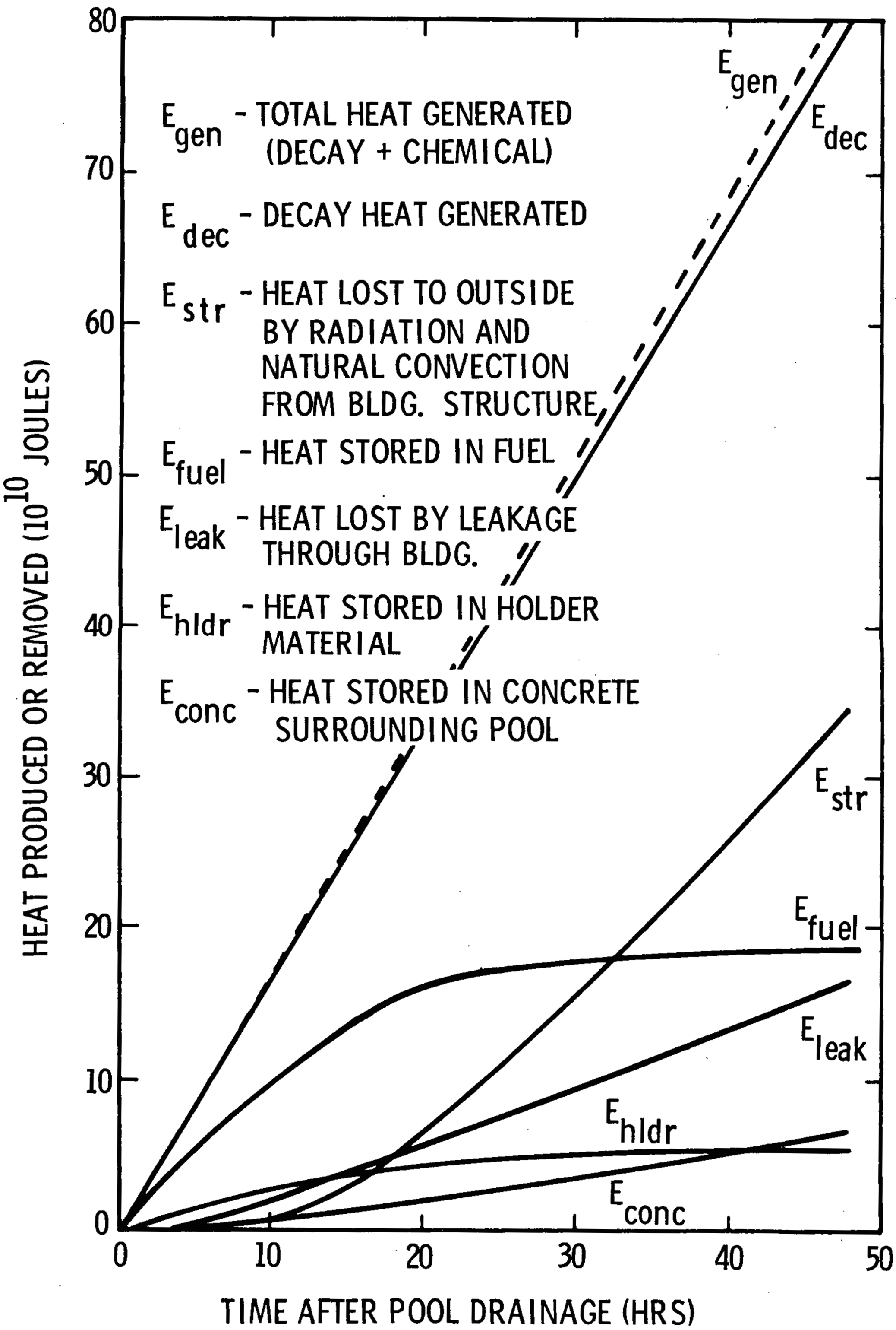

Figure 23. Partitioning of Heat for a Drained Away-From-Reactor Spent Fuel Pool Without Room Ventilation

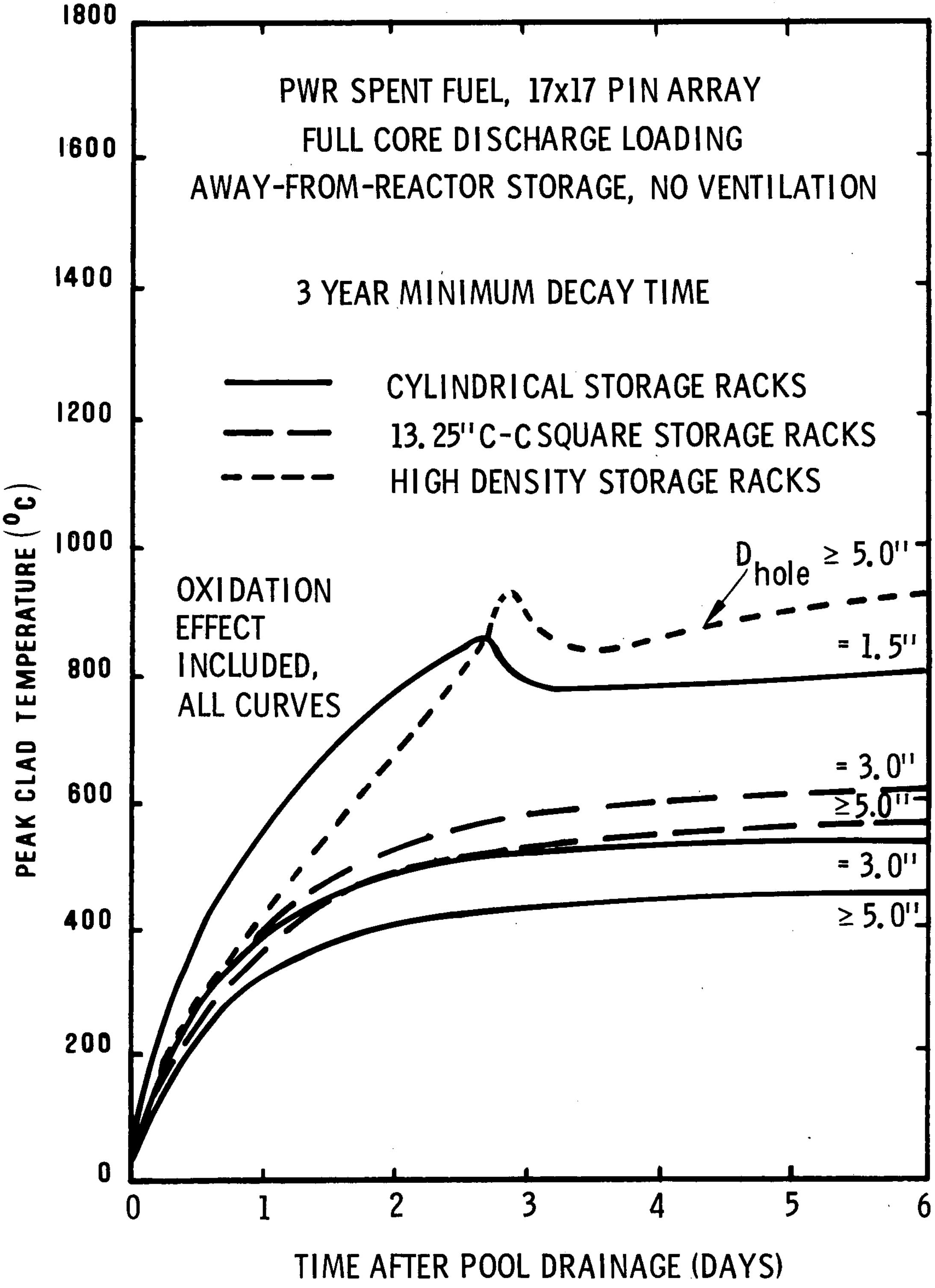

Figure 24. Heatup of PWR Spent Fuel with Complete Ventilation Failure in an Away-From-Reactor Storage Facility, Three Year Minimum Decay Time

only borderline exceptions are the high density storage configuration and the lower density cylindrical configuration with small baseplate holes, both of which produce clad temperatures that may be high enough for rupture to occur. If a half-hour change rate were included, these temperatures would be reduced slightly.

The situation is more favorable for BWR spent fuel than for PWR spent fuel, both because of the lower decay heat produced and the larger room size for reactor storage (1,800,000 cu. ft. assumed). As shown in Figure 25, the peak clad temperature in a BWR reactor pool with a 30-day minimum decay time and a full core discharge loading pattern will increase over the perfectly ventilated case by about 300°C when ventilation is completely unavailable, as compared to about 150°C when ventilation is operative at the rate of two air changes per hour. The latter figure is consistent with the results of Table VII, Case 2. In addition, the amount of heatup occurring in the unventilated or underventilated away-from-reactor storage pool is considerably lower when the pool is filled with BWR fuel (Figure 25) than when it is filled with PWR fuel (Figure 21). The loading pattern assumes that nine BWR spent fuel elements occupy the same space as four PWR spent fuel elements, while only producing about three-quarters as much decay heat.

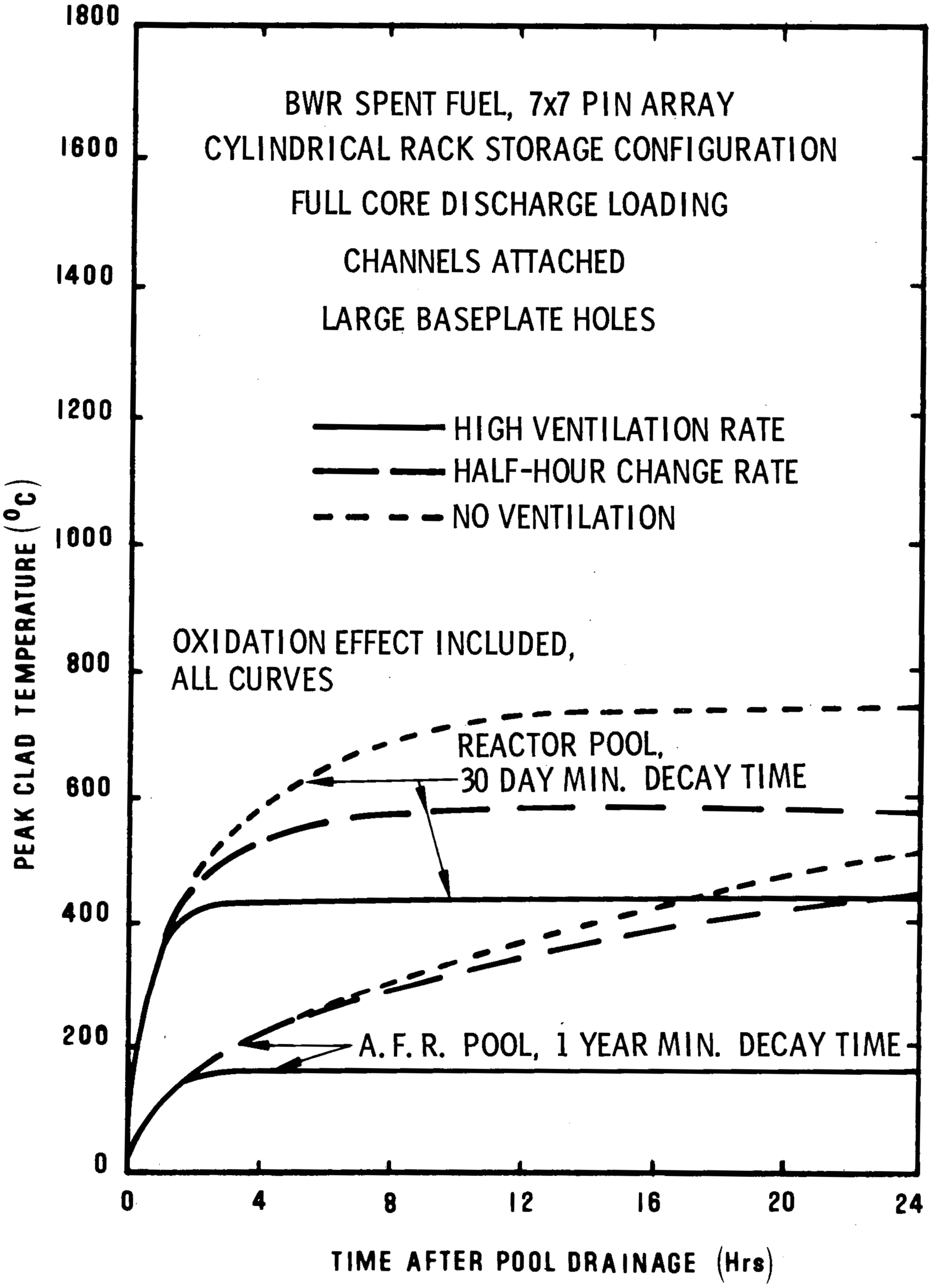

Figure 25. Effect of Ventilation Rate on Heatup of BWR Spent Fuel in Reactor Storage and Away-From-Reactor Storage

5. OTHER CONSIDERATIONS

5.1 Effect of Incomplete Drainage

Many spent fuel holder designs provide only a single inlet hole for convective flow through each fuel element, located in the baseplate or near the bottom of the holder. If there is a complete pool drainage, the air must circulate down and under the fuel elements before passing through the baseplate inlet hole into the fuel assembly. An incomplete drainage could block this flow and reduce the effectiveness of natural convective cooling. Open frame configurations are, of course, exempt from this possibility because the flow does not have to pass through an inlet hole in order to gain proximity to the fuel element.

A detailed analysis of spent fuel heatup in the event of an incomplete drainage has not been undertaken. However, an approximate analysis has been performed to estimate the amount of aggravation that might occur if the water ceased to drain after exposing all but the bottom portion of the fuel elements. The analysis is included in Appendix B and is based, among other things, upon upper and lower bound estimates of the thermal radiation absorbed by the water from the hot fuel rods above. The temperature distribution along the rods is prescribed in this analysis according to estimates made of the likely distribution that would occur just prior to the onset of self-sustaining clad oxidation. The amount of heat produced above the water level is then determined together with the amount that could be removed by various mechanisms, including water boiling (latent heat), convection to the steam produced by boiling (sensible heat), radiation to the building, and convection to the air. If the heat removal rate is determined to be larger than the rate of production, then the configuration is coolable; if the heat removal rate is smaller than the rate of production, overheating resulting in clad rupture or melting will occur.

The results for a 1-year decay time are presented in Table VIII. Consider first the case where the drainage uncovers the upper 80 percent of the fuel rods, leaving the lower 20 percent still covered (third column). The heat transferred to the remaining water by decay from the immersed portions and by radiation from above is 3.6 - 4.9 KW per assembly (line 2c). This implies that about an hour might be required to raise the water temperature to boiling (assuming all the assemblies produce the same decay heat) and that the water recession rate following the inception of boiling will be about 10 cm/h (lines 3 and 4). Meanwhile, the decay heat produced above the water line is about 4.5 KW per assembly (line 5), and the capability for removing heat as the clad temperatures approach the lower limit of self-sustaining oxidation is 5.7 - 8.7 KW per assembly (line 6e). Since the heat removal capability exceeds the heat production (line 7), the geometry is temporarily coolable.

If, however, the drainage were to uncover the whole length of the rods but still to constrict the flow, either by blocking the baseplate holes or by not allowing enough space for unrestricted flow in the base region, then the heat production would exceed the heat removal capability (line 7, first column) and the clad would overheat. The same situation would eventually occur if, rather than immediately draining to this position, the water were to drain part way down the rods and then boil off down to the baseplates over a period of time. Table VIII indicates that there is a good chance of overheating, in

Table VIII.

Estimates of Heat Removal Capability in an Incompletely Drained Pool, One Year Decay Time*

1.	Normalized water level (z_w/L)	0.0	0.1	0.2
2.	Heat transferred to water, per assembly (KW):			
	a. by decay heat	0.0	0.2	0.6
	b. by thermal radiation from above	0.3 - 1.3	1.2 - 2.6	3.0 - 4.3
	c. total	0.3 - 1.3	1.4 - 2.8	3.6 - 4.9
3.	Time to start boiling (hours)	1.0 - 4.3	0.9 - 1.8	0.7 - 1.0
4.	Water surface recession rate (cm/hr)	0.7 - 3.2	3.5 - 7.0	9.0 -12.2
5.	Decay heat produced by spent fuel above water level, per assembly (KW)	5.1	4.9	4.5
6.	Removal of heat produced by spent fuel above water level, per assembly (KW):			
	a. by radiation to water	0.3 - 1.3	1.2 - 2.6	3.0 - 4.3
	b. by radiation to building	0.0 - 0.9	0.0 - 0.9	0.0 - 0.9
	c. by transfer to water vapor	0.2 - 0.8	0.9 - 1.8	2.3 - 3.1
	d. by transfer to air	0.4	0.4	0.4
	e. total	0.9 - 3.4	2.5 - 5.7	5.7 - 8.7
7.	Heat removal surplus (deficit) per assembly (KW), line 6e minus line 5.	(4.2)-(1.7)	(2.4)-0.8	1.2 - 4.2

* PWR spent fuel in cylindrical baskets. One year decay time assumed, uniformly throughout pool. Numerical ranges (e.g., 0.3 - 1.3) give lower and upper-bound estimates. See Appendix B.

fact, if the water were to recede below the level where the lower 10% of the rods is still immersed.

A comparison of the peak clad temperature rise versus time for PWR spent fuel with a 1-year minimum decay time in a well-ventilated room is shown in Figure 26. The temperature rise corresponding to an incomplete drainage down to the bottom of the rods, calculated by utilizing the lower-bound radiation estimate, is compared with previous cases for a complete drainage with varying baseplate hole sizes. The clad oxidation effect has not been calculated for the case of incomplete drainage (blocked inlets), because it is believed to be substantially reduced by the unavailability of oxygen within the assembly. Clearly, a 1-year minimum decay time is not sufficient to preclude overheating for this case.

The approximate method used for bracketing the thermal radiation downward to the water and upward to the building is not considered to be precise enough to allow prediction of the minimum allowable decay time in the event of an incomplete drainage. This problem could be approached by formulating a detailed thermal radiation model to calculate shape factors and include the shadowing of radiating surfaces by fuel rods and tie plates. By incorporating this radiation capability into the overall heat transfer models described in Sections 3.3 and 3.4, a credible prediction of the minimum allowable decay time could be obtained. No attempt to do this, however, has been made.

It is clear, however, that an incomplete drainage can potentially cause a more severe heatup problem than a complete drainage, if the residual water level remains near the baseplates. From a practical point of view, it might be possible to make provisions for either completing the drainage or refilling the pool, if this should happen. However, it would

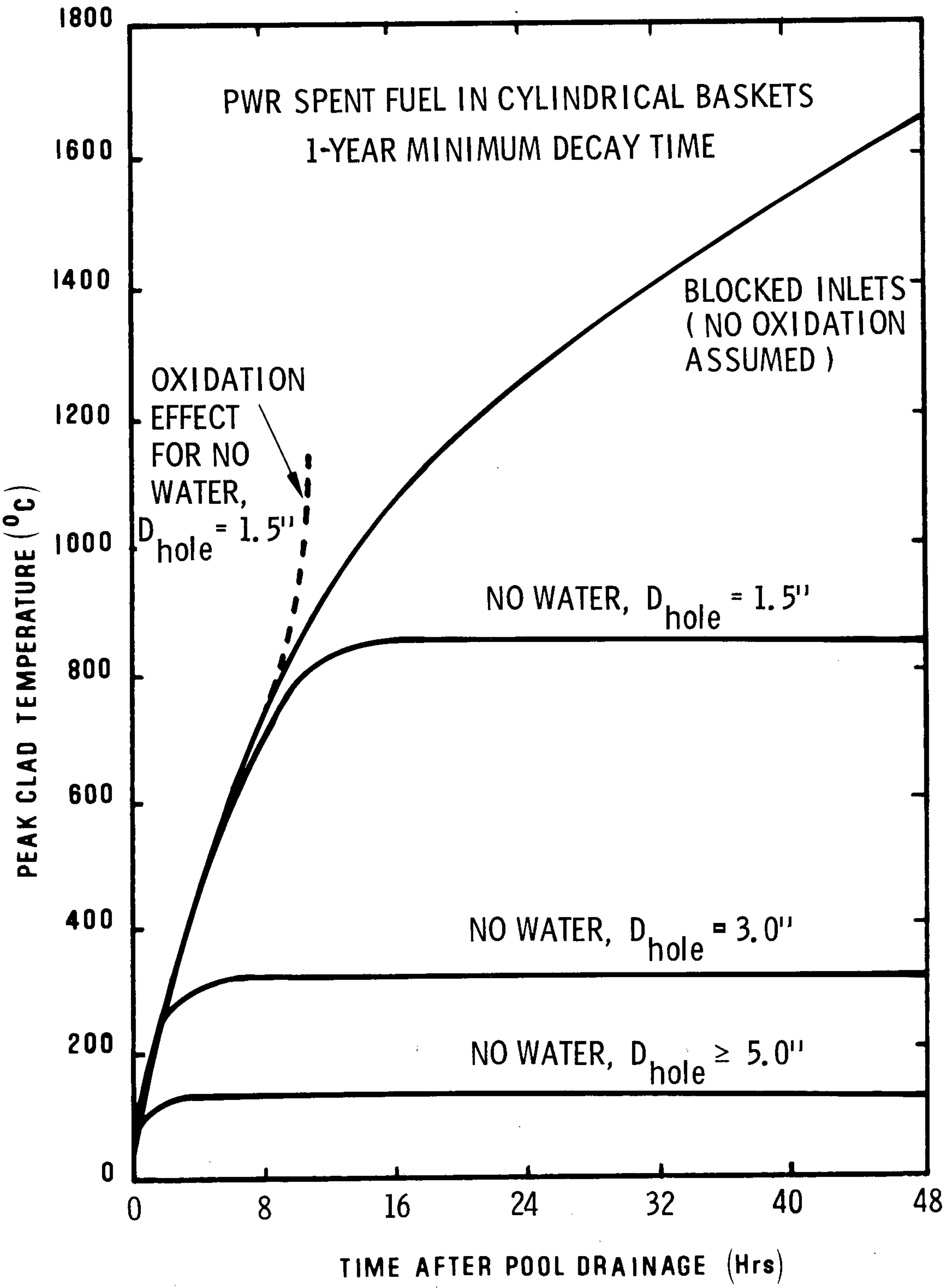

Figure 26. Estimated Heatup of PWR Spent Fuel With Residual Water Sufficient to Block Flow Inlets, Well-Ventilated Room

seem that the special problems associated with an incomplete drainage could best be circumvented by modifying the spent fuel holders to include inlet holes at various elevations along the vertical, rather than just at the baseplate level. According to the predictions, these inlet holes would only be required for the bottom 20 percent of the fuel rod length if the spent fuel were at least a year old. With these additional inlets, the beneficial effect of natural convection would not be cancelled by an incomplete drainage.

5.2 Effect of Surface Crud

Iron oxides are known to deposit upon the outside of the fuel pins during normal operation of the reactor, and these deposits are likely to remain on the fuel pins during storage of the spent fuel. Typically, the iron oxide crud buildup on BWR fuel pins is on the order of 25 to 100 microns and in the form of Fe_2O_3, whereas the buildup on PWR pins is on the order of only 1 to 5 microns and in the form of Fe_3O_4.[16] A calculation was made to determine whether a 100 micron Fe_2O_3 coating on the BWR fuel pins would affect the heatup of these pins during a pool drainage accident, and it was found that the overall effect on the fuel pin temperature was less than one degree.

The question was also raised as to whether some of the crud, which would be contaminated, could be levitated by the air flows produced by natural convection after a pool drainage and thereby produce a health hazard. An analysis of the weight and drag characteristics of iron oxide particles revealed that a BWR fuel assembly having a decay time of 90 days prior to loss of water can produce upward air currents sufficient to levitate a 200-micron sized particle, whereas an assembly allowed to decay for 250 days can levitate a 175-micron sized particle. Since any spallation of the crud would produce particles of roughly the same size as the thickness of the layer (namely 25 to 100 microns), the air currents produced by the exposed assemblies should be sufficient to lift a significant proportion of oxide particulate from the surface of the fuel rods. Since the adhesiveness of the crud is not likely to be sufficient to prevent spallation, it should be assumed that some spallation and levitation will occur.

5.3 Emergency Water Spray

A number of suggestions have been made in the preceding sections to improve the natural convection capabilities of spent fuel storage configurations and to reduce the likelihood of clad failure by overheating. An alternative way to maintain coolability, at least on a temporary basis, would be to provide an emergency water spray of sufficient intensity to remove the decay heat by its latent heat of vaporization. The water supply could be available from onsite hydrants, from onsite storage tanks, from remote portable storage tanks, or, preferably, from a combination of onsite and remote sources in order to reduce the risk of unavailability. Facility personnel would presumably be available to set up fire hoses and initiate the spray in the event of a complete power failure, and the spray would be continued until the source of the leak could be repaired.

The rate of water spray that would be required to maintain coolability can be easily estimated by equating the decay heat produced by the hottest assembly in the pool to the sensible and latent heat of the spray droplets falling in the immediate vicinity of that assembly. Thus

$$\dot{V}_w = \frac{C_P q_{decay}}{\eta\rho(c_p\Delta T + H_v)} \quad (7)$$

where

$\dot{V}_w$ = volume flow rate of water

C_P = storage capacity of pool (metric tons)

q_{decay} = decay power per metric ton, hottest assembly

η = spray efficiency (ratio of water falling within pool to total water sprayed)

ρ_w = density of water (1.0 gm/cm^3)

$c_p \Delta T$ = sensible heat (380 Joule/gm)

H_v = latent heat of vaporization (2250 Joule/gm).

Table IX shows the values of $\dot{V}_w$ obtained for various storage situations and minimum decay times, and also estimates the spray droplet concentrations obtained for a drop size of 1.0 mm and corresponding terminal velocity of 380 cm/sec. It may be noted that the required spray rates, which are under 100 gal/min, are easily achievable with fire hoses that normally produce up to 250 gal/min, and that the quoted terminal velocity is easily sufficient to overcome the updrafts from the spent fuel array, which are on the order of 75 cm/sec.

To verify that these estimated spray rates are sufficient to keep the spent fuel temperatures within safe limits, calculations have been made using the detailed heat transfer model of Section 3.3, modified so as to include the effects of the water spray. In order to be conservative, it was assumed that the spray droplets collect on the holders/baskets without ever coming into contact with the fuel rods. (This assumption may actually be fairly accurate, in view of the fact that the holders usually protrude upward several feet beyond the top of the fuel elements.) The sensible and latent heats of the water droplets were expended in keeping the holder walls at the water saturation temperature, but only down to the depth allowed by the availability of water. Heat transfer from the hot fuel

TABLE IX

Water Spray Rate Required to Insure Spent Fuel Coolability in Various Situations

	Situation	Minimum Decay Time (Days)	Decay Heat (KW/MTU)	Required Spray Rate* (Gal/min)	Required Spray Density** (gm/cm^3)
1.	PWR reactor-sited pool, 2 core capacity	30	53.2	82	2.3×10^{-5}
		90	30.0	46	1.3×10^{-5}
		365	11.0	17	0.5×10^{-5}
2.	BWR reactor-sited pool, 2 core capacity	30	36.9	95	1.5×10^{-5}
		90	21.5	55	0.9×10^{-5}
		365	8.58	22	0.4×10^{-5}
3.	Away-from-reactor pool, 750 MTU capability, PWR spent fuel	365	11.0	71	4.7×10^{-6}
		730	5.90	38	2.5×10^{-6}
		1095	3.76	24	1.6×10^{-6}

*Based on spray efficiency of 0.7
**Based on 1.0 mm drop size

rods to the cooled holder walls was accomplished by radiation and natural convection. No water accumulation at the bottom of the pool was assumed to occur, any excess water being drained immediately.

Some results of calculations utilizing this approach are shown in Figure 27, where it may be seen that a reasonable spent fuel temperature (∿400°C) can be maintained indefinitely by applying a sufficient amount of spray, even in cases where overheating would normally occur very rapidly. A 1-hour delay between the drainage incident and the application of the spray will generally be acceptable.

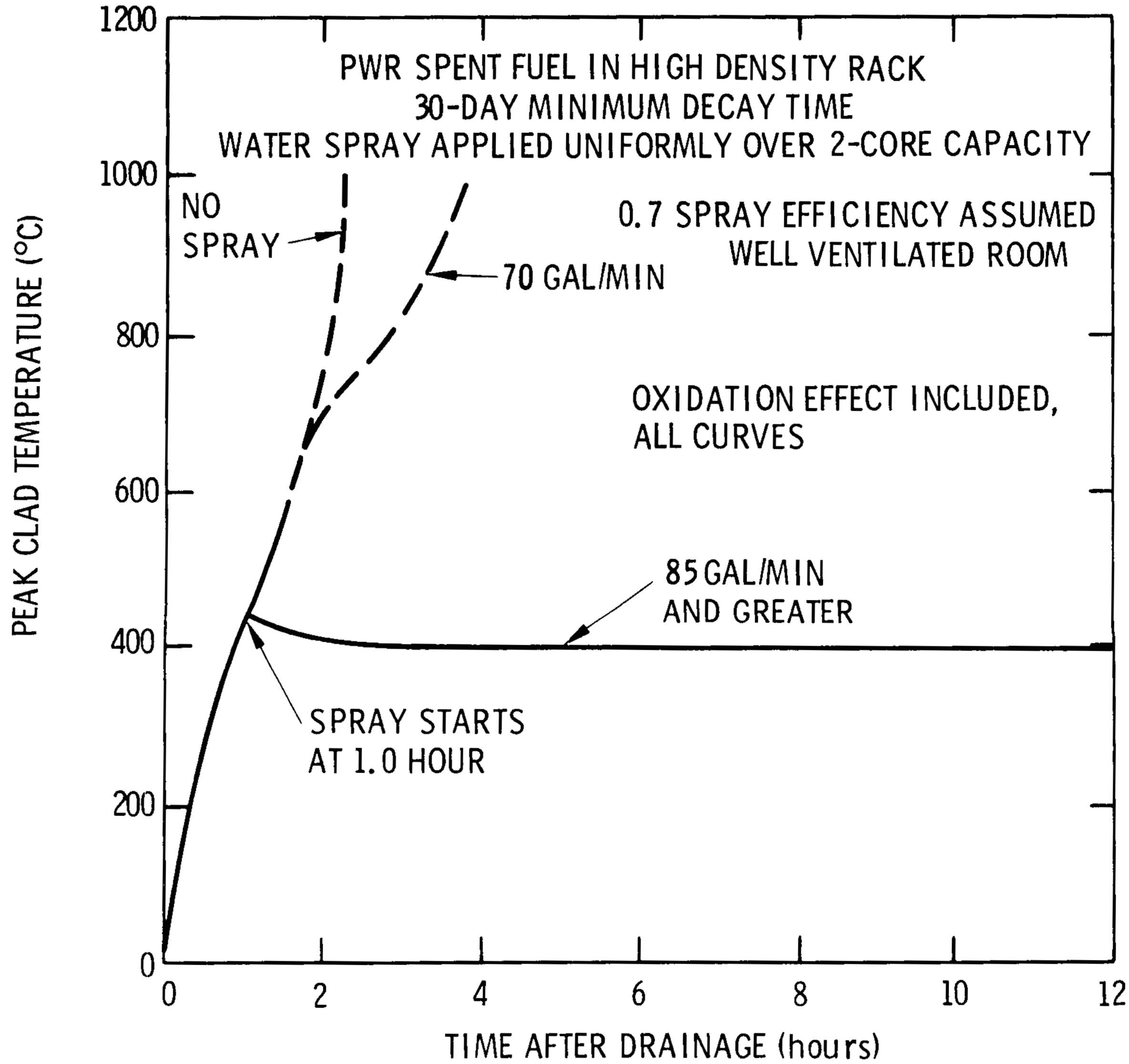

Figure 27. Effect of Emergency Water Spray in Retarding Spent Fuel Heatup in a Drained Storage Pool

To confirm the feasibility of an emergency spray initiated by personnel, it must be confirmed, first of all, that this technique will not increase the reactivity to a critical condition as a result of undermoderation, and secondly, that the radioactive dose will not be severely injurious to the person providing the corrective action. The question of undermoderation is easily resolved by observing that the expected water concentrations in the air (Table IX) are far less than those which would cause an increase in reactivity.[17] The question of dose, however, requires a careful evaluation of the sky-shine radiation emitting from the drained pool. A model for evaluating that radiation has been formulated and is described in Appendix C. The results indicate that a person standing at about 50 feet from the edge of a typical PWR reactor pool, filled to capacity 30 days after a full core discharge, will receive a full body gamma dose of about 200 Rem/hr. While this dose rate is considerable, it is believed that with adequate shielding, it would be easily possible for a person to enter into and remain inside the building long enough to perform necessary emergency measures.

In conclusion, therefore, initiation of an emergency water spray by onsite personnel appears to be a viable means of maintaining coolability in a drained spent fuel pool until repair actions can be undertaken to restore convective water cooling.

6. CONCLUSIONS

An analysis of spent-fuel heatup following drainage of the storage pool has been completed, and the following conclusions have been reached:

Well-Ventilated Rooms

1. Considering a complete pool drainage, the minimum allowable decay time for PWR spent fuel in a well-ventilated room varies from a best value of about 5 days, for open-frame storage configurations, to a worst value of about 700 days, for high-density closed-frame configurations with wall-to-wall spent fuel placement. Other storage configurations fall between these limits. The minimum allowable decay time is defined as the lower limit of safe decay times, such that shorter decay times would produce local clad failures due to rupture or melting.
2. The minimum allowable decay time for BWR spent fuel in a well-ventilated room varies from a best value of 5 days to a worst value of 150 days for the cases considered. A high-density storage rack design for BWRs would result in a somewhat higher value of the allowable decay time than presented here, but not as high as for PWR spent fuel.
3. The allowable decay times can be reduced significantly by widening baseplate holes, opening flow paths between holders, removing BWR channels, and avoiding wall-to-wall storage. Decay times as low as 80 days for the high density racks and 20 days for other

racks could in principle be accommodated with these design modifications at no expense in packing density.

4. The differences between fuel assembly designs are small, i.e., a 17 x 17 PWR pin array and a 15 x 15 PWR pin array produce similar results, as do an 8 x 8 BWR pin array and a 7 x 7 BWR pin array. The effect of surface crud on the fuel pins is also insignificant.

Inadequately Ventilated Rooms

5. Current forced air ventilation systems in typical PWR auxiliary buildings may provide insufficient ventilation to remove the decay heat produced in the spent fuel pool after a complete pool drainage. Consequently, overheating due to inadequate ventilation may occur. Adequate ventilation could be provided by passive methods that utilize a chimney effect.
6. Ventilation systems in typical BWR spent fuel pools inside the reactor containment building are adequate to remove most of the decay heat, owing to the large size of the containment building.
7. Additional ventilation provisions for typical away-from-reactor facilities (750 MTU capacity) will be unnecessary if the spent fuel is sufficiently aged. Minimum decay times of between 2 and 4 years, depending on the storage configuration, are sufficient to prevent overheating in AFR storage pools with inadequate or inoperative ventilation because of the fairly substantial size of the room, the presence of heat sinks, and the capacity of the sheet metal walls to reject heat through thermal radiation to the outside. Shorter decay times can be accomodated by providing additional passive ventilation.

Incomplete Drainage

8. For many spent fuel holder designs where the air must circulate under the fuel elements and pass through a

baseplate hole to enter the elements, a nearly complete drainage can be more severe than a complete drainage. For 1-year-old spent fuel, coolability can be maintained by the process of water boiling and convection of heat to the steam, as long as the lower 20 percent of the fuel rods remains covered by water. If the water drains or boils off to a lower level, but not sufficiently low to open the baseplate passages to air flow, then the removal of heat associated with water boiling, steam convection, and air convection will all be impaired. These circumstances can lead to an increased tendency to overheat.

9. The potentially adverse effects of an incomplete drainage can be counteracted by drilling air inlet holes at various elevations in the lower part of the holders. This will permit air flows to circulate when the water level drops beneath the location of the uppermost inlet holes.

Emergency Water Spray

10. For those cases where overheating is a concern, coolability in a drained spent fuel pool can be maintained indefinitely by providing a water spray. Spray volumes on the order of 100 gal/min and less appear to be sufficient for all the cases considered. The gamma dose rate to a person entering within 50 feet of the edge of the pool to set up a fire hose is about 200 Rem/hr.

References

1. Reactor Safety Study, WASH-1400, Appendix I, 95-99, 1975.

2. Ibid., Appendix VII, 3, 1975.

3. R. H. Chapman, Multirod Burst Test Program Quarterly Progress Report for July - September 1976, ORNL/NUREG/TM-77, 1977.

4. A. S. Benjamin and D. J. McCloskey, "Spent Fuel Heatup Following Loss of Water During Storage," ANS TRANSACTIONS, 28, 333, 1978.

5. A. S. Benjamin and D. J. McCloskey, "Protecting Against Spent-Fuel Overheating in a Pool Drainage Accident," ANS Transactions, 30, 331, 1978.

6. Private communications between T. E. Tehan, General Electric Morris Operation, and A. S. Benjamin, Sandia Labs, November 1977.

7. V. E. Schrock, "Development of a Revised ANS Standard on Decay Heat from Fission Products," ANS Transactions, 28, 421, 1978.

8. M. J. Bell, ORIGEN - The ORNL Isotope Generation and Depletion Code, ORNL-4628, 1973.

9. D. E. Bennett, "Sandia - ORIGEN Input Manual," SAND77-1175, to be published.

10. Private communications between D. McDaniel, General Electric Co., San Jose, and D. E. Bennett, Sandia Labs, January 1978.

11. D. A. Powers, "Chemical and Physical Processes of Reactor Core Meltdown," Chapter 4 in Core-Meltdown Experimental Review, SAND74-0382 (Revision), 4-15, 1977.

12. E. T. Hayes and A. H. Roberson, "Some Effects of Heating Zirconium in Air, Oxygen, and Nitrogen," Jl. Electrochem. Soc., 96, 142, 1949.

13. J. H. White, reported in AEC Fuels and Materials Development Program, Progress Report No. 67, GEMP-67, General Electric Co., 151, 1967.

14. S. Leistikow, et al., "Study on High Temperature Steam Oxidation of Zircaloy-4 Cladding Tubes," Nuclear Safety Project Second Semiannual Report, 1975, KfK-2262, Karlsruhe, 233, 1976.

15. R. R. Biederman, R. D. Sisson, Jr., J. K. Jones, and W. G. Dobson, A Study of Zircaloy-4 Steam Oxidation Reaction Kinetics, Final Report, EPRI NP-734, 1978.

16. Private communication between A. B. Johnson, Jr., Battelle Pacific Northwest Labs, and A. S. Benjamin, Sandia Labs, June 1977.

17. F. M. Alcorn, "Criticality Evaluation of Low-Density Moderation in PWR Fuel Storage," ANS Transactions, 27, 416, 1977.

APPENDIX A

MATHEMATICAL MODELS IN THE COMPUTER CODE SFUEL

CONTENTS

FIGURES

TABLES

A1. Nomenclature

English Symbols

A	Cross-sectional area
A_1	Baseplate hole area
A_2	Internal basket/holder cross-sectional area
C_D	Orifice discharge coefficient (taken as 0.6)
c_f	Skin friction coefficient
c_p	Specific heat at constant pressure
D_H	Hydraulic diameter, $D_H = 4A/P_w$
f	Mass-fraction of oxygen in atmosphere
g	Acceleration of gravity (980 cm/sec^2)
Gr, Gr_x	Grashoff number, $Gr_x = \bar{\rho}^2 g x^3 \Delta T/\bar{\mu}^2 \bar{T}$
H	Specific enthalpy
h	Heat transfer coefficient, $h = \dot{q}/\Delta T$
k	Thermal conductivity
L	Length of a flow path
$\dot{m}$	Mass rate of flow
$\dot{m}_{leak}$	Leakage rate from building to external atmosphere
Nu_D	Nusselt number based on hydraulic diameter, $Nu_D = hD_H/k$
p	Pressure
p_{max}	Maximum pressure that can be sustained by containment building
Pr	Prandtl number

Nomenclature (continued)

English Symbols

P_w	Wetted perimeter
$\dot{q}$	Heat rate per unit surface area
q_{decay}	Decay heat rate per assembly
q_{chem}	Heat rate per assembly due to clad oxidation
R	Gas constant for air (2.871×10^6 dy-cm/gm-°K)
Re	Reynolds number
Re_D	Reynolds number based on hydraulic diameter, $Re_D = \rho U D_H/\mu$
Re_x	Reynolds number based on wetted distance, $Re_x = \rho U x/\mu$
T	Temperature
t	Time
U	Velocity
V_r	Volume of room
$\dot{V}_{vent}$	Volumetric venting rate
$\dot{w}_{ox}$	Oxygen consumption rate per unit surface area
x	Distance along flow path

Greek Symbols

γ	Ratio of specific heats ($\gamma = 1.4$)
δ_s	Thickness of heat sink wall
ε	Free surface emissivity
$\varepsilon_{a,b}$	Effective emissivity from surface a to surface b

Nomenclature (continued)

Greek Symbols

θ	Angle between flow direction and upward-directed vertical
μ	Viscosity
ρ	Density
σ	Stefan-Boltzmann constant (5.67×10^{-12} Watt/cm^{2}-°K^{4})
τ	Shear stress

Subscripts

ℓ	Pool liner
o	Outside atmosphere
ox	Relating to clad oxidation reaction
r	Containment room
s	Heat sink structure in containment building
sf	Spent fuel
t	Tie plate
w	Solid components ("walls") in spent fuel pool
(None)	Properties without subscript generally relate to air flows in spent fuel array

A2. Equations for Air Flows

Refer to Section 3.3 in the main text for the primary assumptions and methodology used in connection with the air flows and the general heat transfer problem in the pool area. In particular Figures 7, 8, and 9 (main text) summarize the nature of the air flows, the heat transfer modes, and the solution procedures used.

The following contribution provides the main equations of the method, presented in integral form. In the computer code SFUEL, these equations are solved in differential form (i.e., by marching application over increments of length, Δx), using a semi-implicit technique. To obtain the differential equations from the integral equations presented below, one may consider L to be a running length and may differentiate the equations with respect to L.

a. <u>Conservation of Mass</u>

$$\Sigma \dot{m}_{out} = \Sigma \dot{m}_{in} - \int_0^L \dot{w}_{ox} \, P_w dx \qquad (A.1)$$

(Mass outflow from control volume)
= (Mass inflow) - (Oxygen consumption)

b. <u>Conservation of Momentum</u>

$$P_{in} - P_{out} = \int_0^L \rho g \cos \theta \, dx + \Sigma \int_0^L \frac{4}{D_H} \tau_w dx + \left[\frac{\dot{m}^2}{2\rho C_D^2} \, \frac{A_2^2 - A_1^2}{A_1^2 A_2^2} \right]_{base} \qquad (A.2)$$

(Pressure drop) = (Buoyancy term) + (Shear stress dissipation) + (Orifice loss across baseplate inlet hole, vertical flows only)

c. Conservation of Energy

$$\frac{d}{dt}\int_0^L \rho HAdx = \Sigma\ (\dot{m}H)_{in} - \Sigma\ (\dot{m}H)_{out} - \int_0^L (\dot{w}H)_{ox}P_w dx$$

$$+ \Sigma \int_0^L h(T_w - T)P_w dx \qquad \text{(A.3)}$$

(Enthalpy rate of change in control volume)
= (Enthalpy inflow) - (Enthalpy outflow)
- (Enthalpy term for oxygen consumed in reaction) + (Heat convection from structures to air flows)

d. Enthalpy-Specific Heat Relationship

$$H = \int_0^T c_p dT \qquad \text{(A.4)}$$

e. Equation of State

$$p = \rho RT \qquad \text{(A.5)}$$

f. Heat Transfer Coefficient

$$h = \frac{k}{D_H} Nu_D(Re,\ Gr,\ Pr) \qquad \text{(A.6)}$$

g. Shear Stress

$$\tau_w = \frac{\dot{m}^2}{2\rho A^2} c_f(Re,\ Pr) \qquad \text{(A.7)}$$

Values of $Nu_D(Re, Gr, Pr)$ and $c_f(Re, Pr)$ are obtained from analyses and correlations (see Section V, below).

At each time step, inlet values of $\dot{m}$ are assumed for each flow path based on the solution obtained from the previous time step, and the equations of conservation are solved for each flow path. Resulting exit pressures obtained for upward-directed vertical flows are compared with the pressure in the room above, p_r, and exit pressures obtained for downward-directed vertical flows are compared with the computed base flow pressures, $p_b(x)$. The assumed inlet mass flows are adjusted in an iterative manner, using a modified Newton-Raphson approach, until the pressure discrepancies are negligibly small for each flow path exit.

A3. Equations for Fuel Rods, Structural Elements, and Concrete Encasement

a. Fuel Rods

$$\frac{d}{dt}\int_0^L \rho_w c_{p,w} T_w A_w dx = q_{decay} + q_{chem} + \left(k_w A_w \frac{\partial T_w}{\partial x}\right)_{x=L} - \left(k_w A_w \frac{\partial T_w}{\partial x}\right)_{x=0} - \Sigma \int_0^L h(T_w - T) P_w dx - \Sigma \int_0^L \varepsilon_{w,w'} \sigma (T_w^4 - T_{w'}^4) P_w dx \qquad (A.8)$$

(Rate of heat storage) = (Decay heat) + (Heat from chemical oxidation) - (Conduction losses) - (Convection from fuel rods to air flows) - (Radiative transfer from fuel rods to neighboring structures)

The heat storage term includes both fuel and clad, viz.

$$(\rho c_p A)_w \equiv (\rho c_p A)_{fuel} + (\rho c_p A)_{clad} \tag{A.9}$$

b. Structural Elements (Channels, Baskets, Liners)

$$\frac{d}{dt} \int_0^L \rho_w c_{p,w} T_w A_w dx = - \Sigma \int_0^L h(T_w - T) P_w dx$$

$$- \Sigma \int_0^L \varepsilon_{w,w'} \sigma (T_w^4 - T_{w'}^4) P_w dx \tag{A.10}$$

(Rate of heat storage) = - (Convection from structure to air flows) - (Radiative transfer from structure to neighboring structures and fuel rods)

c. Concrete Pool Encasement -- The heat absorbed into the concrete sides and bottom of the pool is determined by an approximate technique which proves to be quite accurate. Let $T_\ell(t)$ be the temperature of the pool liner (which is assumed to be equal to the concrete surface temperature) at some point on the liner as a function of time, and let t_n denote the current time. Replace this temperature history with an approximation, $T_\ell'(t)$, defined as being equal to the initial temperature, T_o, from time zero until a time $\hat{t}$, and equal to the temperature $T_\ell(t_n)$ from time $\hat{t}$ to time t_n. Let $\hat{t}$ be defined in such a way as to conserve the integral $\int_0^{t_n} T_\ell(t)\, dt$, viz.

$$\hat{t} = \frac{t_n T_\ell(t_n) - \int_0^{t_n} T_\ell(t) dt}{T_\ell(t_n) - T_o} \tag{A.11}$$

With this approximation, the heat absorbed by the concrete from time zero to time t_n can be shown, via the error-function solution, to be equal to

$$\int_o^{t_n} \dot{q}(t)dt = \left[\frac{(\rho c_p k)_{conc}(t_n - \hat{t})}{\pi}\right]^{\frac{1}{2}} \left[T_\ell(t_n) - T_o\right] \qquad \text{(A.12)}$$

Equations (A.11) and (A.12) are used to determine the accumulated heat absorption into the concrete, with an estimated error, due to the approximation, of no more than six percent.

A4. Equations for Containment Building

Refer to Section 3.4 in the main text for an overall discussion of the heat transfer problem in the containment building and to Figure 10 for an illustrative schematic.

a. Conservation of Mass, Room Atmosphere

$$V_r \frac{d\rho_r}{dt} = -\Sigma\dot{m}_{ox} - \dot{m}_{leak} + \dot{V}_{vent} (\rho_o - \rho_r) \qquad \text{(A.13)}$$

(Mass accumulation rate in room) = - (Oxygen depletion rate, clad reaction) - (Leak rate) + (Air exchange rate by forced venting)

b. Conservation of Species (Oxygen), Room Atmosphere

$$V_r \frac{d(f_r\rho_r)}{dt} = - \Sigma\ \dot{m}_{ox} - f_r\dot{m}_{leak} + \dot{V}_{vent} (f_o\rho_o - f_r\rho_r) \qquad \text{(A.14)}$$

(Oxygen accumulation rate) = - (Oxygen depletion rate, clad reaction) - (Oxygen leak rate) + (Oxygen exchange rate by forced venting)

c. Conservation of Energy, Room Atmosphere

$$V_r \frac{d(\rho_r H_r)}{dt} = \Sigma(\dot{m}H)_{sf,out} - (\Sigma\dot{m}_{sf,in})H_r - \dot{m}_{leak}H_r$$

$$+ \dot{V}_{vent}(\rho_o H_o - \rho_r H_r) - h_s A_s (T_r - T_s) \quad \text{(A.15)}$$

(Enthalpy rate of change) = (Enthalpy outflow from spent fuel array) - (Enthalpy inflow to spent fuel array) - (Enthalpy outflow due to leakage) + (Net enthalpy inflow due to forced venting) - (Convective loss to heat sinks/structures)

The building structure is treated as a single entity with a heat transfer coefficient governed by the correlations for free convection to a vertical plate.

d. Enthalpy-Specific Heat Relationship

$$H = \int_0^T c_p dT \quad \text{(A.16)}$$

e. Equation of State

$$p = \rho RT = \frac{\gamma-1}{\gamma} \rho H \quad \text{(A.17)}$$

The leakage rate is determined by specifying $dp_r/dt = 0$ when the room pressure reaches a maximum allowable value, p_{max}:

f. Leakage Rate

$\dot{m}_{leak} = 0$ if $p_r < p_{max}$ or the expression below ≤ 0.

$$\dot{m}_{leak} = \frac{1}{H_r} \left[\Sigma(\dot{m}H)_{sf,out} - (\Sigma\dot{m}_{sf,in})H_r + \dot{V}_{vent}(\rho_o H_o - \rho_r H_r) - h_s A_s (T_r - T_s) \right] \quad \text{otherwise} \quad \text{(A.18)}$$

g. Heat Sinks/Containment Building Structures

$$(\rho c_p A\delta)_s \frac{dT_s}{dt} = h_s A_s (T_r - T_s) + \Sigma\varepsilon_{ts}\sigma A_t (T_t^4 - T_s^4)$$

$$- h_o A_s (T_s - T_o) - \varepsilon_s \sigma A_s (T_s^4 - T_o^4) \quad \text{(A.19)}$$

(Rate of heat storage) = (Convective heat transfer from room air) + (Radiative transfer from upper tie plates, spent fuel array) - (Convective loss to outside) - (Radiative loss to outside)

A5. Nusselt Number and Skin Friction Coefficient

Expressions for Nu_D(Re, Gr, Pr) and c_f(Re, Pr) used in Equations (A.6) and (A.7) are tabulated in Table A-I, next page. On any occasion when the Nusselt number is required, the program calculates values of the parameter for each of the three cases listed in Table A-I, namely (1) forced convection past a flat plate, (2) forced convection between parallel plates or longitudinally past an array of parallel tubes, and (3) free convection past a vertical plate. The first and third cases correspond to situations where the boundary layer velocity profile is not fully developed and is dominated by either viscous forces or buoyancy forces, respectively. The second case corresponds to a fully-developed velocity profile where, by its nature, viscous forces are predominant. The hydraulic diameter is assumed to be the operative parameter in extending Case 2 to other geometries. As indicated by the footnote under Table A-I, the dominant case is assumed to be that which provides the highest value of Nu_D among the three possibilities. The heat transfer coefficient so obtained is assumed to be driven by the local temperature difference, $T_w - T$, as indicated by Equations

Table A-I.

Equations Used for Nusselt Number and Skin Friction Coefficient*

Flow Geometry	Laminar Flow	Turbulent Flow
Forced Convection Parallel to a Flat Plate	$(Nu_D)_1 = 0.332\ Re_x^{0.5} Pr^{0.33} \left(\frac{D_H}{x}\right)$ $(c_f)_1 = 0.664\ Re_x^{-0.5}$ $Re_x \leq 5 \times 10^5$ Blasius Solution [A.1]	$(Nu_D)_1 = .0296\ Re_x^{0.8} Pr^{0.6} \left(\frac{D_H}{x}\right)$ $(c_f)_1 = .0592\ Re_x^{-0.2}$ $Re_x > 5 \times 10^5$ "Power Law" Solution [A.1]
Forced Convection Between Parallel Plates (Applied Outside Fuel Element)	$(Nu_D)_2 = 7.54 + 0.0234\ Re_D Pr \left(\frac{D_H}{L}\right)$ $(c_f)_2 = 24/Re_D$ $Re_D \leq 3000$ Poiseuille Solution [A.1]	$(Nu_D)_2 = 0.023\ Re_D^{0.8} Pr^{0.4}$ $(c_f)_2 = 0.0014 + 0.125\ Re_D^{-0.32}$ $Re_D > 3000$ Correlation [A.1, A.2]
Longitudinal Forced Convection Between Parallel Tubes in an Infinite Array (Applied Inside Fuel Element)	$(Nu_D)_2 = 8$ $(c_f)_2 = 25/Re_D$ $Re_D \leq 3000$ Sparrow-Loeffler [A.3]	Assumed to be same as (2a).
Free Convection Past a Vertical Plate	$(Nu_D)_3 = 0.36\ Gr_x^{0.25} \left(\frac{D_H}{x}\right)$ $Gr_x \leq 1 \times 10^9$, $Pr = 0.71$ Correlation [A.1]	$(Nu_D)_3 = 0.116\ Gr_x^{0.33} \left(\frac{D_H}{x}\right)$ $Gr_x > 1 \times 10^9$, $Pr = 0.71$ Correlation [A.1]

*To obtain Nusselt number for a particular condition, take the maximum of $(Nu_D)_1$, $(Nu_D)_2$, and $u_D)_3$. To obtain skin friction coefficient, take the maximum of $(c_f)_1$ and $(c_f)_2$.

(A.3) and (A.10). The skin friction coefficient is evaluated by a similar procedure, except that the buoyancy-driven alternative is deleted.

It should be observed that in the process of exercising the code, the flow inside the fuel elements was almost always governed by laminar fully-developed forced convection, Case 2b, except in the immediate entrance region. Flows in the interspaces between baskets or down the liner along the side of the pool were sometimes dominated by forced convection, Cases 1 and 2a, and sometimes by free convection, Case 3.

A6. Code Validation

To validate the SFUEL code, comparisons of SFUEL results were made against (1) hand calculations, (2) approximate analytical solutions, and (3) experimental data [Ref. A.4, A.5]. The code was considered to be validated when all of these comparisons were positive.

The comparison with experimental data is of particular interest because it provides some insight into the accuracy of some of the assumptions. The experimental models consisted of long, narrow, open-ended channels (6.0-ft high, 4.5-ft wide, 1.5-inch to 15-inches deep) suspended vertically in room air (65°F) with the side walls heated to 135°F and the end walls insulated against heat loss. Steady-state heat transfer rates governed by naturally induced convection through the inside of the channel were measured at three elevations, and are shown in Fig. A-1, next page. While the geometries considered in the experiments do not exactly duplicate a typical spent fuel storage configuration, they show some similarity in regard to the large channel heights and narrow wall spacings.

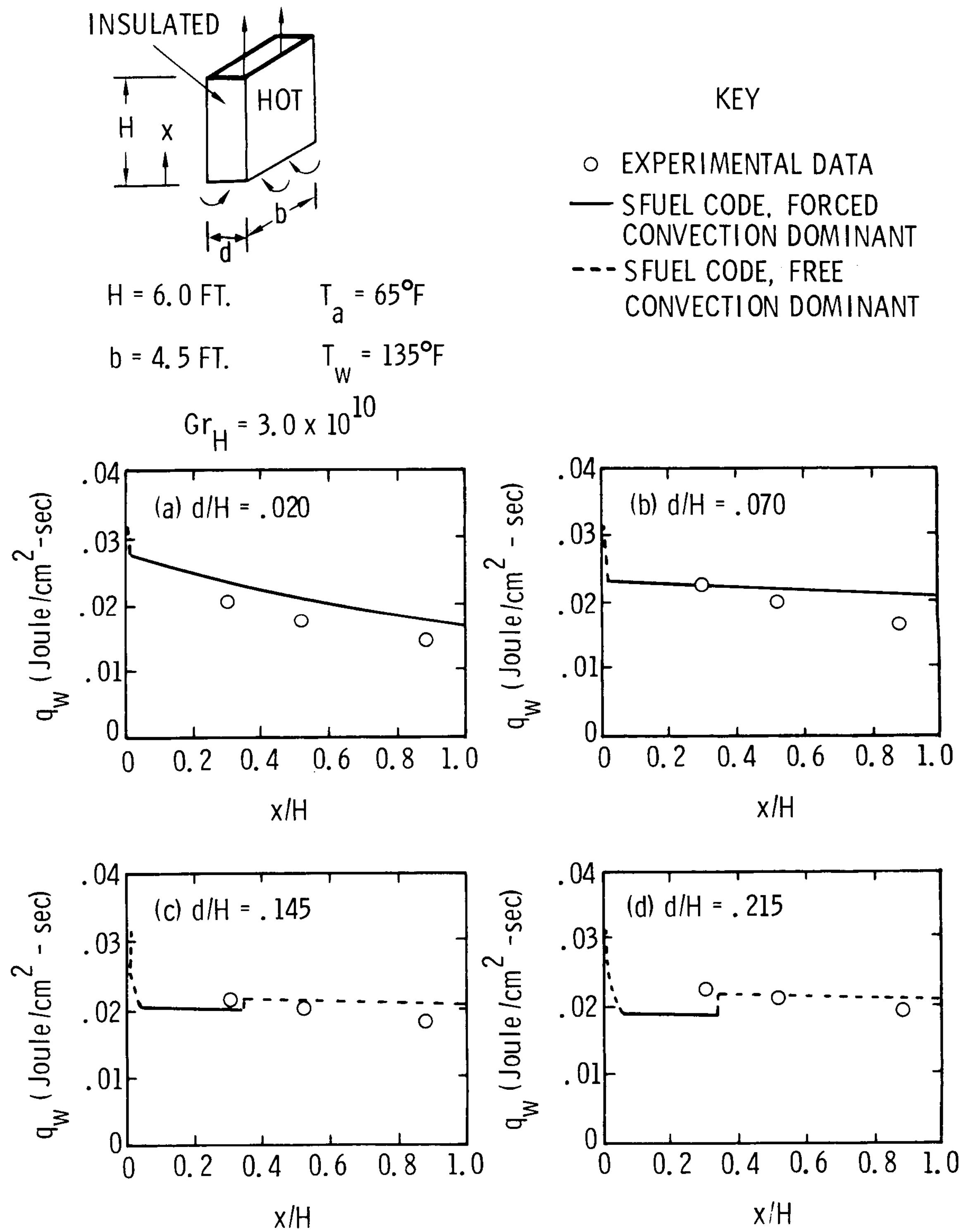

Figure A-1. Comparison of Heat Transfer Predictions With Experiment, Natural Convection Flow Through a Vertical Channel

The solid and dashed curves in Fig. A-1 correspond to SFUEL predictions based on heat transfer coefficients obtained from Table A-I (Cases 2a and 3, respectively), together with solution of the flow conservation equations to obtain the gas-side driving function, $T_w - T$, as a function of elevation. According to the assumption that the dominant heat transfer mechanism is that producing the highest heat rate (Section V), laminar free convection is indicated to be the dominant mode very near the entrance. Fully-developed turbulent, forced convection dominates at the higher elevations, except when the wall-to-wall spacing is fairly large (Fig. A-1, parts c and d), where the predictions indicate a change to turbulent free convection as the driving mechanism near the exit.

It is not certain whether the transition from turbulent forced convection to turbulent free convection in parts c and d of Fig. A-1 is real, there being a reasonable argument to support the idea that the flow is probably in a mixed state for these cases. However, the advantage of the model is not in its ability to predict the mode of heat transfer but in its ability to predict the amount of heat transfer, and in this regard it may be noted that the predictions are generally within 20 percent of the data. This level of accuracy is considered quite reasonable in view of the fact much of the error may be due to experimental uncertainty.

A7. Approximations for Open Frame Configuration

The open frame configuration (Fig. 2a in the main text) is more difficult to analyze because of the lack of defined flow paths. On the other hand, it is obviously a very coolable configuration, because of the openness of the structure and the large spacings between elements, so that a detailed, exact flow calculation was not deemed necessary from a practical viewpoint.

For the open frame configuration, a considerably abbreviated version of SFUEL was created based on an overall heat transfer coefficient approximation that obviated the need to solve the gas phase conservation equations at all. The driving function for the heat transfer coefficient was the difference between the local clad temperature and the room air temperature, $T_w - T_r$, and the values of the heat transfer coefficient were estimated by using experimental data [Ref. A.5] applicable to laminar or turbulent natural convection between narrowly spaced walls or within narrowly spaced channels. These heat transfer coefficients were evaluated in the form of correction factors, having values less than 1.0, to the case of natural convection past an isolated, vertical plate. They were applied to the internal fuel pins of the spent fuel assemblies by estimating an equivalent "wall-to-wall spacing" based on flow area considerations. The correction factor was taken as being 1.0 for the outermost fuel pins.

The calculations for the open frame configuration should be viewed as very approximate, with minimum allowable decay times being accurate, perhaps, to within a factor of two.

References

A.1. D.K. Edwards, V.E. Denny, and A.F. Mills, Transfer Processes, Holt, Rinehart, and Winston, New York, 1973.

A.2. H. Schlichting, Boundary Layer Theory, 4th ed., McGraw Hill, New York, 1960.

A.3. E.M. Sparrow, A.L. Loeffler, Jr., and H.A. Hubbard, "Heat Transfer to Longitudinal Laminar Flow Between Cylinders," Transactions ASME: Jl. Heat Transfer, 415-422, 1961.

A.4. R. Siegel and R.H. Norris, "Tests of Free Convection in a Partially Enclosed Space Between Two Heated Vertical Plates," ASME Transactions, 79, 663, 1957.

A.5. R.H. Norris, F.F. Buckland, N.D. Fitzroy, R.H. Roecker, and D.A. Kaminski, eds., Heat Transfer Data Book, General Electric Co., Schenectady, N.Y., 1978 update.

APPENDIX B

APPROXIMATE ANALYSES ASSOCIATED WITH SPENT FUEL HEATUP CALCULATIONS

CONTENTS

FIGURES

B1. Nomenclature

English Symbols

A	Area of door or chimney opening
A_w	Water surface area inside holder or basket*
C_D	Discharge coefficient (taken as 0.6)
c_p	Specific heat
D	Inner diameter of radiating cylinder
D_H	Hydraulic diameter
g	Acceleration of gravity (980 cm/sec^2)
H	Specific enthalpy
h	Heat transfer coefficient
$H_{v,w}$	Latent heat of vaporization of water (2250 Joule/gm)
L	Length of spent fuel rod*
L_r	Height of containment room
$\dot{m}$	Mass rate of flow
$\dot{m}_{leak}$	Leakage rate from building to external atmosphere
p	Pressure
P_o	Decay power per metric ton of uranium
P_w	Wetted perimeter
q_{ca}	Rate of heat convected to air, per assembly
q_{cs}	Rate of heat convected to steam, per assembly
q_d	Decay heat rate per assembly
Q_{decay}	Total decay heat rate generated in pool

*Asterisks call attention to differences between Appendix B nomenclature and Appendix A nomenclature.

Nomenclature (continued)

English Symbols

q_{dw}	Decay heat rate generated beneath water level, per assembly
q_{rb}	Rate of heat radiation to building, per assembly
q_{rw}	Rate of heat radiation absorbed by water, per assembly
R	Gas constant for air (2.871×10^6 dy-cm/gm-°K)
$\dot{S}_w$	Surface recession rate of water
T	Temperature
t	Time
T_{boil}	Boiling temperature of water
t_{boil}	Time after drainage until initiation of boiling of remaining water
T_c	Clad temperature
$T_{c,max}$	Maximum clad temperature within fuel assembly
T_{max}	Maximum allowable room temperature
V_r	Volume of room
$\dot{V}_{vent}$	Volumetric venting rate
W_U	Weight (metric tons) of uranium per assembly
z	Vertical distance measured from bottom of fuel rods
z_w	Elevation of water surface level, measured from bottom of fuel rods

Nomenclature (continued)

Greek Symbols

δ_w	Depth of residual water, measured from bottom of pool
θ	Angle between radiation path and vertical*
η	Dummy variable
ρ	Density
σ	Stefan-Boltzmann constant (5.67×10^{-12} Watt/cm^2-°K^4)

Subscripts

lb	Lower bound
o	Outside atmosphere
r	Containment room
s	Steam*
sf	Spent fuel
ub	Upper bound
w	Water*

B2. Forced Air Ventilation Requirements

The derivation in this section leads to Equation (5) in Section 4.2 of the main text, and provides the means for calculating the desirable forced air ventilation rates tabulated in Table VII of the main text.

The equations of mass balance and energy balance for the room atmosphere were presented in Appendix A, viz. Equations (A.13) and (A.15). Neglecting heat convection to walls and structures and chemical oxidation of the clad, it is possible to write these equations as follows:

$$V_r \frac{d\rho_r}{dt} = -\dot{m}_{leak} + \dot{V}_{vent} (\rho_o - \rho_r) \tag{B.1}$$

$$V_r \frac{d(\rho_r H_r)}{dt} = \Sigma \dot{m}_{sf} (H_{sf} - H_r) - \dot{m}_{leak} H_r + \dot{V}_{vent} (\rho_o H_o - \rho_r H_r) \tag{B.2}$$

Using the definition of enthalpy (Equation A.16) and the perfect gas equation of state (Equation A.17), together with the following approximation for a very leaky building:

$$p_r = p_o \tag{B.3}$$

and the following assumption of equilibrium between the total decay heat production, Q_{decay}, and its removal by natural convection:

$$\Sigma \dot{m}_{sf} (H_{sf} - H_r) = Q_{decay} \tag{B.4}$$

it is possible to reduce Equations (B.1) and (B.2) to the following differential equation for the temperature of the room air:

$$\frac{dT_r}{dt} = \left[\frac{R\ Q_{decay}}{p_o V_r c_p} + \frac{\dot{V}_{vent}}{V_r}\right] T_r - \frac{\dot{V}_{vent}}{V_r T_o} T_r^{\ 2} \qquad (B.5)$$

Equation (B.5) has a steady-state temperature value given by

$$T_r = \left(1 + \frac{R\ Q_{decay}}{p_o c_p \dot{V}_{vent}}\right) T_o \qquad (B.6)$$

which indicates that if the room air is to remain within a maximum of T_{max} for all time, the venting rate must satisfy the following inequality:

$$\dot{V}_{vent} \geqslant \frac{T_o}{T_{max} - T_o} \ \frac{R\ Q_{decay}}{p_o c_p} \qquad (B.7)$$

B3. Door/Chimney Requirements to Produce Chimney Effect

The question of providing an adequate chimney effect also can be approached from an approximate point of view, from which one can estimate the size of open doors/windows that would be required. Assume that at the time of the pool drainage, a door of area A is opened at ground level to allow fresh air to enter the building, and that a chimney hole of similar area, A, is opened in the ceiling, above the pool, to allow hot air to escape. Air entering the building through the door at temperature T_o is assumed to enter the exposed spent fuel array at the same temperature, to be circulated and then discharged into the room at a higher temperature, T_{sf}. The discharged air is then assumed to mix completely with the room atmosphere (a conservative assumption), so that the air which is expelled to the outside through the chimney hole possesses the temperature of the room, T_r. The room atmosphere itself is assumed to be in thermal equilibrium, so that the rate of air inflow through the door, $\dot{m}$, is equalled by the outflow through the chimney.

Neglecting inertia and viscous effects, which can be shown to be of secondary importance in this problem, one can write an equation expressing conservation of momentum from the door to the chimney hole in terms of entrance and exit losses and buoyancy forces, viz.

$$\Delta p = \frac{1}{2C_D^2} \left(\frac{\dot{m}}{A}\right)^2 \left[\frac{1}{\rho_o} + \frac{1}{\rho_r}\right] + \rho_r g L_r \tag{B.8}$$

The pressure change, Δp, must also be equated to the outside hydrostatic pressure change over the height L_r, viz.

$$\Delta p = \rho_o g L_r \tag{B.9}$$

With the room in thermal equilibrium, however, it can also be assumed that

$$\dot{m} c_p (T_r - T_o) = Q_{decay} \tag{B.10}$$

By combining Equations (B.8), (B.9), and (B.10) to eliminate Δp and $\dot{m}$ and by introducing the perfect gas equation of state, one may derive the following transcendental expression for the steady-state temperature of the room:

$$T_r = T_o + \frac{Q_{decay}}{C_D c_p \rho_o A \sqrt{2gL_r}} \sqrt{\frac{T_r(T_o + T_r)}{T_o(T_r - T_o)}} \tag{B.11}$$

Equation (B.11) can be rearranged as a cubic equation and solved explicitly for T_r. However, the objective is to determine the door/chimney hole size that insures a maximum room temperature of T_{max}, or less. By rearranging Equation (B.11), the following inequality is obtained:

$$A \geq \frac{Q_{decay}}{C_D c_p \rho_o \sqrt{2gL_r}} \sqrt{\frac{T_{max}(T_o + T_{max})}{T_o(T_{max} - T_o)^3}} \qquad \text{(B.12)}$$

Equation (B.12) corresponds to Equation (6) in the main text and is the basis for the door/chimney hole sizes reported in Table VII of the main text.

B4. Effect of Incomplete Drainage

The equations presented in this section support the analysis of incomplete drainage described in Section 5.1 of the main text and, in particular, are the basis for the numbers presented in Table VIII.

a. Heat Transferred to Water by Decay Heat, Per Assembly -- Using Equation (1) of the main text (Section 3.1) to characterize the distribution of decay heat along the fuel rods, the portion produced under the water level can be written as

$$q_{dw} = \frac{W_U P_o}{2} \left\{ 1 - \frac{\cos\left[\frac{\pi}{42}\left(40\frac{z_w}{L} + 1\right)\right]}{\cos\left[\frac{\pi}{42}\right]} \right\} \qquad \text{(B.13)}$$

b. Heat Transferred to Water by Radiation from Above, Per Assembly -- The heat transferred to the water by thermal radiation from the hot fuel rods and structure above is a complicated problem which depends upon the details of the geometry. It is possible, however, to make lower-bound and upper-bound estimates of this radiation contribution by considering two limiting cases. For the lower-bound estimate, assume that the fuel pin array is so dense that one can approximate the radiating source as being a horizontal flat plate located just above the water level and having a temperature equal to the clad temperature at this level. Assuming black-body radiation, the radiation absorbed by the water inside a basket is given by

$$(q_{rw})_{lb} = \sigma A_w \left[T_c^{\,4}(z_w) - T_w^{\,4} \right] \tag{B.14}$$

If the water level is beneath the bottom of the fuel rods, (i.e., if $z_w < 0$), replace $T_c(z_w)$ by $T_c(0)$.

For the upper-bound estimate, consider the radiating surface to be a vertical, right circular cylinder having an axial length equal to that of the full assembly and a cross-sectional internal flow area equal to that of the basket or holder. The temperature distribution on this radiating cylinder is equal to that of the fuel pins, $T_c(z)$, but the fuel pins themselves are considered to be physically absent. This approximation will overestimate the radiation received by the water because of the removal of the blocking or shadowing effects caused by the presence of the pins. As a further approximation in the same direction, consider the radiation flux at the surface of the water to be uniform and equal to that at the centerline. The radiation absorbed by the water within the basket is then given by

$$(q_{rw})_{ub} = \sigma A_w \int_{\theta_1}^{\theta_2} 2 \left[T_c^{\,4}(z) - T_w^{\,4} \right] \sin\theta \cos\theta \, d\theta \tag{B.15}$$

where θ, D, and z are depicted in Fig. B-1. By defining

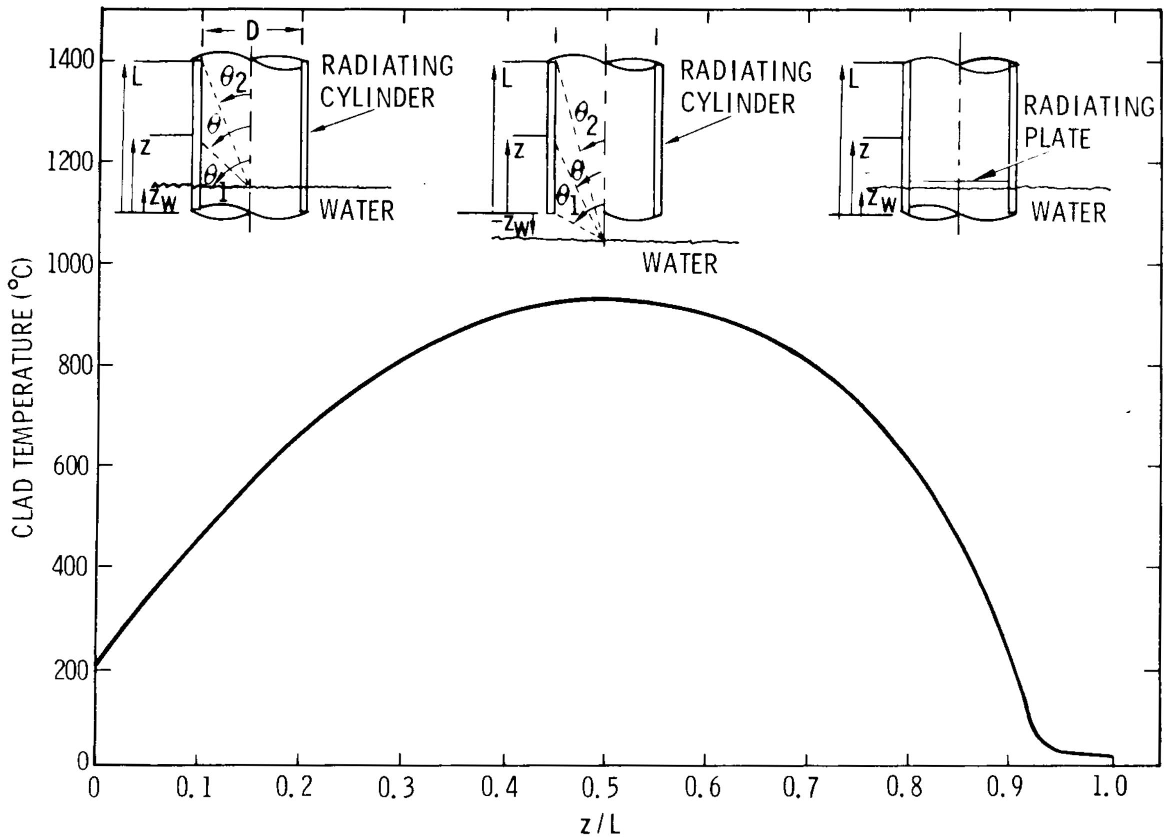

Figure B-1. Clad Temperature Distribution Used to Calculate Radiation to Water

$$\eta(z) = \sin^2\theta(z) = \frac{D^2}{(z - z_w)^2 + D^2} . \tag{B.16}$$

Equation (B.15) may also be written as

$$(q_{rw})_{ub} = \sigma A_w \int_{\eta(L)}^{\eta(z_w)} \left[T_c^{\,4}(\eta) - T_w^{\,4} \right] d\eta \tag{B.17}$$

If $z_w < 0$, replace $\eta(z_w)$ by $\eta(0)$ in Equation (B.17).

To evaluate the radiation received by the water via Equation (B.14) or (B.17), the temperature distribution along the fuel pins must be known a priori. In order to obtain the estimates in Table VIII of the main text, it was assumed that the fuel pin temperature had risen to the point where clad failure was imminent. The particular temperature distribution used is shown in Figure B-1 and was taken from the printout corresponding to the curve labeled "Blocked Inlets" in Fig. 26 of the main text. The low temperatures at the top end of the fuel rods, depicted in Figure B-1, are caused by local natural convection cooling as described in Subsection h.

c. Time to Start Boiling -- Assuming that the water drains instantaneously to the given level, z_w, and that all the fuel elements are of the same age, the time required to raise the water temperature to its saturation or boiling point can be estimated by

$$t_{boil} = \frac{\rho_w c_{p,w} A_w \delta_w (T_{boil} - T_o)}{q_{dw} + q_{rw}} \tag{B.18}$$

This time will be lengthened somewhat if q_{dw} and q_{rw} correspond to the hottest elements in a pool having spent fuel with varying decay times.

d. Water Surface Recession Rate -- Under the same assumption of uniform decay times, the water surface recession rate after initiation of boiling can be estimated by

$$\dot{S}_w = \frac{q_{dw} + q_{rw}}{\rho_w A_w H_{v,w}} \tag{B.19}$$

This recession rate will be reduced somewhat if the pool contains older elements and the water is free to seek a uniform level.

e. Decay Heat Produced Above Water Level, Per Assembly -- Based on Equation (1) of the main text, the portion of decay heat produced above the water level can be written as

$$q_d - q_{dw} = \frac{W_U\ P_o}{2} \left\{ 1 + \frac{\cos\left[\frac{\pi}{42} \left(40\ \frac{z_w}{L} + 1 \right) \right]}{\cos\left[\frac{\pi}{42} \right]} \right\} \qquad (B.20)$$

f. Heat Radiated to Building, Per Assembly -- The lower-bound and upper-bound estimates of heat radiated to the building, analogous to Equations (B.14) and (B.17), are

$$(q_{rb})_{lb} = \sigma A_w \left[T_c^{\,4}(L) - T_o^{\,4} \right] \qquad (B.21)$$

and

$$(q_{rb})_{ub} = \sigma A_w \int_{\eta(z_w)}^{\eta(L)} \left[T_c^{\,4}(\eta) - T_o^{\,4} \right] d\eta \qquad (B.22)$$

where

$$\eta(z) = \frac{D^2}{(L - z)^2 + D^2} \qquad (B.23)$$

Replace $\eta(z_w)$ by $\eta(0)$ in Equation (B.22) if $z_w < 0$.

g. Heat Convected to Steam, Per Assembly -- The maximum amount of heat that can be removed by convection to the vapor produced by boiling is the sensible heat corresponding to a steam temperature rise from the saturation temperature to the maximum clad temperature. This heat convection rate is given by

$$q_{cs} = \frac{q_{dw} + q_{rw}}{H_{v,w}}\ C_{p,s}\ (T_{c,max} - T_{boil}) \qquad (B.24)$$

h. Heat Convected to Air, Per Assembly -- The amount of heat that can be removed by natural convection of air into the fuel assembly is limited by the blockage of the inlets caused by the residual water. In this situation, air must enter and exit through the top of the assembly. Analysis and experiments indicate that for long, narrow channels that are closed at the bottom and open at the top, the effectiveness of natural convection is limited to the top portion of the channel where the vertical penetration distance, L-z, is less than 25 times the wall spacing. Using hydraulic diameter as a common denominator, this implies that only the top 10 percent or so of the fuel assembly is coolable by natural convection of air. This figure will be reduced still further by steam generation from water boiling, which tends to further block the penetration of the air.

Based on the preceding discussion, the heat removed by convection to air is estimated to be

$$q_{ca} = P_w \int_{L-12.5D_H}^{L} h(z) \left[T_c(z) - T_r\right] dz \qquad \text{(B.25)}$$

where

$$D_H = \frac{4A}{P_w} \qquad \text{(B.26)}$$

The heat transfer coefficient, h(z), is taken to be that for natural convection from an isolated vertical plate, Case (3) in Table A-1.

APPENDIX C

RADIATION DOSE FROM A DRAINED SPENT FUEL POOL

CONTENTS

FIGURES

TABLES

C1. Introduction

This appendix supports Section 5.3 of the main text by determining the dose rate to personnel performing emergency actions in the vicinity of the drained spent fuel pool.

The MORSE-SGC code (Ref. C.1), a Monte Carlo radiation transport program, was used to determine the tissue dose rate at ground level at various distances from a drained PWR on-site spent fuel storage pool, 30 days after a full core discharge. To simplify the analysis, the calculation was separated into two parts. In the first part the gamma ray emission rate through the top of an infinite array of spent fuel rods was determined, neglecting the presence of the air, the pool boundaries, and the spent fuel holders. The result of this calculation was then used as the source in a second calculation which determined the dose rates out to a radius of 550 m from the center of the pool. The second calculation included the effects of the air, the sides of the pool, and the ground outside the pool but neglected the presence of the containment building. Division of the analysis into two parts neglects multiple scattering at the sides of the pool, but this effect is small except near the edges of the fuel array.

Only gamma radiation was considered in this analysis. The dose rate on the surface of a PWR spent fuel assembly with a nominal burnup (33,000 MWD/MTU) and a 150-day decay time is approximately 2.4×10^6 rad/hr from gamma rays, compared with 0.25 rem/hr from neutrons. The relative gamma ray and neutron dose rates continue to be of this order of magnitude at longer cooling times of interest in this study, and thus the neutron contribution to the tissue dose rate may be neglected.

The cross sections used in the present calculations were an 11-group, P_3 set generated with the GAMLEG code (Ref. C.2). The energy group structure and dose conversion factors for this cross section set are shown in Table C-I. The dose factors were obtained from Ref. C.3.

TABLE C-I.

Gamma Ray Cross Section Group Structure and Sources

Energy Group	Upper Energy Bound (MeV)	Dose Factor $\left(\frac{mr/hr}{photons/cm^2\text{-}sec}\right)$	Gamma Ray Source in 30-day Cooled PWR Spent Fuel (photons/MTU-sec)	Calculated Gamma Ray Emission Rate Through Top of Spent Fuel Array (photons/MTU-sec)	fsd*
1	3.5	4.36×10^{-3}	3.15×10^{12}	5.63×10^{10}	0.029
2	3.0	4.00	1.48×10^{14}	2.54×10^{12}	0.025
3	2.6	3.71	6.37×10^{14}	1.09×10^{13}	0.030
4	2.2	3.24	1.01×10^{15}	1.69×10^{13}	0.030
5	1.8	2.77	1.56×10^{16}	2.41×10^{14}	0.033
6	1.35	2.30	4.29×10^{15}	8.90×10^{13}	0.044
7	0.9	1.51	1.80×10^{17}	2.67×10^{15}	0.056
8	0.4	0.83	9.31×10^{15}	7.30×10^{14}	0.088
9	0.2	0.36	-	6.09×10^{13}	0.187
10	0.1	0.37	-	-	-
11	0.01	0.37×10^{-3}	-	-	-

*fsd = fractional standard deviation of the Monte Carlo result

C2. Calculation of the Gamma Radiation Escaping Through the Top of the Spent Fuel Storage Array

In a typical PWR storage pool, the fuel assemblies, each containing 264 fuel rods, 24 guide thimble tubes, and 1 instrumentation tube in a 17 x 17 array, are stored upright on a rectangular pitch of 33.02 cm (13 inches). Around each assembly, which is 21.4 cm (8.426 inches) square, is a stainless steel basket or holder and above the fuel pins is a rod cluster control assembly, a nozzle, and a set of alignment pins. Thus the spent fuel array presents a relatively complex geometry for use in a radiation transport analysis. To make the problem tractable, a simplified model was used to determine the intensity of gamma rays escaping through the top of the spent fuel array.

Diffusion of the gamma rays axially through the dry fuel array will be dominated by streaming of the radiation along the coolant paths between the fuel rods and in the gaps between the fuel elements and the stainless steel racks. To account for this streaming, a geometry model consisting of an infinite array of equally-spaced PWR fuel rods having a pitch of 1.905 cm (0.75 inch) was used (see Fig. C-1). This pitch was chosen to provide the correct amount of void space for a group of assemblies on 13-inch centers, and not to duplicate the actual rod-to-rod spacing within a single assembly. The steel racks were not included in the geometry.

The source used in this calculation was generated with the ORIGEN code (see Refs. 8 and 9 in the main text). The fresh fuel was assumed to be 3.3 percent enriched in ^{235}U. The 33,000 MWD/MTU burnup was achieved over a 3-year operating life assuming an 80 percent use factor and 30-day annual refueling intervals. Decay heat for this case was presented in the main text, Table III, Case (1). The corresponding gamma ray source for 30-day-cooled spent fuel discharged after the third cycle is shown in Table C-I, normalized to 1 metric ton of uranium charged to the reactor.

Source photons with energies below 200 keV are produced by bremsstrahlung, by Auger reactions, and by other sources. They are significantly lower both in intensity and penetration than the gamma rays with energies above 200 keV and have been neglected in the present calculation.

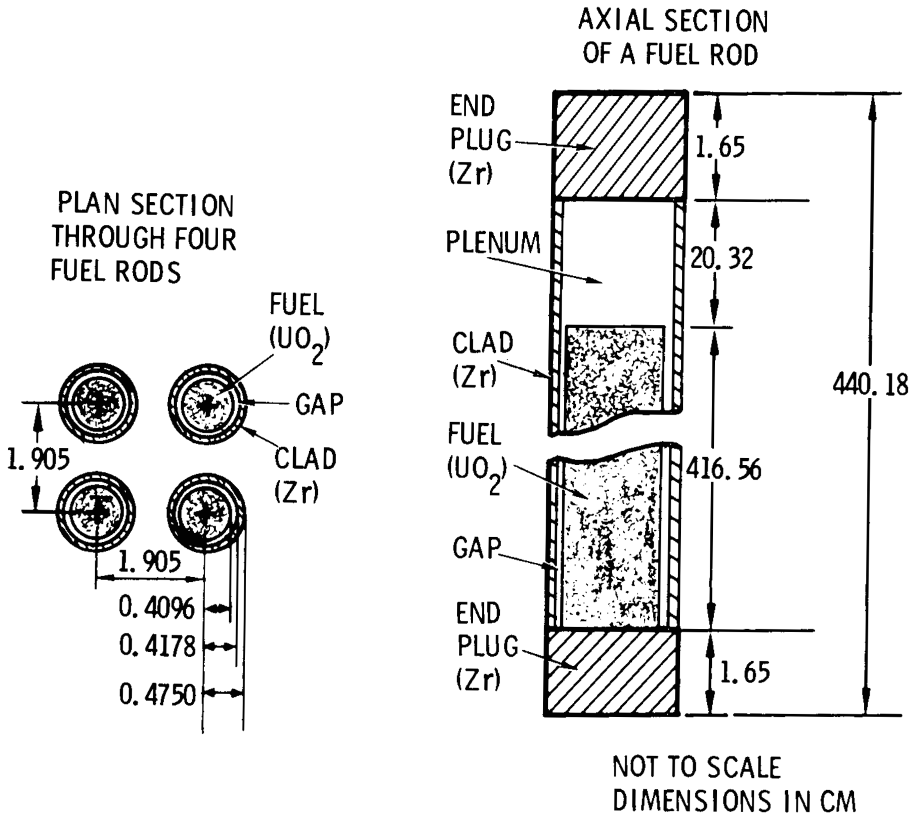

Figure C-1. MORSE Geometry Model of a PWR Spent-Fuel Storage Array

The energy spectrum of gamma rays emitted from spent fuel softens with increasing decay time; therefore, to be conservative (i.e., to maximize the calculated gamma dose rate above the fuel), all the gamma rays were assumed to be born with the 30-day energy spectrum of Table C-I, regardless of the age of the fuel. Furthermore, the gamma source varies with axial position in a fuel rod due to the buckling of the neutron flux, the presence of partially withdrawn control rods, and other factors. The maximum gamma intensity is usually located at a point near the axial center of the core. In addition, the escape probability of a gamma ray varies markedly with the axial location at which it is born, being much higher near the top of the fuel pins than at the center or bottom. However, for the present calculation, the gamma source obtained from ORIGEN was assumed to be constant along the entire length of the active fuel and equal to the average value. The conservatism in this assumption is estimated to be around 30 percent.

The calculated gamma ray leakage through the top of the spent fuel array is shown as a function of energy in the last two columns of Table C-I for 30-day cooled spent fuel. Under the present model the average probability of a gamma ray, born at random in the spent fuel rods, escaping through the top of the array was determined to be 0.0181 ± 0.0008.

The photons leaking through the top of the spent fuel array have an anisotropic angular distribution from streaming through the coolant channels. Thus, in the MORSE calculation, the escaping gamma rays were "scored" as a function of their velocity vector with respect to the upward-directed normal to the top surface of the spent fuel array. The calculated angular distribution, summed over energy, is shown in Figure C-2. The error bars represent the Monte Carlo statistical standard deviation. It is apparent that relatively few photons are emitted tangential to the top of the array and that most of the gamma rays are emitted in a cone with a solid angle of about π steradians. The average escape angle for the gamma rays is about 47° to normal.

The energy and angular dependences of Table C-I and Figure C-2 were used to define the source in the second part of this analysis. The angular variation was assumed to be the same for all energy groups. A major source of uncertainty in the results of the calculation to this point is in the simplified geometry model of the spent fuel storage array. However, several conservative assumptions were made (e.g., the uniform distribution of the gamma source over the length of the fuel rods and the omission of the upper fuel element hardware), which make it highly unlikely that the gamma ray leakage through the top of the spent fuel array has been underestimated.

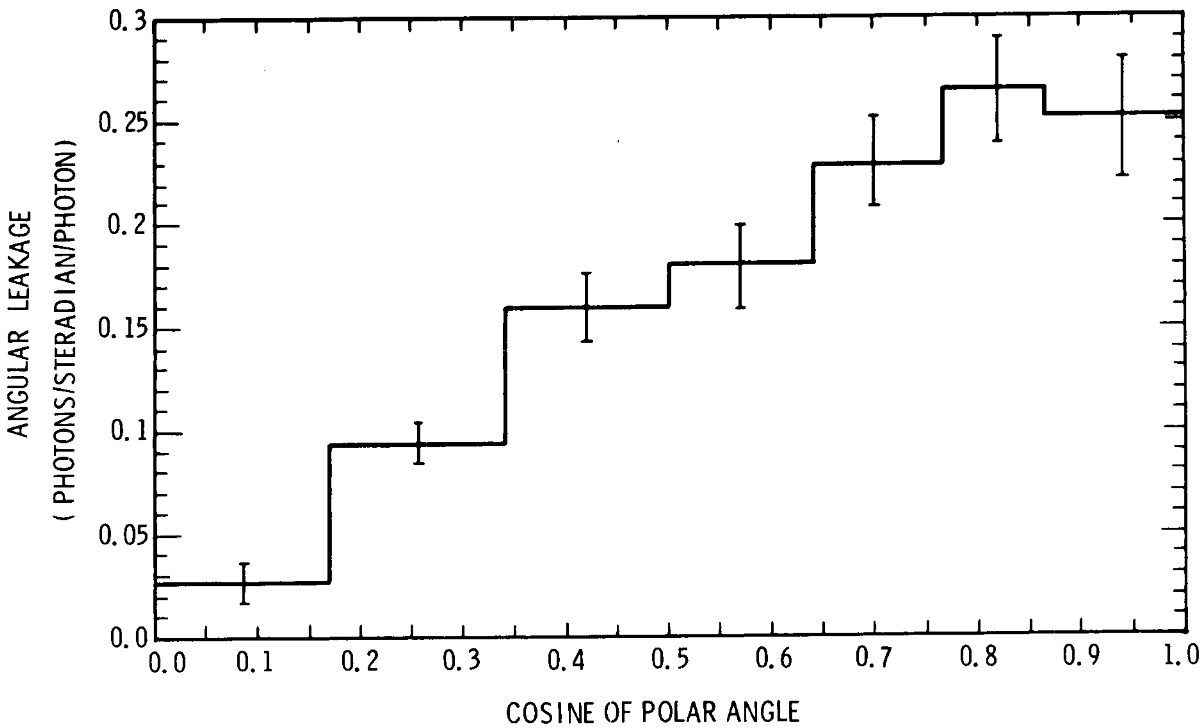

Figure C-2. Angular Dependence of Photons Escaping Through the Top of the Spent Fuel Storage Array

C3. Calculation of the Gamma Ray Tissue Dose Rate at Various Distances from the Pool

To complete the calculation of the gamma dose rate at ground level, the leakage determined in the first calculation was input to the air-over-ground geometry shown in Figure C-3. The source plane was located 762 cm (25 ft) below ground level in a concrete pool 825.5 by 1056.64 cm (27.08 by 34.67 ft). The pool can thus hold 32 rows of 25, or 800 total, PWR spent fuel assemblies on a 33.02 cm (13 inch) pitch. This represents a capacity of approximately 4 PWR cores at 193 fuel assemblies per core.

For the present calculation the assumption has been made that the storage pool is full of spent fuel. From a radiation

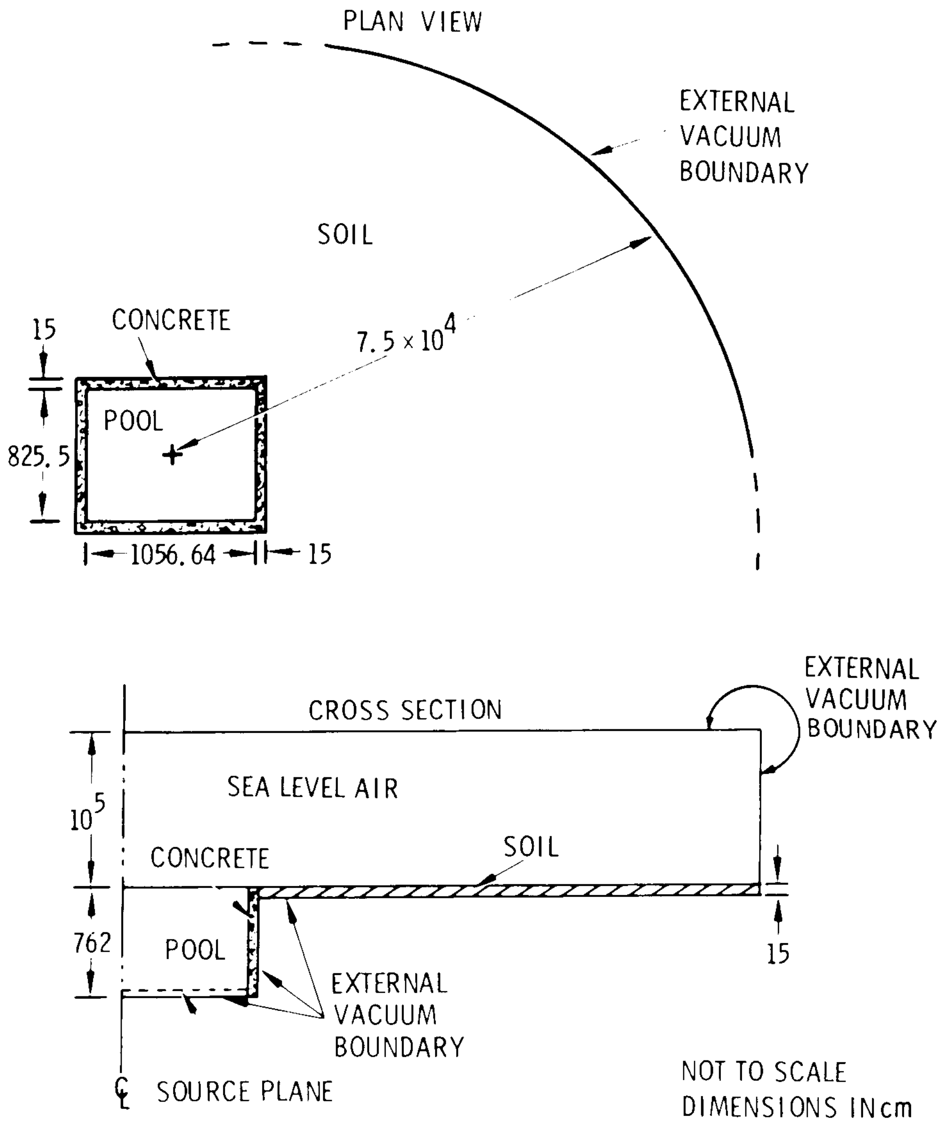

Figure C-3. MORSE Geometry Model of a PWR Spent Fuel Storage Pool and Surroundings

standpoint this may not be the worst case. In the absence of water, empty portions of the pool would provide a streaming path for the escape of radiation emitted from points at the center and bottom of the fuel rods. Thus a partially empty storage pool might result in a higher radiation dose rate on the surface than the fully loaded pool considered here.

For the present analysis, a severe fuel loading pattern has been assumed, in which the most active elements correspond to a full core of 30-day-old spent fuel divided into thirds having burnups of 33,000, 22,000 and 11,000 MWD/MTU, respectively (i.e., a full core discharge). The remaining positions in the pool are filled with full cores having decay times of 1, 2 and 3 years, respectively, and a uniform burnup of 33,000 MWD/MTU.

No systematic attempt was made to determine the worst-case distribution of the fuel elements from the four cores; instead, the distribution shown in Figure C-4 was assumed. In this distribution, photons emitted at 45° to normal from the 30-day-cooled core assemblies have approximately a 20-percent probability of being emitted in an azimuthal direction that will give them a direct line-of-sight to the surface. The loading distribution shown in Figure C-4 is believed to be more severe than, say, a uniform or random distribution of the six types of fuel elements.

The source strength for each source region is also shown in Figure C-4 in units of photons/cm^2-sec. (The source shown for the 30-day-cooled core is the average for the 3 burnups used.) These figures were obtained by multiplying the ORIGEN-calculated gamma source rates for each source region (photons/MTU-sec) by the escape probability (.0181) and the weight loading of the pool (7.5×10^{-9} MTU/cm^2). The total source from the pool is 4.1×10^{17} photons/sec, of which approximately 77 percent is contributed by the 30-day-cooled elements.

The calculated gamma ray tissue dose rate at ground level from the dry PWR spent fuel storage pool is shown in Figure C-5. The results are based on calculated free field gamma ray fluxes 1 meter above ground level, and hence represent whole-body dose rates to personnel standing on the ground. These dose rates have been averaged over the direction taken from the center of the pool, and therefore represent a mean dose rate for all points on a circle having the radius given by the abscissa. The variation of dose rate with azimuthal angle is small at large distances from the center of the pool (about 25 m or more), but becomes large as the detector approaches the lip of the pool. Thus the azimuthally-averaged dose rate becomes less meaningful as the edge of the pool is approached, and the results are therefore indicated by dashed lines in this region.

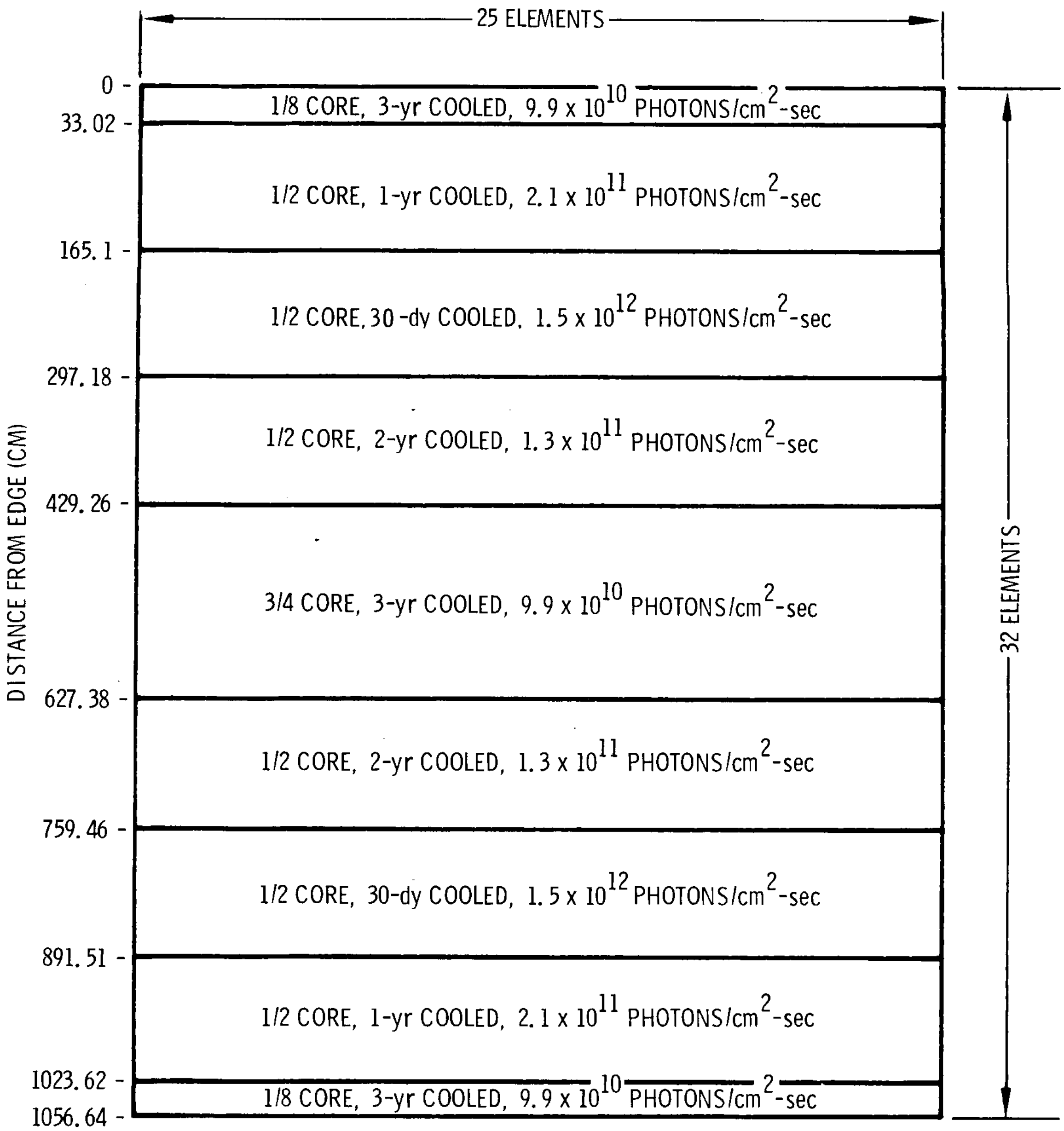

Figure C-4. Source Distribution in Spent Fuel Storage Pool

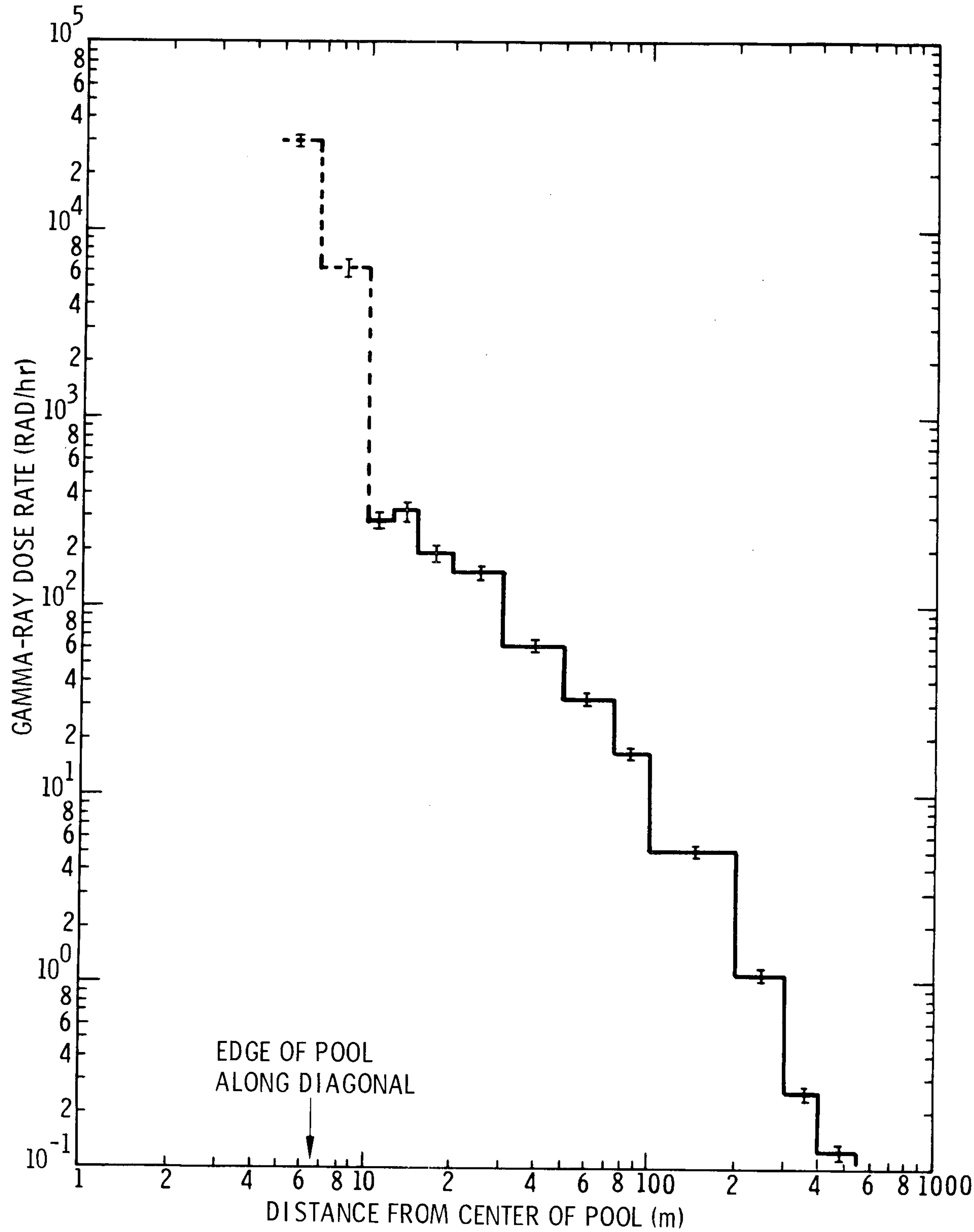

Figure C-5. Whole Body Gamma Ray Dose Rate at Ground Level as a Function of Distance From a Dry PWR Spent Fuel Storage Pool

The error bars shown in Figure C-5 indicate the statistical standard deviation of the Monte Carlo results and are not a measure of the overall accuracy of the solution. Such accuracy is a function of the calculational models, the source definition, the cross sections, the material compositions, and other factors, including the statistical uncertainty. Because a series of conservative assumptions was made in obtaining the present results, the upside uncertainty in the data shown in Figure C-5 is probably +25 to +30 percent, whereas the downside uncertainty is probably -30 to -50 percent.

References

C.1. S.K. Fraley, User's Guide to MORSE-SGC, ORNL/CSD-7, Oak Ridge National Laboratory, 1976.

C.2. J.H. Renken and K.G. Adams, An Improved Capability for Solution of Photon Transport Problems by the Method of Discrete Ordinates, SC-RR-69-739, Sandia Laboratories, 1969.

C.3. American National Standard Neutron and Gamma Ray Flux-to-Dose-Rate Factors, ANSI/ANS-6.1.1-1977 (N666), American Nuclear Society, 1977.

APPENDIX D

SFUEL INPUT, OUTPUT, AND PROGRAM LISTING

CONTENTS

TABLES

D1. SFUEL Input

The input for SFUEL is entered via namelist under the heading $INPUT. The following list provides the names and dimensions of the variables, their definitions and units, and the nominal values built into the program.

INPUT VARIABLE NAME	DEFINITION	NOMINAL VALUE
ASINK	Surface area of sheet metal walls and ceilings in containment building (cm^2)	0.
CPCØN	Specific heat of concrete (Joule/gm-°K)	1.047
CPL	Specific heat of liner material (Joule/gm-°K)	0.460
CPNI	Specific heat of nitrogen (Joule/gm-°K)	1.130
CPØX	Specific heat of oxygen (Joule/gm-°K)	1.130
CPS	Specific heat of channel structure, BWR elements (Joule/gm-°K)	0.364
CPW	Specific heat of holder wall (Joule/gm-°K)	0.883
CSINK	Heat capacity of sheet metal walls and ceilings in containment building (Joule/°K)	0.
DAMP	Damping factor for mass flow iteration	0.
DELT	Computational time step (sec)	50.
DLFACT	Factor by which time step is reduced if fuel rod temperature exceeds TRDELT	1.
DMWTR(3)	Mass rate of spray water addition per per assembly (gm/sec):	3*0.

INPUT VARIABLE NAME	DEFINITION	NOMINAL VALUE
	DMWTR(1): amount collecting on fuel rods	
	DMWTR(2): amount collecting on channels (BWR)	
	DMWTR(3): amount collecting on holders	
EPC	Emissivity of the clad	0.7
EPL	Emissivity of the pool liner	0.3
EPS	Emissivity of the channel structure, BWR elements	0.7
EPT	Emissivity of the tie plates	0.7
EPW	Emissivity of the holder walls	0.2
FDECAY(8)	Decay power per unit fuel weight, for each section of pool (KW/MTU). Operative only if FMULT<0.	-
FL	Active length of the fuel rods (cm)	-
FMULT	Multiplier on decay heat rate. If negative, program multiplies FDECAY input by absolute value of FMULT. If positive, program uses built-in tables of decay power ratio versus cooling time, and multiplies these values by FMULT.	1.0
FSTR	Flag indicating whether holders are directional (FSTR=0.5) or nondirectional (FSTR=1.0). Fig. 2e in the main text shows a directional holder.	-
IBLØCK	Flag indicating which vertical flow paths are blocked.	0
	IBLØCK=0: all flow paths open	
	IBLØCK=1: no flow through fuel elements	
	IBLØCK=2: no flow between channel and holder (BWRs)	
	IBLØCK=3: no flow between holders.	

INPUT VARIABLE NAME	DEFINITION	NOMINAL VALUE
ICHEM	Flag for chemical oxidation of clad: 0 - off, 1 - on	0
IPLØT	Plot flag: 0 - off, 1 - on	0
KMAX	Maximum mass flow iterations per time step	15
N	Number of node points in vertical direction	21
NASS(8)	Number of assemblies for each section of pool, counted along a single row from the middle to the edge of the pool	-
NCEND	Flag indicating last case (if NCEND=1) of a series of stacked cases	0
NDECAY	Number of entries in FDECAY, only if FMULT<0.	-
NPRINT	Number of time intervals between printouts. Also a flag indicating long print (if positive) or short print (if negative).	36
NPRNEW	Number of time intervals between printouts if fuel rod temperature exceeds TRPNT	1
NRØD	Number of rods per assembly (including control rods, if present)	-
NSECT	Number of sections in pool. I.e., number of separate fuel clusters in a row from the center to an edge of the pool.	-
PØWØ	If FMULT<0, number of metric tons of uranium per assembly. If FMULT>0, operating power per assembly (KW).	-
PRMAX	Maximum room pressure (absolute) sustainable without leakage (dyne/cm^2)	1.151×10^6
RCI	Inner clad radius (cm)	-
RCØ	Outer clad radius (cm)	-
RF	Fuel radius (cm)	-
RHØC	Density of clad material (gm/cm^3)	6.5

INPUT VARIABLE NAME	DEFINITION	NOMINAL VALUE
RHØCØN	Density of concrete (gm/cm^3)	2.34
RHØF	Density of UO_2 fuel (gm/cm^3)	10.4
RHØL	Density of pool liner material (gm/cm^3)	7.82
RHØS	Density of channel structure material, BWR elements (gm/cm^3)	6.5
RHØW	Density of holder wall material (gm/cm^3)	2.79
RØWS	Number of rows of fuel elements evaluated so that the total number of assemblies in the pool is equal to RØWS*(NASS(1)+ NASS(2)+---+NASS(NSECT))	-
SMB	Constant in decay power axial distribution equation, Eqn. (1) in main text	.025
SMKCØN	Thermal conductivity of concrete (Watt/ cm-°K)	.012
TIMAX	Termination time in spent fuel heat-up calculation (sec)	36000.
TIMEØ(8)	Decay time for each section of pool (used only if FMULT<0)	-
TIMWØF	Time when water spray is turned off (sec)	$1. \times 10^9$
TIMWØN	Time when water spray is turned on, TIMWØN<TIMWØF (sec)	0
TØ	Outside ambient temperature (°K)	283.
TRDELT	Maximum fuel rod temperature allowed before cutback of time step (°K)	$1. \times 10^9$
TRMAX	Maximum fuel rod temperature allowed before termination of case (°K)	$1. \times 10^9$
TRPNT	Maximum fuel rod temperature allowed before change of print interval (°K)	$1. \times 10^9$
UL	Length of inactive part of fuel rods (cm)	0
VENT	Volume exchange rate for forced air room ventilation system (cm^3/sec)	0

INPUT VARIABLE NAME	DEFINITION	NOMINAL VALUE
VRØØM	Containment room volume (cm^3)	-
WS	Inside distance between parallel walls of a channel if present, BWR elements (cm)	-
WW	Inside distance between parallel walls of a holder or basket (cm)	-
XB	Thickness of liner on bottom of pool (cm)	.635
XKBØT	Coefficient of $(\frac{1}{2})\rho U^2$ in equation for pressure drop due to constriction of flow through baseplate hole	0.
XKTØP	Coefficient of $(\frac{1}{2})\rho U^2$ in equation for pressure drop due to constriction of flow at top of assembly	0.
XL	Thickness of liner on bottom of pool (cm)	.635
XS	Thickness of channel structure if present, BWR element (cm)	0.
XTB	Distance from bottom pool liner to lower tie plate or baseplate (cm)	40.6
XW	Thickness of holder or basket wall (cm)	-
XWL	Distance from sidewall pool liner to nearest holder or basket wall (cm)	-
XWW	Distance between adjacent holder or basket walls (cm)	-

A sample input listing is shown in Table D-I. This particular case corresponds to PWR spent fuel with a 1-year minimum decay time, full core discharge loading, cylindrical baskets, large baseplate hole, perfect ventilation (see Fig. 12, lowest curve, in main text).

TABLE D-I

Sample Input Listing

SFX4

ASINK=	0
CSINK=	0
DAMP=	0
DELT=	5.000E+01
DLFACT=	1.000E+00
DMWTR=	0
	0
	0
FL=	3.660E+02
FSTR=	1.000E+00
IBLOCK=	3
ICHEM=	0
IPLOT=	0
N=	21
NCEND=	1
NPRINT=	-36
NPRNEW=	1
NROD=	289
NSECT=	6
POWO=	4.614E-01
PRMAX=	1.151E+06
RCI=	4.180E-01
RCO=	4.750E-01
RF=	4.010E-01
ROWS=	0
SMB=	2.500E-02
TIMAX=	9.000E+03
TIMWOF=	1.000E+09
TIMWON=	0
TRDELT=	1.000E+09
TRMAX=	2.073E+03
TRPNT=	1.000E+09
UL=	0
VENT=	0
VROOM=	4.250E+09
WS=	2.140E+01
WW=	2.800E+01
XB=	6.350E-01
XL=	6.350E-01
XS=	0
XTB=	4.060E+01
XW=	3.510E-01
XWL=	4.060E+01
XWW=	3.690E+00

CPCON=	1.047E+00
CPL=	4.600E-01
CPNI=	1.130E+00
CPOX=	1.130E+00
CPS=	3.640E-01
CPW=	4.600E-01
EPC=	7.000E-01
EPL=	3.000E-01
EPS=	7.000E-01
EPT=	7.000E-01
EPW=	3.000E-01
FMULT=	-1.000E+00
KMAX=	15
NDECAY=	16
RHOC=	6.500E+00
RHOCON=	2.340E+00
RHOF=	1.040E+01
RHOL=	7.820E+00
RHOS=	6.500E+00
RHOW=	7.820E+00
SMKCON=	1.200E-02
TO=	2.830E+02
XKBOT=	0
XKTOP=	0

J	NASS	FDECAY
1	1	2.720E+00
2	4	3.760E+00
3	4	5.050E+00
4	4	5.900E+00
5	4	8.200E+00
6	4	1.104E+01

D2. SFUEL Output

The user has a choice of long or short output format, depending upon the sign of the input quantity NPRINT (see preceding definition of input quantities). The only difference between the two options is that the long output format includes a printout for each identified section of the pool, whereas the short output format provides output only for the section of the pool containing the hottest elements (j = NSECT). A sample short-format output is shown in Table D-II, these results corresponding to the input of Table D-I with an elapsed real time of t = 2.0 hours. The variables shown in Table D-II are defined below in the order of their appearance in the output.

Table D-II

Sample Short-Format Output

```
SFX4                                   *** TIME = 7.200E+03 ***

KIT= 1   DPFRAC= 9.817E-03   DGFRAC= 2.439E-03   TRMAX= 1.210E+02   TROOM= 1.000E+01   PROOM= 1.013E+06   TSINK= 1.000E+01
```

I	TL(I)	J	TB(J)	TA4AVE(J)	PA4AVE(J)	FOXAVB(J)	GNIAVB(J)	GNI(J,1)	GNI(J,2)	GNI(J,3)
1	1.031E+01	1	1.029E+01	1.090E+01	4.236E+02	2.300E-01	2.456E+02	1.257E+01	1.000E-10	-5.039E+02
2	1.032E+01	2	1.038E+01	1.090E+01	4.276E+02	2.300E-01	4.536E+02	7.500E+01	1.000E-10	-2.000E-10
3	1.035E+01	3	1.038E+01	1.091E+01	4.251E+02	2.300E-01	3.729E+02	8.680E+01	1.000E-10	-2.000E-10
4	1.038E+01	4	1.037E+01	1.092E+01	4.251E+02	2.300E-01	2.829E+02	9.322E+01	1.000E-10	-2.000E-10
5	1.041E+01	5	1.037E+01	1.093E+01	4.246E+02	2.300E-01	1.814E+02	1.099E+02	1.000E-10	-2.000E-10
6	1.045E+01	6	1.038E+01	1.096E+01	4.244E+02	2.300E-01	6.323E+01	1.265E+02	1.000E-10	-2.000E-10
7	1.049E+01									
8	1.052E+01									
9	1.056E+01									
10	1.058E+01									
11	1.060E+01									
12	1.060E+01									
13	1.061E+01									
14	1.059E+01									
15	1.058E+01									
16	1.053E+01									
17	1.050E+01									
18	1.044E+01									
19	1.039E+01									
20	1.030E+01									

J= 6

I	TR	TAVE1	I1	TS	TAVE2	I2	TW	TAVE3	I3	FCT	FCX	IS
1	1.555E+01	1.160E+01	3	1.198E+01	1.000E+01	0	1.198E+01	1.197E+01	1	1.538E-04	2.300E-01	0
2	2.082E+01	1.347E+01	3	1.426E+01	1.000E+01	0	1.426E+01	1.423E+01	1	1.538E-04	2.300E-01	0
3	2.713E+01	1.647E+01	3	1.770E+01	1.000E+01	0	1.770E+01	1.764E+01	1	1.538E-04	2.300E-01	0
4	3.419E+01	2.057E+01	3	2.220E+01	1.000E+01	0	2.220E+01	2.209E+01	4	1.538E-04	2.300E-01	0
5	4.185E+01	2.568E+01	3	2.771E+01	1.000E+01	0	2.771E+01	2.756E+01	4	1.538E-04	2.300E-01	0
6	4.994E+01	3.168E+01	3	3.406E+01	1.000E+01	0	3.406E+01	3.366E+01	4	1.538E-04	2.300E-01	0
7	5.828E+01	3.845E+01	3	4.114E+01	1.000E+01	0	4.114E+01	4.087E+01	4	1.538E-04	2.300E-01	0
8	6.672E+01	4.581E+01	3	4.874E+01	1.000E+01	0	4.874E+01	4.842E+01	4	1.538E-04	2.300E-01	0
9	7.509E+01	5.362E+01	3	5.671E+01	1.000E+01	0	5.671E+01	5.631E+01	4	1.538E-04	2.300E-01	0
10	8.322E+01	6.168E+01	3	6.482E+01	1.000E+01	0	6.482E+01	6.438E+01	4	1.538E-04	2.300E-01	0
11	9.094E+01	6.982E+01	3	7.291E+01	1.000E+01	0	7.291E+01	7.237E+01	4	1.538E-04	2.300E-01	0
12	9.810E+01	7.785E+01	3	8.073E+01	1.000E+01	0	8.073E+01	8.016E+01	4	1.538E-04	2.300E-01	0
13	1.045E+02	8.557E+01	3	8.812E+01	1.000E+01	0	8.812E+01	8.744E+01	4	1.538E-04	2.300E-01	0
14	1.101E+02	9.279E+01	3	9.485E+01	1.000E+01	0	9.485E+01	9.416E+01	4	1.538E-04	2.300E-01	0
15	1.147E+02	9.935E+01	3	1.008E+02	1.000E+01	0	1.008E+02	9.996E+01	4	1.538E-04	2.300E-01	0
16	1.181E+02	1.051E+02	3	1.057E+02	1.000E+01	0	1.057E+02	1.049E+02	4	1.538E-04	2.300E-01	0
17	1.202E+02	1.098E+02	3	1.094E+02	1.000E+01	0	1.094E+02	1.085E+02	4	1.538E-04	2.300E-01	0
18	1.210E+02	1.134E+02	3	1.119E+02	1.000E+01	0	1.119E+02	1.110E+02	4	1.538E-04	2.300E-01	0
19	1.203E+02	1.158E+02	3	1.130E+02	1.000E+01	0	1.130E+02	1.120E+02	4	1.538E-04	2.300E-01	0
20	1.155E+02	1.163E+02	3	1.118E+02	1.000E+01	0	1.118E+02	1.106E+02	4	1.538E-04	2.300E-01	0

```
EGEN=    4.602E+08   ECHEM=  0.          EFUEL=  1.744E+08   ESTR=   0.          EHOLCR= 4.741E+07   ERAD=   2.551E+06
ELINRS= 1.304E+04    ELINRB= 1.571E+04   ECONCS= 5.670E+04   ECONCB= 9.647E+04   ECONV1= 1.426E+09   ECCNV2= 0.
ECONV3=-1.190E+09    ESTAIR= 3.292E+05   EREMOR= 1.352E-02   EROOM=  0.          ESINK=  0.          ELCSS=  0.

PGEN=    6.391E+04   PCHEM=  0.          PFUEL=  1.928E+03   PSTR=   0.          PHOLCR= 1.185E+03   PRAD=   7.217E+02
PLINRS= 1.696E+00    PLINRB= 2.010E+00   PCONCS= 1.372E+01   PCONCB= 1.871E+01   PCONV1= 2.693E+05   PCCNV2= 0.
PCONV3=-2.093E+05    PSTAIR= 3.804E+00   PREMOR= 2.243E-06   QROOM=  0.          QSINK=  0.          CLCSS=  0.
```

OUTPUT VARIABLE NAME	DEFINITION
TIME	Elapsed real time (sec)
KIT	Number of mass flow iterations performed
DPFRAC	Relative pressure change between last two mass flow iterates
DGFRAC	Relative mass flow change between last two mass flow iterates
TRMAX	Maximum fuel rod temperature in pool (°C)
TRØØM	Room temperature (°C)
PRØØM	Room pressure, absolute (dyne/cm^2)
TSINK	Temperature of heat sinks in containment building (°C)
I	Nodal index for vertical direction. Vertical distance from bottom of fuel rods = $(I-\frac{1}{2})\Delta X$.
TL(I)	Temperature of sidewall liner (°C)
J	Section of pool, measured from pool side toward center of pool. J = NSECT corresponds to hottest elements, which are located in center of pool. Each section consists of the number of fuel assemblies given in the input under NASS, assumed to be aligned in a single row.
TB(J)	Temperature of liner along bottom of pool (°C)
TA4AVE(J)	Temperature of air flow along bottom of pool (°C)
PA4AVE(J)	Gage pressure of air flow along bottom of pool (dyne/cm^2)
FØXAVB(J)	Oxygen mass fraction for air flow along bottom of pool
GNIAVB(J)	Nitrogen mass flow rate along bottom of pool, for a one-assembly flow path width (gm/sec)
GNI(J,1)	Nitrogen mass flow rate within fuel assemblies located in Section J, positive upward (gm/sec)

OUTPUT VARIABLE NAME	DEFINITION
GNI(J,2)	Nitrogen mass flow rate between channel structure and holder/basket for assemblies located in Section J, BWR elements (gm/sec)
GNI(J,3)	Nitrogen mass flow rate between adjacent holder walls for assemblies located in Section J (gm/sec)
TR	Temperature of fuel rods (°C)
TAVE1	Temperature of air flow within fuel assemblies (°C)
I1	Index indicating which heat transfer correlation was used for air flow within fuel assemblies: 1: laminar free convection 2: laminar forced convection, entrance flow 3: laminar forced convection, fully developed 4: turbulent free convection 5: turbulent forced convection, entrance flow 6: turbulent forced convection, fully developed
TS	Temperature of channel structure, if present (°C)
TAVE2	Temperature of air flow between channel structure and holder/basket, BWR elements (°C)
I2	Index indicating which heat transfer correlation was used for air flow between channel structure and holder/basket, BWR elements
TW	Temperature of holder or basket wall
TAVE3	Temperature of air flow between adjacent holder walls (°C)
I3	Index indicating which heat transfer correlation was used for air flow between adjacent holder walls
RCT	Depth of chemical oxidation of clad (cm)
FØX	Oxygen mass fraction for air flow within fuel assembly
IS	Index indicating type of chemical reaction - 1: kinetics rate limited; 2: oxygen diffusion limited

OUTPUT VARIABLE NAME	DEFINITION
EGEN	Total energy generated by decay heat, per row (Joule)
ECHEM	Total energy produced by chemical reaction, per row (Joule)
EFUEL	Total energy absorbed by fuel rods, per row (Joule)
ESTR	Total energy absorbed by channel structures if present, per row (Joule)
EHØLDR	Total energy absorbed by holders/baskets, per row (Joule)
ERAD	Total energy radiated to building by upper tie plates, per row (Joule)
ELINRS	Total energy absorbed by sidewall liner, per row (Joule)
ELINRB	Total energy absorbed by bottom liner, per row (Joule)
ECØNCS	Total energy conducted into sidewall concrete, per row (Joule)
ECØNCB	Total energy conducted into bottom concrete, per row (Joule)
ECØNV1	Total energy convected out of spent fuel array by air flows within fuel assemblies, per row (Joule)
ECØNV2	Total energy convected out of spent fuel array by air flows between channel structures and holder walls, BWR elements, per row (Joule)
ECØNV3	Total energy convected out of spent fuel array by air flows between adjacent holders, per row (Joule)
ESTAIR	Total energy assigned to air currently within spent fuel array (Joule)
EREMDR	Total energy balance error for spent fuel pool, per row (Joule)

OUTPUT VARIABLE NAME	DEFINITION
EINTØ	Total energy transferred into room atmosphere by spent fuel air flows (Joule)
ESINK	Total energy absorbed by containment building heat sinks (Joule)
ELØSS	Total energy lost to outside atmosphere by leakage, forced venting, and radiation/convection from building structure (Joule)
PGEN	Current rate of heat (power) generation by decay, per row (Watt)
PCHEM	Current rate of heat production by chemical reaction, per row (Watt)
PFUEL	Current rate of heat absorption by fuel rods, per row (Watt)
PSTR	Current rate of heat absorption by channel structures if present, per row (Watt)
PHØLDR	Current rate of heat absorption by holders/ baskets, per row (Watt)
PRAD	Current rate of heat radiation to building by upper tie plates, per row (Watt)
PLINRS	Current rate of heat absorption by sidewall liner, per row (Watt)
PLINRB	Current rate of heat absorption by bottom liner, per row (Watt)
PCØNCS	Current rate of heat conduction into sidewall concrete, per row (Watt)
PCØNCB	Current rate of heat conduction into bottom concrete, per row (Watt)
PCØNV1	Current rate of heat convection out of spent fuel array by air flows within fuel assemblies, per row (Watt)
PCØNV2	Current rate of heat convection out of spent fuel array by air flows between channel structures and holder walls, BWR elements, per row (Watt)

OUTPUT VARIABLE NAME	DEFINITION
PCØNV3	Current rate of heat convection out of spent fuel array by air flows between adjacent holders, per row (Watt)
PSTAIR	Rate of energy increase of air within spent fuel array (Watt)
PREMDR	Current heat rate balance error for spent fuel pool, per row (Watt)
PINTØ	Current rate of heat transferral into room atmosphere by spent fuel air flows (Watt)
PSINK	Current rate of heat absorption by containment building heat sinks (Watt)
PLØSS	Current rate of heat loss to outside atmosphere by leakage, forced venting, and radiation/ convection from building structure (Watt)

```
      PROGRAM SFUEL(INPUT,OUTPUT,TAPE5=INPUT,TAPE6=OUTPUT,TAPE40)
C
C        GLOBAL TWO-DIMENSIONAL PROGRAM TO CALCULATE FUEL
C        TEMPERATURE RISE IN A BWR OR PWR SPENT FUEL POOL
C        WITH NO WATER.
C
      DIMENSION AB(8), AC(8), AF(8), AR(8), AS(8), ASPL(8), AT(8)
      DIMENSION AW(8), AWPL(8), AXA1(8), AXA2(8), AXA3(8), CB(8)
      DIMENSION COEFF1(3), COEFF2(3), CS(8), CW(8), DELY(8)
      DIMENSION DGNI(8,3), DMWTR(3), DP(8,3), DPO1(8,3), DPO2(8,3)
      DIMENSION DPO3(8,3), DPO4(8,3), DQB(8), DQL(31), DQS(31,8)
      DIMENSION DQW(31,8), FACS(8), FASK(8), FATB(8), FATSNK(8)
      DIMENSION FDBWR(21), FDECAY(21), FDPWR(21), FOX(31,8), FOXAVB(8)
      DIMENSION GCPB(8,3), GNI(8,3), GNIAVB(8), GNIB(9), GNIO1(8,3)
      DIMENSION GNIO2(8,3), GNIO3(8,3), GNIO4(8,3)
      DIMENSION GOX(31), GOXB(9), GOXBOT(8,3), HBA4(8), HDR(31,8)
      DIMENSION HRA1(31,8), HRA2(31,8), HSA1(31,8), HSA2(31,8)
      DIMENSION HTA4(8), HWA2(31,8), HWA3(31,8), HWJM1(31,8)
      DIMENSION IDECAY(8), IND1(31,8), IND2(31,8), IND3(31,8), IS(31,8)
      DIMENSION NASS(8), NOT(3), OXM(31,8), PA1(31), PA2(31), PA3(31)
      DIMENSION PA4(9), PA4AVE(8), PTAU(9), PTAUAV(8)
      DIMENSION Q(31), QB(8), QCB(8), QCBTOT(8), QCHEM(31,8)
      DIMENSION QCL(31), QCLTOT(31), QCOND(31), QDECAY(31,8)
      DIMENSION QL(31), QR(31,8), QS(31,8), QTBOT(8)
      DIMENSION QTTOP(8), QW(31,8), RCT(31,8), RHOA1(31)
      DIMENSION RHOA2(31), RHOA3(31), RHOA4(9), TAVE1(31,8)
      DIMENSION TAVE10(31,8), TAVE2(31,8), TAVE20(31,8), TAVE3(31,8)
      DIMENSION TAVE30(31,8), TA1(31,8), TA2(31,8), TA3(31,8)
      DIMENSION TA4(9), TA4AVE(8), TA4AVO(8), TB(8), TBTOT(8)
      DIMENSION TCOOL(21), TIMEC(8), TITLE(5), TL(31), TLTOT(31)
      DIMENSION TR(31,8), TS(31,8), TW(31,8), TWJM1(31), X(31)
      DIMENSION XLAB(5), XPL(100), YLAB(5), YPL(100)
      COMMON /FLOW/ FOXAVB, GCPB, GNI, GNIB, GOXB, GOXBOT
      NAMELIST /INPUT/ ASINK, CSINK, DAMP, DELT, DLFACT, DMWTR, FL,
     1   FSTR, IBLOCK, ICHEM, IPLOT, N, NASS, NCEND, NPRINT, NPRNEW,
     2   NROD, NSECT, POWO, PRMAX, RCI, RCO, RF, ROWS, SMB, TIMAX,
     3   TIMEC, TRDELT, TRMAX, TRPNT, TIMWOF, TIMWON, UL, VENT, VROOM,
     4   WS, WW, XB, XL, XS, XTB, XW, XWL, XWW,
     5   CPCON, CPL, CPNI, CPOX, CPS, CPW, EPC, EPL, EPS, EPT,
     6   EPW, FDECAY, FMULT, KMAX, NDECAY, RHOC, RHOCON, RHOF,
     7   RHOL, RHOS, RHOW, SMKCON, TCOOL, TO, XKBOT, XKTOP
      DATA CPCON, CPL, CPNI, CPOX /1.047, .460, 1.130, 1.130/
      DATA CPS, CPW, EPC, EPL /.364, .883, .7, .3/
      DATA EPS, EPT, EPW, KMAX /.7, .7, .2, 15/
      DATA PI, PO, RA, RHOC /3.14159265, 1.013E6, 2.871E6, 6.5/
      DATA RHOCON, RHOF, RHOL, RHOS /2.34, 10.4, 7.82, 6.5/
      DATA RHOW, SIG, SMG, SMKCON /2.79, 5.67E-12, 980., .012/
      DATA TO, XKBOT, XKTOP /283., 0., 0./
      DATA NDECAY, FMULT, TCOOL, FDBWR, FDPWR /16, 1.00,
     1   1.E-1,   1.E0,    1.E1,    1.E2,    1.E3,    1.E4,
     2   1.E5,    8.64E5,  2.592E6, 7.776E6, 1.555E7, 3.155E7,
     3   6.311E7, 9.466E7, 1.578E8, 3.155E8, 5*0.,
     4   5.33E-2, 4.78E-2, 3.92E-2, 2.59E-2, 1.45E-2, 7.61E-3,
     5   3.76E-3, 2.39E-3, 1.49E-3, 9.65E-4, 5.74E-4, 3.45E-4,
     6   1.93E-4, 1.28E-4, 7.80E-5, 4.99E-5, 5*0.,
     7   5.33E-2, 4.78E-2, 3.92E-2, 2.59E-2, 1.45E-2, 7.61E-3,
     8   3.76E-3, 2.32E-3, 1.43E-3, 8.05E-4, 5.15E-4, 2.96E-4,
     9   1.61E-4, 1.01E-4, 5.70E-5, 3.42E-5, 5*0./
      DATA DAMP, DELT, DLFACT, DMWTR, IPLOT /0., 50., 1., 3*0., 0/
      DATA N, NPRINT, NPRNEW, PRMAX /21, 36, 1, 1.151E6/
      DATA SMB, TIMAX, TRDELT, TRMAX /.025, 36000., 1.E9, 1.E9/
      DATA TRPNT, TIMWOF, TIMWON, XB /1.E9, 1.E9, 0., .635/
      DATA XL, XTB /.635, 40.6/
      DATA TITLE /5*10H          /
```

```
      DATA XLAE /10HTIME (SEC), 4*10H          /
      DATA YLAE /10HPEAK CLAD , 10HTEMPERATUR, 10HE (C)      ,
     1   2*10H          /
      DATA XMAX, YMAX, XPMAX, YPMAX /28., 1400., 28., 1400./
C
      ISTART=1
      NPLOT=0
   80 IEOF=0
   81 READ(5,4890) TITLE(1)
 4890 FORMAT(A7)
      IF (EOF(5)) 82, 85
   82 IF (IEOF.EQ.1) GO TO 999
      IEOF=1
      GO TO 81
   85 READ(5,INPUT)
      IF (ISTART.EQ.0) GO TO 87
      IF (IPLOT.EQ.0) GO TO 87
      CALL HDCOPY(40)
      ISTART=0
   87 WCS=WS
      IF (XS.NE.0.) GO TO 90
      WS=WW
C
C          INITIAL VALUES
C
   90 DELX=FL/(N-1)
      WSPL=WS+2.*XS
      WWPL=WW+2.*XW
      XSW=(WW-WSPL)/2.
      DELZ=WW+XW
      IF (FSTR.EQ.0.5) GO TO 95
      DELZ=WWPL
      IF (XWW.LT.1000.) DELZ=WWPL+XWW
   95 DZDX=DELZ*DELX
      WWDX=DZDX
      IF (FSTR.EQ.1.) WWDX=WWPL*DELX
      SMAR=2.*PI*RCO*DELX*NROD
      SMAF=PI*RF*RF*NROD
      SMAC=PI*(RCO*RCO-RCI*RCI)*NROD
      SMAS=4.*WS*DELX
      SMASPL=4.*WSPL*DELX
      SMAW=4.*WW*DELX
      SMAWPL=2.*DELZ*DELX
      IF (FSTR.EQ.1.0) SMAWPL=4.*WWPL*DELX
      SMAT=WSPL*WSPL
      SMAB=(WWPL+XWW)*DELZ
      IF (FSTR.EQ.1.0) SMAB=DELZ*DELZ
      SMAXA1=WS*WS-PI*RCO*RCO*NROD
      SMAXA2=WW*WW-WSPL*WSPL
      SMAXA3=XWW*DELZ
      IF (FSTR.EQ.1.0) SMAXA3=DELZ*DELZ-WWPL*WWPL
      AXA4=XTB*DELZ
      DO 100 J=1,NSECT
      AR(J)=SMAR*NASS(J)
      AF(J)=SMAF*NASS(J)
      AC(J)=SMAC*NASS(J)
      AS(J)=SMAS*NASS(J)
      ASPL(J)=SMASPL*NASS(J)
      AW(J)=SMAW*NASS(J)
      AWPL(J)=SMAWPL*NASS(J)
      AT(J)=SMAT*NASS(J)
      AB(J)=SMAB*NASS(J)
      IF (J.EQ.1) AB(J)=AB(J)+DELZ*(XWL-XWW)
      IF (J.EQ.NSECT) AB(J)=AB(J)+.5*DELZ*XWW
```

```
      AXA1(J)=SMAXA1*NASS(J)
      AXA2(J)=SMAXA2*NASS(J)
      AXA3(J)=SMAXA3*NASS(J)
      IF (J.EQ.1) AXA3(J)=AXA3(J)+DELZ*(XWL-XWW)
      IF (J.EQ.NSECT) AXA3(J)=AXA3(J)+.5*DELZ*XWW
  100 CONTINUE
      NPRNTA=IABS(NPRINT)
      NP=NPRNTA
      NM1=N-1
      BL=0.
      DO 105 J=1,NSECT
      DELY(J)=(WWPL+XWW)*NASS(J)
      BL=BL+DELY(J)
  105 CONTINUE
      DELY(1)=DELY(1)+XWL-XWW
      DELY(NSECT)=DELY(NSECT)+.5*XWW
      BL=BL+(XWL-XWW)+.5*XWW
      CL=RHCL*CFL*DELZ*DELX*XL
      DO 110 J=1,NSECT
      CS(J)=RHCS*CPS*(WSPL*WSPL-WS*WS)*DELX*NASS(J)
      CW(J)=RHCW*CPW*(WWPL*(WWPL-2.*(1.-FSTR)*XW)-WW*WW)*DELX*NASS(J)
      CB(J)=RHCL*CPL*AB(J)*XB
  110 CONTINUE
      FAWL=DZDX/(DZDX/(EPW*WWDX)+1./EPL-1.)
      FAWW=WWDX/(2./EPW-1.)
      DO 115 J=1,NSECT
      FACS(J)=FSTR*AS(J)/(1./EPC+1./EPS-1.)
      IF (XS.NE.0.) GO TO 112
      ACS=4.*WCS*DELX*NASS(J)
      FACS(J)=FSTR*AW(J)/(AW(J)/(EPC*ACS)+1./EPW-1.)
  112 FASW(J)=FSTR*AW(J)/(AW(J)/(EPS*ASFL(J))+1./EPW-1.)
      FATB(J)=AB(J)/(1./EPT+1./EPL-1.)
      FATSNK(J)=AB(J)/(1./EPT+1./0.7-1.)
  115 CONTINUE
      TMAX=TO
      PMIN=-PO
      WSMG=SMG*DELX/RA
      RHOO=PO/(RA*TO)
      FO=.23
      CPO=FO*CPOX+(1.-FO)*CPNI
      FPL=SMG*RHOO*FL
      UPL=SMG*RHOO*UL
      APL=FPL+UPL
      PW=4.*WS+2.*PI*RCO*NROD
      DE=4.*SMAXA1/PW
      EL=FL*(1.+2.*SMB)/PI
      QDENOM=COS(SMB*FL/EL)-COS((1.+SMB)*FL/EL)
      EGEN=0.
      ECHEM=0.
      EFUEL=0.
      ESTR=0.
      EHOLDR=0.
      ERAD=0.
      ELINRS=0.
      ELINRB=0.
      ECONCS=0.
      ECONCB=0.
      ECONV1=0.
      ECONV2=0.
      ECONV3=0.
      ESTAIR=0.
      EREMOR=0.
      EROOM=0.
      ESINK=0.
```

```
      ELOSS=0.                                                          SFU02020
      PCONCS=0.                                                         SFU02030
      PCONCB=0.                                                         SFU02040
      QSINK=0.                                                          SFU02050
      QASINK=0.                                                         SFU02060
      QLSINK=0.                                                         SFU02070
      QLOSS=0.                                                          SFU02080
      QOUT=0.                                                           SFU02090
      DELTC=DELT                                                        SFU02100
      TIME=0.                                                           SFU02110
      X(1)=0.                                                           SFU02120
      DO 120 I=1,NM1                                                    SFU02130
      X(I+1)=I*DELX                                                     SFU02140
      Q(I)=(COS((X(I)+SMB*FL)/EL)-COS((X(I+1)+SMB*FL)/EL))/QDENOM       SFU02150
  120 CONTINUE                                                          SFU02160
      DO 130 I=1,NM1                                                    SFU02170
      TL(I)=TO+1.E-10                                                   SFU02180
      TLTOT(I)=0.                                                       SFU02190
      QCL(I)=0.                                                         SFU02200
      QCLTOT(I)=0.                                                      SFU02210
  130 CONTINUE                                                          SFU02220
      DO 140 J=1,NSECT                                                  SFU02230
      TB(J)=TO+1.E-10                                                   SFU02240
      TBTOT(J)=0.                                                       SFU02250
      QCB(J)=0.                                                         SFU02260
      QCBTOT(J)=0.                                                      SFU02270
      QTBOT(J)=0.                                                       SFU02280
      QB(J)=0.                                                          SFU02290
      TA4(J)=TO                                                         SFU02300
      TA4AVE(J)=TO                                                      SFU02310
      PA4AVE(J)=APL                                                     SFU02320
      FOXAVB(J)=FO                                                      SFU02330
      IDECAY(J)=1                                                       SFU02340
  140 CONTINUE                                                          SFU02350
      DO 160 J=1,NSECT                                                  SFU02360
      GNI(J,1)=1.E-10                                                   SFU02370
      GNI(J,2)=1.E-10                                                   SFU02380
      GNI(J,3)=-2.E-10                                                  SFU02390
      GCXBOT(J,2)=0.                                                    SFU02400
      DGNI(J,1)=0.                                                      SFU02410
      DGNI(J,2)=0.                                                      SFU02420
      DGNI(J,3)=0.                                                      SFU02430
  160 CONTINUE                                                          SFU02440
      DO 165 J=1,NSECT                                                  SFU02450
      DO 162 I=1,NM1                                                    SFU02460
      TA3(I,J)=TO                                                       SFU02470
      TA2(I,J)=TO                                                       SFU02480
      TA1(I,J)=TO                                                       SFU02490
      TAVE3(I,J)=TO                                                     SFU02500
      TAVE2(I,J)=TO                                                     SFU02510
      TAVE1(I,J)=TO                                                     SFU02520
      TW(I,J)=TO+1.E-10                                                 SFU02530
      TS(I,J)=TO+1.E-10                                                 SFU02540
      TR(I,J)=TO+1.E-10                                                 SFU02550
      OXM(I,J)=0.                                                       SFU02560
      QDECAY(I,J)=0.                                                    SFU02570
      QCHEM(I,J)=0.                                                     SFU02580
      RCT(I,J)=1./6500.                                                 SFU02590
      IS(I,J)=0                                                         SFU02600
      HWA2(I,J)=0.                                                      SFU02610
      HSA2(I,J)=0.                                                      SFU02620
      HRA2(I,J)=0.                                                      SFU02630
  162 CONTINUE                                                          SFU02640
  165 CONTINUE                                                          SFU02650
```

```
      PROOM=PO
      TROOM=TO
      FROOM=FO
      RHORM=RHOO
      DPMAX=0.
      DGMAX=0.
      GNIMAX=1.E10
      TSINK=TO
      NPL=0
      IPL=IPLOT
      TRPL=TO
C
      IVENT=0
      IF (PROOM.GE.PRMAX) IVENT=1
      NOT(1)=0
      IF (IBLOCK.EQ.1) NOT(1)=1
      NOT(2)=0
      IF (XS.EQ.0..OR.IBLOCK.EQ.2) NOT(2)=1
      NOT3=0
      IF (IBLOCK.EQ.3) NOT3=1
C
      IF (FMULT.LT.0.)GO TO 169
      IF (NROD.GT.100) GO TO 167
      DO 166 IDCY=1,NDECAY
  166 FDECAY(IDCY)=FDBWR(IDCY)*FMULT
      GO TO 169
  167 DO 168 IDCY=1,NDECAY
  168 FDECAY(IDCY)=FDPWR(IDCY)*FMULT
C
C          WRITE INPUT
C
  169 WRITE(6,4900) TITLE(1), ASINK, CSINK, DAMP, DELT, DLFACT, DMWTR,
     1    FL, FSTR, IBLOCK, ICHEM, IPLOT, N, NCEND, NPRINT, NPRNEW, NROD,
     2    NSECT, POWO, PRMAX, RCI, RCO, RF, ROWS, SMB, TIMAX, TIMWOF,
     3    TIMWON, TRDELT, TRMAX, TRPNT, UL, VENT, VROOM, WCS, WW, XB, XL,
     4    XS, XTB, XW, XWL, XWW
 4900 FORMAT(*1*,A7 // * ASINK= *,1PE10.3 / * CSINK= *,E10.3 /
     1    * DAMP=   *,E10.3 / * DELT=   *,E10.3 / * DLFACT=*,E10.3 /
     2    * DMWTR= *,E10.3/8X,E10.3/8X,E10.3 /
     3    * FL=     *,E10.3 / * FSTR=   *,E10.3 / * IBLOCK=*,I5 /
     4    * ICHEM= *,I5 / * IPLOT= *,I5 / * N=      *,I5 / * NCEND= *,
     5    I5 / * NPRINT=*,I5 / * NPRNEW=*,I5 / * NROD=   *,I5 /
     6    * NSECT= *,I5 / * POWO=   *,E10.3 / * PRMAX= *,E10.3 /
     7    * RCI=    *,E10.3 / * RCO=    *,E10.3 / * RF=     *,E10.3 /
     8    * ROWS=   *,E10.3 / * SMB=    *,E10.3 / * TIMAX= *,E10.3 /
     9    * TIMWOF=*,E10.3 / * TIMWON=*,E10.3 / * TRDELT=*,E10.3 /
     +    * TRMAX= *,E10.3 / * TRPNT= *,E10.3 / * UL=     *,E10.3 /
     1    * VENT=   *,E10.3 / * VROOM= *,E10.3 / * WS=     *,E10.3 /
     2    * WW=     *,E10.3 / * XE=     *,E10.3 / * XL=     *,E10.3 /
     3    * XS=     *,E10.3 / * XTB=    *,E10.3 / * XW=     *,E10.3 /
     4    * XWL=    *,E10.3 / * XWW=    *,E10.3)
      WRITE(6,4910)
 4910 FORMAT(/*    J    NASS         TIMEO*/)
      WRITE(6,4920) (J, NASS(J), TIMEO(J), J=1,NSECT)
 4920 FORMAT(I4,I6,1PE12.3)
      WRITE(6,4930) CPCON, CPL, CPNI, CPOX, CPS, CPW, EPC, EPL,
     1    EPS, EPT, EPW, FMULT, KMAX, NDECAY, RHOC, RHOCON, RHOF,
     2    RHOL, RHOS, RHOW, SMKCON, TO, XKBOT, XKTOP
 4930 FORMAT(/* CPCON= *,1PE10.3 / * CPL=    *,E10.3 / * CPNI=   *,
     1    E10.3 / * CPOX=   *,E10.3 / * CPS=    *,E10.3 / * CPW=    *,
     2    E10.3 / * EPC=    *,E10.3 / * EPL=    *,E10.3 / * EPS=    *,
     3    E10.3 / * EPT=    *,E10.3 / * EPW=    *,E10.3 / * FMULT= *,
     4    E10.3 / * KMAX=   *,I5 / * NDECAY=*,
     5    I5 / * RHOC=   *,E10.3 / * RHOCON=*,E10.3 / * RHOF=   *,
```

```
     6    E10.3 / * RHOL=   *,E10.3 / * RHOS=   *,E10.3 / * RHOW=   *,
     7    E10.3 / * SMKCON=*,E10.3 / * TO=      *,E10.3 / * XKBOT= *,
     8    E10.3 / * XKTOP= *,E10.3)
      WRITE(6,4940)
 4940 FORMAT(/*    I         TCOOL        FDECAY*/)
      WRITE(6,4950) (I, TCOOL(I), FDECAY(I), I=1,NDECAY)
 4950 FORMAT(I4,1P2E12.3)
C
C         START TIME LOOP
C
  170 DO 174 J=1,NSECT
      DO 172 I=1,NM1
      TAVE10(I,J)=TAVE1(I,J)
      TAVE20(I,J)=TAVE2(I,J)
      TAVE30(I,J)=TAVE3(I,J)
  172 CONTINUE
      TA4AVO(J)=TA4AVE(J)
  174 CONTINUE
      DO 178 J=1,NSECT
      DO 176 L=1,3
      AGNI=AXA1(J)
      IF (L.EQ.2) AGNI=AXA2(J)
      IF (L.EQ.3) AGNI=AXA3(J)
      GNIO1(J,L)=-200.*AGNI
      DPO1(J,L)=-PO
      GNIO2(J,L)=GNIO1(J,L)
      DPO2(J,L)=DPO1(J,L)
      GNIO3(J,L)=200.*AGNI
      DPO3(J,L)=PO
      GNIO4(J,L)=GNIO3(J,L)
      DPO4(J,L)=DPO3(J,L)
  176 CONTINUE
  178 CONTINUE
  180 DO 550 K=1,KMAX
      KIT=K
      PCONV1=0.
      PCONV2=0.
      PCONV3=0.
      PSTAIR=0.
      IDIREC=-1
C
C         START LOOP THROUGH SECTIONS OF POOL
C
  190 DO 325 J=1,NSECT
C
C         START DETERMINATION OF AIR PROPERTIES
C         CHANNEL 3, BETWEEN HOLDERS
C         P IS PRESSURE ABOVE ROOM PRESSURE
C
      IF (GNI(J,3)*IDIREC.LT.0.) GO TO 245
      IF (GNI(J,3).GT.0.) GO TO 200
      PA3(N)=0.+UPL
      TA3(N,J)=TROOM
      FOXO=FROOM
      GO TO 210
  200 PA3(1)=PA4AVE(J)
      TA3(1,J)=TA4AVE(J)
      FOXO=FOXAVB(J)
  210 GOXO=FOXO/(1.-FOXO)*GNI(J,3)
      GCP=GOXO*CPOX+GNI(J,3)*CPNI
      GCPA=ABS(GCP)
      GI=GNI(J,3)+GOXO
      CP=FOXO*CPOX+(1.-FOXO)*CPNI
      PCA=PROOM*CP*AXA3(J)*DELX/(RA*DELT)
```

```
      IF (IDIREC.EQ.-1) PA3(N)=PA3(N)-(XKTOP*GI*GI*RA*TA3(N,J))
     1 /(2.*PROOM*AXA3(J)*AXA3(J))
      IF (IDIREC.EQ.+1) PA3(1)=PA3(1)-(XKBOT*GI*GI*RA*TA3(1,J))
     1 /(2.*PROOM*AXA3(J)*AXA3(J))
      DO 240 II=1,NM1
      I=N*((1-IDIREC)/2)+II*IDIREC
      IBACK=I+(1-IDIREC)/2
      IFWD=I+(1+IDIREC)/2
      XPATH=(II-.5)*DELX
      XNC=FL*((1-IDIREC)/2)+XPATH*IDIREC
      IF (J.NE.1) GO TO 220
      TWJM1(I)=TL(I)
      XWWJM1=XWL
      WZDX=DZDX
      GO TO 230
  220 TWJM1(I)=TW(I,J-1)
      XWWJM1=XWW
      WZDX=WWDX
  230 DH=2.*XWWJM1
      CALL APROP(1, XPATH, XNC, FL, GI, DH, TWJM1(I), TA3(IBACK,J),
     1   RHOA3(IBACK), PROOM, RE3, HWJM1(I,J), SMFJM1, AXA3(J), FOXO,
     2   HDR(I,J), IND3(I,J))
      IF (J.EQ.1) CALL APROP(1, XPATH, XNC, FL, GI, DH, TW(I,J),
     1   TA3(IBACK,J), RHOA3(IBACK), PROOM, RE3, HTEMP, SMFTEM,
     2   AXA3(J), FOXO, HDR(I,J), IND3(I,J))
      DH=2.*XWW
      CALL APROP(1, XPATH, XNC, FL, GI, DH, TW(I,J), TA3(IBACK,J),
     1   RHOA3(IBACK), PROOM, RE3, HWA3(I,J), SMFWA3, AXA3(J), FOXO,
     2   HDR(I,J), IND3(I,J))
      IF (HWA3(I,J).EQ.0.) HWA3(I,J)=1.E-100
      AWA3=AWPL(J)-WZDX
      IF (J.EQ.NSECT) AWA3=AWA3+WWDX
      IF (J.NE.1) GO TO 232
      HWA3(I,J)=(HWA3(I,J)*(AWA3-WWDX)+HTEMP*WWDX)/AWA3
      SMFWA3=(SMFWA3*(AWA3-WWDX)+SMFTEM*WWDX)/AWA3
  232 WK1=HWA3(I,J)*AWA3+HWJM1(I,J)*WZDX
      HAT=HWA3(I,J)*AWA3*TW(I,J)+HWJM1(I,J)*WZDX*TWJM1(I)
      TAVE3(I,J)=(2.*GCPA*TA3(IBACK,J)+PCA+HAT)/(2.*GCPA+PCA/TAVE30(I,J)
     1   +WK1)
      TA3(IFWD,J)=2.*TAVE3(I,J)-TA3(IBACK,J)
      PSTAIR=PSTAIR+PCA*(TAVE3(I,J)-TAVE30(I,J))/TAVE30(I,J)
  235 ALPH=2.0
      IF (RE3.GE.3000.) ALPH=1.1
            ALPH=0.
      PA3(IFWD)=PA3(IBACK)-WSMG*PROOM/TAVE3(I,J)*IDIREC-(GI*GI*RA)
     1  /(PROOM*AXA3(J)*AXA3(J))*(ALPH*(TA3(IFWD,J)-TA3(IBACK,J))
     2  +(SMFWA3*AWA3+SMFJM1*WZDX)/2.*TAVE3(I,J)/AXA3(J))
  240 CONTINUE
      IF (GNI(J,3).GT.0.) DP(J,3)=PA4AVE(J)-PA3(N)
     1   +SMG*(PROOM/(RA*TA3(N,J)))*UL
C    2   +(XKTOP*GI*GI*RA*TA3(N,J))/(2.*PROOM*AXA3(J)*AXA3(J))
      IF (GNI(J,3).LT.0.) DP(J,3)=PA3(1)-0.
C    1   -(XKBOT*GI*GI*RA*TA3(1,J))/(2.*PROOM*AXA3(J)*AXA3(J))
      GOXBOT(J,3)=GOXO
      PCONV3=PCONV3+GCP*TA3(N,J)
C
C          CHANNEL 2, BETWEEN STRUCTURE AND HOLDER
C
  245 IF (XS.EQ.0.) GO TO 290
      IF (GNI(J,2)*IDIREC.LT.0.) GO TO 290
      IF (GNI(J,2).GT.0.) GO TO 250
      PA2(N)=0.+UPL
      TA2(N,J)=TROOM
      FOXO=FROOM
```

```
      GO TO 260
  250 PA2(1)=PA4AVE(J)
      TA2(1,J)=TA4AVE(J)
      FOXO=FOXAVB(J)
  260 GOXO=FOXO/(1.-FOXO)*GNI(J,2)
      GCP=GOXO*CPOX+GNI(J,2)*CPNI
      GCPA=ABS(GCP)
      GI=GNI(J,2)+GOXO
      CP=FOXO*CPOX+(1.-FOXO)*CPNI
      PCA=PROOM*CP*AXA2(J)*DELX/(RA*DELT)
      IF (IDIREC.EQ.-1) PA2(N)=PA2(N)-(XKTOP*GI*GI*RA*TA2(N,J))
     1   /(2.*PROOM*AXA2(J)*AXA2(J))
      IF (IDIREC.EQ.+1) PA2(1)=PA2(1)-(XKBOT*GI*GI*RA*TA2(1,J))
     1   /(2.*PROOM*AXA2(J)*AXA2(J))
      DO 270 II=1,NM1
      I=N*((1-IDIREC)/2)+II*IDIREC
      IBACK=I+(1-IDIREC)/2
      IFWD=I+(1+IDIREC)/2
      XPATH=(II-.5)*DELX
      XNC=FL*((1-IDIREC)/2)+XPATH*IDIREC
      DH=SMAXA2/(WSPL+WW)
      CALL APROP(1, XPATH, XNC, FL, GI, DH, TW(I,J), TA2(IBACK,J),
     1   RHOA2(IBACK), PROOM, RE2, HWA2(I,J), SMFWA2, AXA2(J), FOXO,
     2   HDR(I,J), IND2(I,J))
      CALL APROP(1, XPATH, XNC, FL, GI, DH, TS(I,J), TA2(IBACK,J),
     1   RHOA2(IBACK), PROOM, RE2, HSA2(I,J), SMFSA2, AXA2(J), FOXO,
     2   HDR(I,J), IND2(I,J))
      IF (HWA2(I,J).EQ.0.) HWA2(I,J)=1.E-100
      WK1=HWA2(I,J)*AW(J)+HSA2(I,J)*ASPL(J)
      HAT=HWA2(I,J)*AW(J)*TW(I,J)+HSA2(I,J)*ASPL(J)*TS(I,J)
      SMFA=(SMFWA2*AW(J)+SMFSA2*ASPL(J))/2.
      IF (FSTR.EQ.1.0) GO TO 262
      CALL APROP(1, XPATH, XNC, FL, GI, DH, TR(I,J), TA2(IBACK,J),
     1   RHOA2(IBACK), PROOM, RE2, HRA2(I,J), SMFRA2, AXA2(J), FOXO,
     2   HDR(I,J), I2)
      WK1=WK1/2.+HRA2(I,J)*(AW(J)+ASPL(J))/2.
      HAT=HAT/2.+HRA2(I,J)*(AW(J)+ASPL(J))*TR(I,J)/2.
      SMFA=SMFA/2.+SMFRA2*(AW(J)+ASPL(J))/4.
  262 TAVE2(I,J)=(2.*GCPA*TA2(IBACK,J)+PCA+HAT)/(2.*GCPA+PCA/TAVE20(I,J)
     1   +WK1)
      TA2(IFWD,J)=2.*TAVE2(I,J)-TA2(IBACK,J)
      PSTAIR=PSTAIR+PCA*(TAVE2(I,J)-TAVE20(I,J))/TAVE20(I,J)
  265 ALPH=2.0
      IF (RE2.GE.3000.) ALPH=1.1
                ALPH=0.
      PA2(IFWD)=PA2(IBACK)-WSMG*PROOM/TAVE2(I,J)*IDIREC-(GI*GI*RA)
     1   /(PROOM*AXA2(J)*AXA2(J))*(ALPH*(TA2(IFWD,J)-TA2(IBACK,J))
     2   +SMFA*TAVE2(I,J)/AXA2(J))
  270 CONTINUE
      IF (GNI(J,2).GT.0.) DP(J,2)=PA4AVE(J)-PA2(N)
     1   +SMG*(PROOM/(RA*TA2(N,J)))*UL
C    2   +(XKTOP*GI*GI*RA*TA2(N,J))/(2.*PROOM*AXA2(J)*AXA2(J))
      IF (GNI(J,2).LT.0.) DP(J,2)=PA2(1)-0.
C    1   -(XKBOT*GI*GI*RA*TA2(1,J))/(2.*PROOM*AXA2(J)*AXA2(J))
      GOXBOT(J,2)=GOXO
      PCONV2=PCONV2+GCP*TA2(N,J)
C
C        CHANNEL 1, WITHIN ASSEMBLY
C
  290 IF (GNI(J,1)*IDIREC.LT.0.) GO TO 325
      IF (GNI(J,1).GT.0.) GO TO 300
      PA1(N)=0.+UPL
      TA1(N,J)=TROOM
      FOX(N,J)=FROOM
```

```
      GCX(N)=FCX(N,J)/(1.-FOX(N,J))*GNI(J,1)                            SFU05220
      GI=GOX(N)+GNI(J,1)                                                SFU05230
      GC TC 310                                                         SFU05240
  300 PA1(1)=PA4AVE(J)                                                  SFU05250
      TA1(1,J)=TA4AVE(J)                                                SFU05260
      FCX(1,J)=FOXAVB(J)                                                SFU05270
      GOX(1)=FOX(1,J)/(1.-FOX(1,J))*GNI(J,1)                            SFU05280
      GI=GOX(1)+GNI(J,1)                                                SFU05290
  310 IF (IDIREC.EQ.-1) PA1(N)=PA1(N)-(XKTOP*GI*GI*RA*TA1(N,J))         SFU05300
     1   /(2.*PROOM*AXA1(J)*AXA1(J))                                    SFU05310
      IF (IDIREC.EQ.+1) PA1(1)=PA1(1)-(XKBOT*GI*GI*RA*TA1(1,J))         SFU05320
     1   /(2.*PROOM*AXA1(J)*AXA1(J))                                    SFU05330
      DO 320 II=1,NM1                                                   SFU05340
      I=N*((1-IDIREC)/2)+II*IDIREC                                      SFU05350
      IBACK=I+(1-IDIREC)/2                                              SFU05360
      IFWD=I+(1+IDIREC)/2                                               SFU05370
      XPATH=(II-.5)*DELX                                                SFU05380
      XNC=FL*((1-IDIREC)/2)+XPATH*IDIREC                                SFU05390
      GCX(IFWD)=GOX(IBACK)-CXM(I,J)*IDIREC                              SFU05400
      IF (GOX(IFWD)*GOX(IBACK).LE.0.) GOX(IFWD)=0.                      SFU05410
      FCX(IFWD,J)=GOX(IFWD)/(GOX(IFWD)+GNI(J,1))                        SFU05420
      FOXAV=(FOX(IBACK,J)+FOX(IFWD,J))/2.                               SFU05430
      GI=.5*(GCX(IBACK)+GOX(IFWD))+GNI(J,1)                             SFU05440
      CALL APRCF(2, XPATH, XNC, FL, GI, DE, TS(I,J), TA1(IBACK,J),      SFU05450
     1   RHOA1(IBACK), PROOM, RE1, HSA1(I,J), SMFSA1, AXA1(J),          SFU05460
     2   FOX(IBACK,J), HDR(I,J), IND1(I,J))                             SFU05470
      CALL APRCF(2, XPATH, XNC, FL, GI, DE, TR(I,J), TA1(IBACK,J),      SFU05480
     1   RHOA1(IBACK), PROOM, RE1, HRA1(I,J), SMFRA1, AXA1(J),          SFU05490
     2   FOX(IBACK,J), HDR(I,J), IND1(I,J))                             SFU05500
      GCP1=GOX(IBACK)*CPOX+GNI(J,1)*CPNI                                SFU05510
      GCP2=GOX(IFWD)*CPOX+GNI(J,1)*CPNI                                 SFU05520
      GCP=(GCP1+GCP2)/2.                                                SFU05530
      GCPA=ABS(GCP)                                                     SFU05540
      CP=FOXAV*CPOX+(1.-FOXAV)*CPNI                                     SFU05550
      PCA=PROOM*CP*AXA1(J)*DELX/(RA*DELT)                               SFU05560
      IF (HRA1(I,J).EQ.0.) HRA1(I,J)=1.E-100                            SFU05570
      WK1=HRA1(I,J)*AR(J)+HSA1(I,J)*AS(J)                               SFU05580
      HAT=HSA1(I,J)*AS(J)*TS(I,J)+HRA1(I,J)*AR(J)*TR(I,J)               SFU05590
      SMFA=(SMFSA1*AS(J)+SMFRA1*AR(J))/2.                               SFU05600
      IF (FSTR.EQ.1.0) GO TO 312                                        SFU05610
      WK1=WK1+(HRA1(I,J)-HSA1(I,J))*AS(J)/2.                            SFU05620
      HAT=HAT+(HRA1(I,J)*TR(I,J)-HSA1(I,J)*TS(I,J))*AS(J)/2.            SFU05630
      SMFA=SMFA+(SMFRA1-SMFSA1)*AS(J)/4.                                SFU05640
  312 TAVE1(I,J)=(2.*GCPA*TA1(IBACK,J)+PCA+HAT)/(2.*GCPA+PCA/TAVE10(I,J)SFU05650
     1   +WK1)                                                          SFU05660
      TA1(IFWD,J)=2.*TAVE1(I,J)-TA1(IBACK,J)                            SFU05670
      PSTAIR=PSTAIR+PCA*(TAVE1(I,J)-TAVE10(I,J))/TAVE10(I,J)            SFU05680
  315 ALPH=2.0                                                          SFU05690
      IF (RE1.GE.3000.) ALPH=1.1                                        SFU05700
                ALPH=0.                                                 SFU05710
      PA1(IFWD)=PA1(IBACK)-WSMG*PROOM/TAVE1(I,J)*IDIREC-(GI*GI*RA)      SFU05720
     1   /(PROOM*AXA1(J)*AXA1(J))*(ALPH*(TA1(IFWD,J)-TA1(IBACK,J))      SFU05730
     2   +SMFA*TAVE1(I,J)/AXA1(J))                                      SFU05740
  320 CONTINUE                                                          SFU05750
      IF (GNI(J,1).GT.0.) DP(J,1)=PA4AVE(J)-PA1(N)+(XKTOP*GI*GI*RA      SFU05760
     1   *TA1(N,J))/(2.*PROOM*AXA1(J)*AXA1(J))+SMG*(PROOM/(RA           SFU05770
     2   *TA1(N,J)))*UL                                                 SFU05780
      IF (GNI(J,1).LT.0.) DP(J,1)=PA1(1)-(XKBOT*GI*GI*RA                SFU05790
     1   *TA1(1,J))/(2.*PROOM*AXA1(J)*AXA1(J))-0.                       SFU05800
      GCXBOT(J,1)=GOX(1)                                                SFU05810
      PCONV1=PCONV1+(GOX(N)*CPOX+GNI(J,1)*CPNI)*TA1(N,J)                SFU05820
C                                                                       SFU05830
  325 CONTINUE                                                          SFU05840
      IF (IDIREC.EQ.-1) GO TO 422                                       SFU05850
```

```
C
C         HEAT FLUXES TO VERTICAL STRUCTURE ELEMENTS
C
      DO 350 J=1,NSECT
      DO 340 I=1,NM1
      IF (J.NE.1) GO TO 326
      TWJM1(I)=TL(I)
      FAJM1=FAWL
      WZDX=DZDX
      GO TO 328
  326 TWJM1(I)=TW(I,J-1)
      FAJM1=FAWW
      WZDX=WWDX
  328 QRWJM1=FAJM1*SIG*(TW(I,J)**4-TWJM1(I)**4)
      QWJM1=HWJM1(I,J)*WZDX*(TAVE3(I,J)-TWJM1(I))+QRWJM1
      IF (J.NE.1) GO TO 330
      QL(I)=QWJM1-QCL(I)
      DQL(I)=-HWJM1(I,J)*WZDX-4.*FAJM1*SIG*TWJM1(I)**3
      GO TO 335
  330 QW(I,J-1)=QW(I,J-1)+QWJM1
      DQW(I,J-1)=DQW(I,J-1)-HWJM1(I,J)*WZDX-4.*FAJM1*SIG*TWJM1(I)**3
  335 QRSW=FASW(J)*SIG*(TS(I,J)**4-TW(I,J)**4)
      QW(I,J)=HWA3(I,J)*(AWPL(J)-WZDX)*(TAVE3(I,J)-TW(I,J))+HWA2(I,J)
     1    *AW(J)*FSTR*(TAVE2(I,J)-TW(I,J))+QRSW-QRWJM1
      DQW(I,J)=-HWA3(I,J)*(AWPL(J)-WZDX)-HWA2(I,J)*AW(J)*FSTR
     1    -4.*(FASW(J)+FAJM1)*SIG*TW(I,J)**3
      IF (J.NE.NSECT) GO TO 337
      QW(I,J)=QW(I,J)+HWA3(I,J)*WWDX*(TAVE3(I,J)-TW(I,J))
      DQW(I,J)=DQW(I,J)-HWA3(I,J)*WWDX
  337 QRRS=FACS(J)*SIG*(TR(I,J)**4-TS(I,J)**4)
      QS(I,J)=(HSA2(I,J)*ASPL(J)*(TAVE2(I,J)-TS(I,J))+HSA1(I,J)*AS(J)
     1    *(TAVE1(I,J)-TS(I,J)))*FSTR+QRRS-QRSW
      DQS(I,J)=-(HSA2(I,J)*ASPL(J)+HSA1(I,J)*AS(J))*FSTR
     1    -4.*(FACS(J)+FASW(J))*SIG*TS(I,J)**3
      IF (XS.NE.0.) GO TO 338
      QW(I,J)=QW(I,J)+QS(I,J)
      DQW(I,J)=DQW(I,J)+DQS(I,J)
  338 QR(I,J)=HRA1(I,J)*AR(J)*(TAVE1(I,J)-TR(I,J))-QRRS
      IF (FSTR.EQ.0.5) QR(I,J)=QR(I,J)+.5*(HRA2(I,J)*(AW(J)+ASPL(J))
     1    *(TAVE2(I,J)-TR(I,J))+HRA1(I,J)*AS(J)*(TAVE1(I,J)-TR(I,J)))
  340 CONTINUE
  350 CONTINUE
      GO TO 434
C
C         BASE FLOW PROPERTIES, MASS FLOWS
C
  422 GNIB(1)=0.
      GCXB(1)=0.
      GNIB(NSECT+1)=0.
      GCXB(NSECT+1)=0.
      PTAU(1)=0.
      DO 424 J=1,NSECT
      GNIB(J+1)=GNIB(J)-GNI(J,1)-GNI(J,2)-GNI(J,3)
      GNIAVB(J)=.5*(GNIB(J)+GNIB(J+1))
  424 CONTINUE
      J=0
      JJ=0
  426 J=J+1
      JJJ=J
      IF (J.GT.NSECT) GO TO 430
      IF (GNIB(J+1).LT.0.) GO TO 426
      CALL BFLOW(J)
      IF ((J-JJ).GT.1) GO TO 428
      JJ=J
```

```
      GO TO 426
  428 J=J-1
      CALL BFLOW(J)
      IF ((J-JJ).GT.1) GO TO 428
      JJ=JJJ
      J=JJJ
      GO TO 426
  430 XPATH=0.
            XPATH=1.E10
      XNC=0.
      TA4(1)=TA3(1,1)
      DO 432 J=1,NSECT
      XPATH=XPATH+.5*DELY(J)
      IF (J.NE.1) XPATH=XPATH+.5*DELY(J-1)
      GI=.5*(GNIB(J)+GOXB(J)+GNIB(J+1)+GOXB(J+1))
      IF (GI.EQ.0.) GI=1.E-50
      IDIRB=+1
      IF (GI.LT.0.) IDIRB=-1
      DH=2.*XTB
      CALL APROP(-1, XPATH, XNC, BL, GI, DH, TR(1,J), TA4(J),
     1   RHOA4(J), PROOM, RE4, HTA4(J), SMFTA4, AXA4, FOXAVB(J),
     2   HDRB, INDB)
      CALL APROP(-1, XPATH, XNC, BL, GI, DH, TB(J), TA4(J),
     1   RHOA4(J), PROOM, RE4, HBA4(J), SMFBA4, AXA4, FOXAVB(J),
     2   HDRB, INDB)
      GCP1=GOXB(J)*CPOX+GNIB(J)*CPNI
      GCP2=GOXB(J+1)*CPOX+GNIB(J+1)*CPNI
      GCP=(GCP1+GCP2)/2.
      CP=FOXAVB(J)*CPOX+(1.-FOXAVB(J))*CPNI
      PCA=PROOM*CP*AB(J)*XTB/(RA*DELT)
      IF (HBA4(J).EQ.0.) HBA4(J)=1.E-100
      WK1=HTA4(J)*AT(J)+HBA4(J)*AB(J)
      HAT=HTA4(J)*AT(J)*TR(1,J)+HBA4(J)*AB(J)*TB(J)
      GIN=(ABS(GNI(J,1)+GOXBOT(J,1))-GNI(J,1)-GOXBOT(J,1)+ABS(GNI(J,2)
     1   +GOXBOT(J,2))-GNI(J,2)-GOXBOT(J,2)+ABS(GNI(J,3)+GOXBOT(J,3))
     2   -GNI(J,3)-GOXBOT(J,3))/2.
      GCPTIN=((ABS(GCPB(J,1))-GCPB(J,1))*TA1(1,J)+(ABS(GCPB(J,2))
     1   -GCPB(J,2))*TA2(1,J)+(ABS(GCPB(J,3))-GCPB(J,3))*TA3(1,J))/2.
      TA4AVE(J)=(2.*GCP*TA4(J)+GCPTIN+PCA+HAT)/(2.*GCP+GIN*CP+PCA
     1   /TA4AVO(J)+WK1)
      PSTAIR=PSTAIR+PCA*(TA4AVE(J)-TA4AVO(J))/TA4AVO(J)
      TA4(J+1)=2.*TA4AVE(J)-TA4(J)
      ALPH=2.0
      IF (RE4.GE.3000.) ALPH=1.1
            ALPH=0.
      DPTAU=-(GI*GI*RA)/(PROOM*AXA4*AXA4)*(ALPH*(TA4(J+1)-TA4(J))
     1   +(SMFTA4*AT(J)+SMFBA4*AB(J))/2.*TA4AVE(J)/AXA4)*IDIRB
      PTAU(J+1)=PTAU(J)+DPTAU
      PTAUAV(J)=.5*(PTAU(J)+PTAU(J+1))
  432 CONTINUE
      IDIREC=+1
      GO TO 190
C
C        BASE FLOW PROPERTIES, PRESSURE
C
  434 PNUMER=0.
      PDENOM=0.
      DFMAX=0.
      NOT(3)=0
      DO 450 J=1,NSECT
      IF (J.NE.1) NOT(3)=NOT3
      DO 440 L=1,3
      IF (NOT(L).EQ.1) GO TO 439
      IF (DP(J,L).GT.PA4AVE(J)) GO TO 436
```

```
      GNIO2(J,L)=GNI(J,L)
      DPO2(J,L)=DP(J,L)
      IF (DPO3(J,L).GT.PA4AVE(J)) GO TO 436
      GNIO3(J,L)=GNIO4(J,L)
      DPO3(J,L)=DPO4(J,L)
      GO TO 438
  436 GNIO3(J,L)=GNI(J,L)
      DPO3(J,L)=DP(J,L)
      IF (DPO2(J,L).LT.PA4AVE(J)) GO TO 438
      GNIO2(J,L)=GNIO1(J,L)
      DPO2(J,L)=DPO1(J,L)
  438 COEFF2(L)=(GNIO3(J,L)-GNIO2(J,L))/(DPO3(J,L)-DPO2(J,L))
      COEFF1(L)=COEFF2(L)*(DP(J,L)-PTAUAV(J))
      GO TO 440
  439 COEFF2(L)=0.
      COEFF1(L)=0.
  440 CONTINUE
      PNUMER=PNUMER+COEFF1(1)+COEFF1(2)+COEFF1(3)
      PDENOM=PDENOM+COEFF2(1)+COEFF2(2)+COEFF2(3)
  450 CONTINUE
      PA4(1)=PNUMER/PDENOM
      NOT(3)=0
      DO 470 J=1,NSECT
      IF (J.NE.1) NOT(3)=NOT3
      PA4(J+1)=PA4(1)+PTAU(J+1)
      PA4AVE(J)=.5*(PA4(J)+PA4(J+1))
      DO 460 L=1,3
      IF (NOT(L).EQ.1) GO TO 460
      DPMAX=AMAX1(DPMAX,ABS(DP(J,L)-PA4AVE(J)))
  460 CONTINUE
  470 CONTINUE
C
C         HEAT FLUXES TO HORIZONTAL STRUCTURAL ELEMENTS
C
      QRSINK=0.
      DO 480 J=1,NSECT
      QTTOP(J)=-FATSNK(J)*SIG*(TR(NM1,J)**4-TSINK**4)
      QRSINK=QRSINK-QTTOP(J)
      QRB=-FATB(J)*SIG*(TB(J)**4-TR(1,J)**4)
      QTBOT(J)=HTA4(J)*AT(J)*(TA4AVE(J)-TR(1,J))-QRB
      QB(J)=HBA4(J)*AB(J)*(TA4AVE(J)-TB(J))+QRB-QCB(J)
      DQB(J)=-HBA4(J)*AB(J)-4.*FATB(J)*SIG*TB(J)**3
  480 CONTINUE
C
C         CONVERGENCE OF MASS FLOWS
C
      GNIMAX=0.
      DGMAX=0.
      NOT(3)=0
      DO 510 J=1,NSECT
      IF (J.NE.1) NOT(3)=NOT3
      DO 500 L=1,3
      IF (NOT(L).EQ.1) GO TO 500
      DGNI(J,L)=-(GNIO3(J,L)-GNIO2(J,L))*(DP(J,L)-PA4AVE(J))
     1   /(DPO3(J,L)-DPO2(J,L))
      GNIMAX=AMAX1(GNIMAX,ABS(GNI(J,L)))
      DGMAX=AMAX1(DGMAX,ABS(DGNI(J,L)))
  500 CONTINUE
  510 CONTINUE
      IF (DPMAX.LT.0.01*AFL.AND.DGMAX.LT.0.01*GNIMAX) GO TO 560
      IF (TIME.EQ.0.) GO TO 560
      DO 530 J=1,NSECT
      DO 520 L=1,3
  520 GNI(J,L)=GNI(J,L)+DGNI(J,L)*(1.-DAMP)
```

```
 530 CONTINUE
 550 CONTINUE
     DPFRAC=DPMAX/APL
     DGFRAC=DGMAX/GNIMAX
     WRITE(6,5010) TIME, DPFRAC, DGFRAC
5010 FORMAT(/38H MASS FLOWS FAILED TO CONVERGE AT TIME,1PE10.3,
    1   10H,  DPFRAC=,E10.3,10H,  DGFRAC=,E10.3)
C
C        PRINTOUT
C
 560 NP=NP+1
     IF (NP.LT.NPRNTA.AND.TMAX.LT.TRMAX) GO TO 680
     IF (IPL.EQ.0) GO TO 565
     NPL=NPL+1
     XPL(NPL)=TIME/3600.
     YPL(NPL)=TRPL-273.
 565 DPFRAC=DPMAX/APL
     DGFRAC=DGMAX/GNIMAX
     DTFRAC=1.0
     IF (TIME.GT.0.) DTFRAC=DTMAX*TIME/(TMAX-TO)
     TROOMC=TROOM-273.
     TSINKC=TSINK-273.
     TRPLC=TRPL-273.
     WRITE(6,5020) TITLE(1), TIME, KIT, DPFRAC, DGFRAC, TRPLC,
    1   TROOMC, PROOM, TSINKC
5020 FORMAT(1H1,A7,43X,10H*** TIME =,1PE10.3,4H ***//6H  KIT=,I3,
    1   10H   DPFRAC=,E10.3,10H   DGFRAC=,E10.3,9H   TRMAX=,E10.3,
    2   9H   TROOM=,E10.3,9H   PROOM=,E10.3,9H   TSINK=,E10.3)
     WRITE(6,5030)
5030 FORMAT(//4X, *I* 7X, *TL(I)* 11X, *J* 7X, *TB(J)* 3X,
    1   *TA4AVE(J)* 3X, *PA4AVE(J)* 3X, *FOXAVB(J)* 3X,
    2   *GNIAVB(J)* 4X, *GNI(J,1)* 4X, *GNI(J,2)* 4X,
    3   *GNI(J,3)*/)
     MAXIJ=MAX0(NM1,NSECT)
     DO 590 IJ=1,MAXIJ
     IF (IJ.GT.NSECT) GO TO 570
     IF (IJ.GT.NM1) GO TO 580
     TLIJ=TL(IJ)-273.
     TBIJ=TB(IJ)-273.
     TA4IJ=TA4AVE(IJ)-273.
     WRITE(6,5040) IJ, TLIJ, IJ, TBIJ, TA4IJ,
    1   PA4AVE(IJ), FOXAVB(IJ), GNIAVB(IJ), GNI(IJ,1), GNI(IJ,2),
    2   GNI(IJ,3)
5040 FORMAT(2X,I3,1PE12.3,9X,I3,8E12.3)
     GO TO 590
 570 TLIJ=TL(IJ)-273.
     WRITE(6,5050) IJ, TLIJ
5050 FORMAT(2X,I3,1PE12.3)
     GO TO 590
 580 TBIJ=TB(IJ)-273.
     TA4IJ=TA4AVE(IJ)-273.
     WRITE(6,5060) IJ, TBIJ, TA4IJ, PA4AVE(IJ),
    1   FOXAVB(IJ), GNIAVB(IJ), GNI(IJ,1), GNI(IJ,2), GNI(IJ,3)
5060 FORMAT(26X,I3,1P8E12.3)
 590 CONTINUE
     DO 610 J=1,NSECT
     IF (NPRINT.LT.0.AND.J.LT.NSECT) GO TO 610
     WRITE(6,5070) J
5070 FORMAT(//*  J=*,I2)
     WRITE(6,5080)
5080 FORMAT(/4X, *I* 10X, *TR* 7X, *TAVE1* 4X, *I1* 10X, *TS*
    1   7X, *TAVE2* 4X, *I2* 10X, *TW* 7X, *TAVE3* 4X, *I3*
    2   9X, *RCT* 9X, *FCX* 4X, *IS*/)
     DO 600 I=1,NM1
```

```
      TRIJ=TR(I,J)-273.
      TA1IJ=TAVE1(I,J)-273.
      TSIJ=TS(I,J)-273.
      TA2IJ=TAVE2(I,J)-273.
      TWIJ=TW(I,J)-273.
      TA3IJ=TAVE3(I,J)-273.
      WRITE(6,5090) I, TRIJ, TA1IJ, IND1(I,J),
     1   TSIJ, TA2IJ, IND2(I,J), TWIJ,
     2   TA3IJ, IND3(I,J), RCT(I,J), FOX(I,J), IS(I,J)
 5090 FORMAT(2X,I3,1P2E12.3,I6,2E12.3,I6,2E12.3,I6,2E12.3,I6)
  600 CONTINUE
  610 CONTINUE
      WRITE(6,6000) EGEN, ECHEM, EFUEL, ESTR, EHOLDR, ERAD,
     1   ELINRS, ELINRB, ECONCS, ECONCB, ECONV1, ECONV2, ECONV3,
     2   ESTAIR, EREMDR, EROOM, ESINK, ELOSS
 6000 FORMAT(//*  EGEN=   *,1PE10.3, *   ECHEM= *,E10.3,*   EFUEL= *,
     1   E10.3, *   ESTR=   *,E10.3, *   EHOLDR=*,E10.3, *   ERAD=   *,
     2   E10.3/ *  ELINRS=*,E10.3, *   ELINRB=*,E10.3, *   ECONCS=*,
     3   E10.3, *   ECONCB=*,E10.3, *   ECONV1=*,E10.3, *   ECONV2=*,
     4   E10.3/ *  ECONV3=*,E10.3, *   ESTAIR=*,E10.3, *   EREMDR=*,
     5   E10.3, *   EROOM= *,E10.3, *   ESINK= *,E10.3, *   ELOSS= *,
     6   E10.3)
      NF=0
C
  680 IF (TIME.GE.TIMAX) GO TO 900
      IF (TMAX.GE.TRMAX) GO TO 900
      IF (TMAX.GE.TRDELT) DELT=DELTO/DLFACT
      IF (TMAX.GE.TRPNT) NPRNTA=IABS(NPRNEW)
      IF (IPL.EQ.0) GO TO 685
      IF (TRPL-273..LT.YPMAX.AND.TIME/3600..LT.XPMAX) GO TO 685
      IPL=0
      CALL PLOTPR(0, 0, XPL, YPL, NPL, 1, 1, 0, 1H , TITLE, XLAB,
     1   YLAB, 2, 1, 0., XMAX, 1, 0., YMAX)
      NPLOT=NPLOT+1
      CALL PLOTND(940)
C
C        ADVANCE TIME
C
  685 TIME=TIME+DELT
      ECONV1=ECONV1+PCONV1*DELT
      ECONV2=ECONV2+PCONV2*DELT
      ECONV3=ECONV3+PCONV3*DELT
      ESTAIR=ESTAIR+PSTAIR*DELT
C
C        CALCULATE NEW TEMPERATURES THROUGH WALLS AND STRUCTURES
C
      PGEN=0.
      PCHEM=0.
      PFUEL=0.
      PSTR=0.
      PHOLDR=0.
      PRAD=0.
      PLINRS=0.
      PLINRB=0.
      OXMTOT=0.
      DTMAX=0.
      TMAX=0.
      TRPL=0.
      QREML=0.
      IF (TIME.GT.TIMWON.AND.TIME.LE.TIMWOF) QREML=2566.*DMWTR(3)
      DO 690 II=1,NM1
      I=N-II
      QLI=(373.-TL(I))*DQL(I)/(EXP(DQL(I)*DELT/QL)-1.)
      QLI=AMIN1(QLI,QL(I))
```

```
      IF ((QL(I)-QLI).GT.QREML) QLI=QL(I)-QREML                         SFU09060
      QREML=QREML-QL(I)+QLI                                             SFU09070
      TLNEW=TL(I)+QLI/DQL(I)*(EXP(DQL(I)*DELT/CL)-1.)                   SFU09080
      TLTOT(I)=TLTOT(I)+((TL(I)-TO)*(TIME-DELT)+(TLNEW-TO)*TIME)*DELT/2.SFU09090
      TL(I)=TLNEW                                                       SFU09100
      PLINRS=PLINRS+QL(I)                                               SFU09110
  690 CONTINUE                                                          SFU09120
      DO 750 J=1,NSECT                                                  SFU09130
      QREM3=0.                                                          SFU09140
      QREM2=0.                                                          SFU09150
      QREM1=0.                                                          SFU09160
      IF (TIME.LE.TIMWON.OR.TIME.GT.TIMWOF) GO TO 700                   SFU09170
      QREM3=2586.*DMWTR(3)*NASS(J)                                      SFU09180
      QREM2=2586.*DMWTR(2)*NASS(J)                                      SFU09190
      QREM1=2586.*DMWTR(1)*NASS(J)                                      SFU09200
  700 QCOND(1)=QTBOT(J)                                                 SFU09210
      QCOND(N)=-QTTOP(J)                                                SFU09220
      PRAD=PRAD+QCOND(N)                                                SFU09230
      IF (FMULT.GT.0.) GO TO 701                                        SFU09240
      F=FDECAY(J)                                                       SFU09250
      GO TO 710                                                         SFU09260
  701 TIMEC=TIMEO(J)+TIME-DELT                                          SFU09270
  702 IDCY=IDECAY(J)                                                    SFU09280
      IF (TIMEC.LE.TCOOL(IDCY)) GO TO 704                               SFU09290
      IF (IDCY.EQ.NDECAY) GO TO 704                                     SFU09300
      IDECAY(J)=IDECAY(J)+1                                             SFU09310
      GO TO 702                                                         SFU09320
  704 IF (IDCY.GT.1) GO TO 706                                          SFU09330
      F=FDECAY(1)                                                       SFU09340
      GO TO 710                                                         SFU09350
  706 IF (TCOOL(IDCY-1).GT.0.) GO TO 708                                SFU09360
      F=FDECAY(IDCY-1)+(TIMEC-TCOOL(IDCY-1))/(TCOOL(IDCY)               SFU09370
     1   -TCOOL(IDCY-1))*(FDECAY(IDCY)-FDECAY(IDCY-1))                  SFU09380
      GO TO 710                                                         SFU09390
  708 F=FDECAY(IDCY-1)*(FDECAY(IDCY)/FDECAY(IDCY-1))**(ALOG(TIMEC       SFU09400
     1   /TCOOL(IDCY-1))/ALOG(TCOOL(IDCY)/TCOOL(IDCY-1)))               SFU09410
  710 F=F*ABS(FMULT)                                                    SFU09420
      DO 740 II=1,NM1                                                   SFU09430
      I=N-II                                                            SFU09440
      CWW=(2.*FSTR+1.)/3.*CW(J)                                         SFU09450
      QWIJ=(373.-TW(I,J))*DQW(I,J)/(EXP(DQW(I,J)*DELT/CWW)-1.)          SFU09460
      QWIJ=AMIN1(QWIJ,QW(I,J))                                          SFU09470
      IF ((QW(I,J)-QWIJ).GT.QREM3) QWIJ=QW(I,J)-QREM3                   SFU09480
      QREM3=QREM3-QW(I,J)+QWIJ                                          SFU09490
      TW(I,J)=TW(I,J)+QWIJ/DQW(I,J)*(EXP(DQW(I,J)*DELT/CWW)-1.)         SFU09500
      PHOLDR=PHOLDR+QW(I,J)                                             SFU09510
      IF (XS.EQ.0.) GO TO 712                                           SFU09520
      CSS=FSTR*CS(J)                                                    SFU09530
      QSIJ=(373.-TS(I,J))*DQS(I,J)/(EXP(DQS(I,J)*DELT/CSS)-1.)          SFU09540
      QSIJ=AMIN1(QSIJ,QS(I,J))                                          SFU09550
      IF ((QS(I,J)-QSIJ).GT.QREM2) QSIJ=QS(I,J)-QREM2                   SFU09560
      QREM2=QREM2-QS(I,J)+QSIJ                                          SFU09570
      TS(I,J)=TS(I,J)+QSIJ/DQS(I,J)*(EXP(DQS(I,J)*DELT/CSS)-1.)         SFU09580
      PSTR=PSTR+QS(I,J)                                                 SFU09590
      GO TO 713                                                         SFU09600
  712 TS(I,J)=TW(I,J)                                                   SFU09610
  713 IF (I.EQ.1) GO TO 715                                             SFU09620
      CALL FPROF(TR(I,J), CF, CC, SMKF, SMKC, 0)                        SFU09630
      CALL FPROF(TR(I-1,J), CF, CC, SMKF1, SMKC1, 0)                    SFU09640
      QCOND(I)=(AF(J)*(SMKF+SMKF1)/2.+AC(J)*(SMKC+SMKC1)/2.)            SFU09650
     1   *(TR(I-1,J)-TR(I,J))/DELX                                      SFU09660
  715 QDECAY(I,J)=1000.*PCWO*NASS(J)*Q(I)*F                             SFU09670
      IF (ICHEM.EQ.0) GO TO 730                                         SFU09680
      CALL CHEM(TR(I,J), DELT, RCI, RCO, RCT(I,J), RCN, QC)             SFU09690
```

```
      OXMK=((32.*6.5)/91.22)*AR(J)*(RCN-RCT(I,J))/DELT
      OXMD=AR(J)*HDR(I,J)*PROOM/(RA*TAVE1(I,J))*(FOX(I,J)+FOX(I+1,J))/2.
C        IS=1 -- PARABOLIC KINETICS LIMITED
      IS(I,J)=1
      OXM(I,J)=OXMK
      IF (OXMK.LT.OXMD) GO TO 720
C        IS=2 -- DIFFUSION LIMITED
      IS(I,J)=2
      OXM(I,J)=OXMD
      RCN=RCT(I,J)+(91.2/(32.*6.5))*OXMD*DELT/AR(J)
      QC=7.8E4*(RCN-RCT(I,J))/DELT
  720 RCT(I,J)=RCN
      QCHEM(I,J)=AR(J)*QC
  730 CALL FPRCF(TR(I,J), CF, CC, SMKF, SMKC, 1)
      CR=(RHOF*CF*AF(J)+RHOC*CC*AC(J))*DELX
      IF (FSTR.EQ.0.5) CR=CR+CS(J)/2.+CW(J)/3.
      QRT=QDECAY(I,J)+QCHEM(I,J)+QCOND(I)-QCOND(I+1)+QR(I,J)
      QRIJ=(373.-TR(I,J))*CR/DELT
      QRIJ=AMIN1(QRIJ,QRT)
      IF ((QRT-QRIJ).GT.QREM1) QRIJ=QRT-QREM1
      QREM1=QREM1-QRT+QRIJ
      TR(I,J)=TR(I,J)+QRIJ*DELT/CR
      PFUEL=PFUEL+QRT
      PGEN=PGEN+QDECAY(I,J)
      PCHEM=PCHEM+QCHEM(I,J)
      OXMTOT=OXMTOT+OXM(I,J)
      DTMAX=AMAX1(DTMAX,ABS(QRT/CR))
      TMAX=AMAX1(TMAX,TR(I,J))
      IF (J.EQ.NSECT) TRPL=AMAX1(TRPL,TR(I,J))
  740 CONTINUE
      TBNEW=TB(J)+QB(J)/DQB(J)*(EXP(DQB(J)*DELT/CB(J))-1.)
      TBTOT(J)=TBTOT(J)+((TB(J)-TO)*(TIME-DELT)+(TBNEW-TO)*TIME)*DELT/2.
      TB(J)=TBNEW
      PLINRB=PLINRB+QB(J)
  750 CONTINUE
      EGEN=EGEN+PGEN*DELT
      ECHEM=ECHEM+PCHEM*DELT
      EFUEL=EFUEL+PFUEL*DELT
      ESTR=ESTR+PSTR*DELT
      EHOLDR=EHOLDR+PHOLDR*DELT
      ERAD=ERAD+PRAD*DELT
      ELINRS=ELINRS+PLINRS*DELT
      ELINRB=ELINRB+PLINRB*DELT
C
C        DETERMINE HEAT FLUX INTO CONCRETE
C
      IF (RHOCON.LE.0.) GO TO 800
      PCONCS=0.
      PCONCB=0.
      DO 760 I=1,NM1
      PCONCS=PCONCS+QCL(I)
      QCL(I)=(4.*TLTOT(I)*DZDX*(RHOCON*CPCON*SMKCON/(PI*TIME**3))**.5
     1   -QCLTOT(I))/DELT
      QCLTOT(I)=QCLTOT(I)+QCL(I)*DELT
  760 CONTINUE
      DO 770 J=1,NSECT
      PCONCB=PCONCB+QCB(J)
      QCB(J)=(4.*TBTOT(J)*AB(J)*(RHOCON*CPCON*SMKCON/(PI*TIME**3))**.5
     1   -QCBTOT(J))/DELT
      QCBTOT(J)=QCBTOT(J)+QCB(J)*DELT
  770 CONTINUE
      ECONCS=ECONCS+PCONCS*DELT
      ECONCB=ECONCB+PCONCB*DELT
C
```

```
C        DETERMINE ROOM AIR PROPERTIES
C
  800 CPROOM=FROOM*CPOX+(1.-FROOM)*CPNI
      IF (CSINK*ASINK.EQ.0.) GO TO 802
      CALL APROP(3, 1.E10, 1.E10, 1.E10, 1.E-10, 1.E10, TSINK, TROOM,
     1   RHOX, FROOM, RE, HRM, SMFX, ASINK, FROOM, HDRM, INDX)
      CALL APROP(3, 1.E10, 1.E10, 1.E10, 1.E-10, 1.E10, TSINK, TO,
     1   RHOX, FO, RE, HOUT, SMFX, ASINK, 0.23, HDRM, INDX)
      QLSINK=ASINK*(HOUT*(TSINK-TO)+.7*SIG*(TSINK**4-TO**4))
      QASINK=HRM*ASINK*(TROOM-TSINK)
      QSINK=QASINK+QRSINK*ROWS-QLSINK
      ESINK=ESINK+QSINK*DELT
      TSINK=TSINK+QSINK*DELT/CSINK
  802 QINTO=(PCONV1+PCONV2+PCONV3)*ROWS
      QVENT=VENT*(RHORM*CPROOM*TROOM-RHOO*CPO*TO)
      GRMOUT=0.
      IF (IVENT.EQ.1) GRMOUT=(QINTO-QASINK-QVENT)/(CPROOM*TROOM)
      QALOSS=GRMOUT*CPROOM*TROOM
      QLOSS=QALOSS+QLSINK+QVENT
      ELOSS=ELOSS+QLOSS*DELT
      RHONEW=(RHORM*VROOM-(OXMTOT*ROWS+GRMOUT+VENT*(RHORM-RHOO))
     1   *DELT)/VROOM
      FNEW=(FROOM*RHORM*VROOM-(OXMTOT*ROWS+FROOM*GRMOUT+VENT*(RHORM
     1   *FROOM-RHOO*FO))*DELT)/(RHONEW*VROOM)
      CPNEW=FNEW*CPOX+(1.-FNEW)*CPNI
      QROOM=QINTO-QASINK-QVENT-QALOSS
      EROOM=EROOM+QROOM*DELT
      TROOM=(RHORM*VROOM*CPROOM*TROOM+QROOM*DELT)/(RHONEW*VROOM*CPNEW)
      FROOM=FNEW
      RHORM=RHONEW
      CPROOM=CPNEW
      IF (IVENT.EQ.1) GO TO 805
      PROOM=RHORM*RA*TROOM
      IF (PROOM.GE.PRMAX) IVENT=1
      UPL=SMG*RHORM*UL
C
C        CLOSURE
C
  805 EREMDR=EGEN+ECHEM-EFUEL-ESTR-EHOLDR-ERAD-ELINRS-ELINRB
     1   -ECONCS-ECONCB-ECONV1-ECONV2-ECONV3-ESTAIR
      PREMDR=PGEN+PCHEM-PFUEL-PSTR-PHOLDR-PRAD-PLINRS-PLINRB
     1   -PCONCS-PCONCB-PCONV1-PCONV2-PCONV3-PSTAIR
      IF (NP.EQ.0) WRITE(6,6010) PGEN, PCHEM, PFUEL, PSTR, PHOLDR,
     1   PRAD, PLINRS, PLINRB, PCONCS, PCONCB, PCONV1, PCONV2,
     2   PCONV3, PSTAIR, PREMDR, QROOM, QSINK, QLOSS
 6010 FORMAT(/*  PGEN=  *,1PE10.3, *   PCHEM= *,E10.3, *   PFUEL= *,
     1   E10.3, *   PSTR=  *,E10.3, *   PHOLDR=*,E10.3, *   PRAD=  *,
     2   E10.3/ *  PLINRS=*,E10.3, *   PLINRB=*,E10.3, *   PCONCS=*,
     3   E10.3, *   PCONCB=*,E10.3, *   PCONV1=*,E10.3, *   PCONV2=*,
     4   E10.3/ *  PCONV3=*,E10.3, *   PSTAIR=*,E10.3, *   PREMDR=*,
     5   E10.3, *   QROOM= *,E10.3, *   QSINK= *,E10.3, *   QLOSS= *,
     6   E10.3)
      GO TO 170
  900 IF (IPL.EQ.0) GO TO 910
      CALL PLOTPR(0, 0, XPL, YPL, NPL, 1, 1, 0, 1H , TITLE, XLAB,
     1   YLAB, 2, 1, 0., XMAX, 1, 0., YMAX)
      NPLOT=NPLOT+1
      CALL PLOTND(940)
  910 IF (NCEND.EQ.0) GO TO 80
  999 IF (NPLOT.GT.0) CALL EXTFLM(0)
      STOP
      END
```

```
      SUBROUTINE AFROF(ID, XPATH, XNC, XL, G, DE, TW, TA, RHOA,
     1   PRCOM, RE, H, SMF, A, FOX, HD, IND)
C
C        AIR PROPERTIES
C
      DIMENSION FI(7), HM(7)
      DATA NF, FI, HM /7, 0., .045, .070, .105, .145, .213, .285,
     1   0., .52, .64, .73, .79, .86, .92/
      AMAIR=1./(FOX/32.00+(1.-FOX)/28.16)
      RA=8.3144E+7/AMAIR
      SMG=980.
      TBAR=(TW+TA)/2.
      RHOA=PRCOM/(RA*TA)
      XMU=0.146E-4*TBAR**1.5/(TBAR+109.58)
      RE=ABS(G)*DE/(XMU*A)
      REX=RE*XPATH/DE
      PR=.714
      SC=.748
      CP=.27*4.184
      SMK=CP*XMU/PR
      DIF=XMU/(RHOA*SC)
C
      DNU1=0.
      IF (ID.LT.0) GO TO 20
      TBARNC=TW-0.38*(TW-TA)
      RHONC=PRCOM/(RA*TBARNC)
      XMUNC=0.146E-4*TBARNC**1.5/(TBARNC+109.58)
      BETA=1./TBARNC
      GRL=SMG*BETA*(RHONC**2)*(XL**3)*ABS(TW-TA)/(XMUNC**2)
      GRX=GRL*(XNC/XL)**3
C
      IF (GRX.GT.1.E+9) GO TO 10
C
C        LAMINAR NATURAL CONVECTION ON A VERTICAL PLATE
C
      DNU1=0.360*(GRX**0.25)*(DE/XNC)
      IND1=1
      GO TO 20
C
C        TURBULENT NATURAL CONVECTION ON A VERTICAL PLATE
C
   10 DNU1=0.1160*(GRX**0.33333333)*(DE/XNC)
      IND1=2
C
C        CORRECTION FOR PARALLEL PLATES, TURBULENT NATURAL CONVECTION
C
C        FOLLOWING STATEMENT DELETES CORRECTION FACTOR
         IF (IND1.EQ.2) GO TO 20
      F=(DE/(2.*XL))*(GRL*PR/1.8E10)**(1./6.)
      I=2
   12 IF (F.LE.FI(I)) GO TO 14
      IF (I.EQ.NF) GO TO 14
      I=I+1
      GO TO 12
   14 HMULT=HM(I-1)+(F-FI(I-1))/(FI(I)-FI(I-1))*(HM(I)-HM(I-1))
      IF (HMULT.LT.0.) HMULT=0.
      IF (HMULT.GT.1.) HMULT=1.
      HDIV=.94+.77*F-.33*(XNC/XL)
      IF (HDIV.GT.1.) HDIV=1.
      DNU1=DNU1*HMULT/HDIV
C
   20 IF (ID.NE.3) GO TO 25
      DNU=DNU1
      GO TO 100
```

```
   25 IF (REX.GT.5.E+5) GO TO 30
C
C        LAMINAR FORCED FLOW PAST A PLATE
C
      DNU2=.332*(REX**0.5)*(PR**0.33)*(DE/XPATH)
      SMF2=0.664/(REX**0.5)
      IND2=1
      GO TO 40
C
C        TURBULENT FORCED FLOW PAST A PLATE
C
   30 DNU2=.0296*(REX**0.8)*(PR**0.6)*(DE/XPATH)
      SMF2=.0592/(REX**0.2)
      IND2=2
C
   40 IF (IABS(ID).EQ.2) GO TO 60
      IF (RE.GE.3000.) GO TO 50
C
C        LAMINAR FORCED FLOW BETWEEN PARALLEL PLATES
C
      DNU3=7.54+.0234*RE*PR*DE/XL
      SMF3=24./RE
      IND3=1
      GO TO 80
C
C        TURBULENT FORCED FLOW BETWEEN PARALLEL PLATES
C
   50 DNU3=.023*(RE**.8)*(PR**.4)
      SMF3=.00140+.125/(RE**.32)
      IND3=2
      GO TO 80
C
   60 IF (RE.GE.3000.) GO TO 70
C
C        LAMINAR FORCED FLOW THROUGH AN ARRAY OF TUBES
C
      DNU3=8.
      SMF3=25./RE
      IND3=1
      GO TO 80
C
C        TURBULENT FORCED FLOW THROUGH AN ARRAY OF TUBES
C
   70 DNU3=.023*(RE**.8)*(PR**.4)
      SMF3=.00140+.125/(RE**.32)
      IND3=2
C
   80 DNU=DNU1
      IND=3*IND1-2
      IF (DNU1.GT.DNU2) GO TO 90
      DNU=DNU2
      IND=3*IND2-1
      IF (DNU2.GT.DNU3) GO TO 100
   90 IF (DNU1.GT.DNU3) GO TO 100
      DNU=DNU3
      IND=3*IND3
  100 SMF=AMAX1(SMF2,SMF3)
      H=SMK*DNU/DE
      HD=DIF*DNU/DE
      RETURN
      END
```

```
      SUBROUTINE BFLOW(J)
C
C        BASE MASS FLOWS
C
      DIMENSION FOXAVB(8), GCPB(8,3), GNI(8,3), GNIB(9)
      DIMENSION GOXB(9), GOXBOT(8,3)
      COMMON /FLOW/ FOXAVB, GCPB, GNI, GNIB, GOXB, GOXBOT
      GNIIN=0.
      GOXIN=0.
      CPNI=1.130
      CPOX=1.130
      DO 10 L=1,3
      IF (GNI(J,L).GE.0.) GO TO 10
      GNIIN=GNIIN-GNI(J,L)
      GOXIN=GOXIN-GOXBOT(J,L)
   10 CONTINUE
      IF (GNIB(J).LE.0.) GO TO 20
      GNIIN=GNIIN+GNIB(J)
      GOXIN=GOXIN+GOXB(J)
   20 IF (GNIB(J+1).GE.0.) GO TO 30
      GNIIN=GNIIN-GNIB(J+1)
      GOXIN=GOXIN-GOXB(J+1)
   30 FOXAVB(J)=GOXIN/(GNIIN+GOXIN)
      IF (GNIB(J).LE.0.) GOXB(J)=FOXAVB(J)/(1.-FOXAVB(J))*GNIB(J)
      IF (GNIB(J+1).GE.0.) GOXB(J+1)=FOXAVB(J)/(1.-FOXAVB(J))
     1   *GNIB(J+1)
      DO 50 L=1,3
      IF (GNI(J,L).LT.0.) GO TO 40
      GOXBOT(J,L)=FOXAVB(J)/(1.-FOXAVB(J))*GNI(J,L)
   40 GCPB(J,L)=GNI(J,L)*CPNI+GOXBOT(J,L)*CPOX
   50 CONTINUE
      RETURN
      END
```

```
      SUBROUTINE CHEM(TC, DELT, RCI, RC, RCT, RCN, QC)
C
C        KINETICS OF ZIRCONIUM OXIDE REACTION
C
      QC=0.
      RCL=RC-RCI
      IF (RCT.GE.RCL) GO TO 40
C     NOMINAL EXPRESSION
C     C1=4.7E+4
C     C2=6.8E+3
C     C3=6.4E+6
      C1=9340.
      C2=13760.
      C3=0.
      IF (TC.LT.1193.) GO TO 10
      C1=4.68E8
      C2=26670.
      IF (TC.LT.1429.) GO TO 10
      C1=5.04E5
      C2=14630.
   10 RHOZR=6.5E+3
      DELH=7.8E+4
      RATEK=C1*EXP(-(C2+C3/TC)/TC)
      RCN=RCT
      W=(RATEK*DELT)/(RHOZR*RHOZR)+RCT*RCT
      IF (W.LE.0.) GO TO 20
      RCN=SQRT(W)
   20 CONTINUE
      IF (RCN.GE.RCL) RCN=RCL
      QC=DELH*(RCN-RCT)/DELT
   40 CONTINUE
      RETURN
      END
```

```
      SUBROUTINE FPROP(T, CF, CC, SMKF, SMKC, ICALL)
C
C        FUEL AND CLAD PROPERTIES
C
      IF (ICALL.EQ.0) GO TO 20
      IF (T.GE.3200.) GO TO 4
      THETA=535.285
      EO=37.6946
      CAPK1=19.1450
      CAPK2=7.84733E-4
      CAPK3=5.64373E+6
      R=1.9865E-3
      THETT=THETA/T
      EXPT=EXP(THETT)
      CF=(CAPK1*THETT*THETT*EXPT/((EXPT-1.)**2)+2.*CAPK2*T+((CAPK3
     1   *EO)/(R*T*T))*EXP(-EO/(R*T)))*4.184/270.13
      GO TO 6
    4 CF=51.*4.184/270.13
    6 CONTINUE
      IF (T.GT.1223.) GO TO 10
      CC=(7.1E-2+1.7E-5*T-0.89E+3/(T*T))*4.184
      RETURN
   10 CC=0.087*4.184
      RETURN
   20 SMKF=0.030
      SMKC=0.30
      RETURN
      END
```

DISTRIBUTION:

U.S. Nuclear Regulatory Commission
(356 copies for R3)
Division of Document Control
Distribution Services Branch
7920 Norfolk Avenue
Bethesda, MD 20014

R. L. Stanford (5)
Fuel Process Systems Standards Branch
Materials Safety Standards
Division of Engineering Standards
Office of Standards Development
U.S. Nuclear Regulatory Commission
Washington, DC 20555

4231	S. A. Dupree
4400	A. W. Snyder
4414	G. B. Varnado
4414	A. S. Benjamin (30)
4441	M. Berman
4550	R. M. Jefferson
4552	R. B. Pope
5511	D. F. McVey
5512	H. C. Hardee
5831	D. A. Powers
8266	E. A. Aas
3141	T. L. Werner (5)
3151	W. L. Garner (3) For DOE/TIC (Unlimited Release)
3172-3	R. P. Campbell (25) For NRC Distribution to NTIS